

Resource Allocation Techniques for Non-Orthogonal Multiple Access Systems

Haitham Al-Obiedollah

Doctor of Philosophy

University of York

Electronic Engineering

September 2019

To my family ...

Acknowledgements

I would like to thank my supervisor, Dr. Kanapathippillai Cumanan, for his generous support, guidance, and unbounded enthusiasm. It has been a privilege working under his supervision. Thank you also to my co-supervisor, Prof. Alister G. Burr, for his kind support and guidance. In fact, the accomplishment of this study would not have been feasible without the kind support and cooperation of my supervisors. Many thanks also go to my research collaborators: Dr. Jeyarajan Thiyagalingam, Prof. Zhiguo Ding and Prof. Octavia A. Dobre. Their help, support, and contribution are much appreciated. I would like also to thank Dr. Rami Al-Obiedollah, who has helped me very much in the very first few days of my arrival to the United Kingdom and has been always there to support during my PhD journey. All my thanks and love to my wife Lara, my son Moffaq, and my daughter Lana who brought great deal of inspiration to my life, despite of the long distances that separated us during this journey, they were always there for me to brighten my way and motivate me to work harder. Furthermore, I would like to extend my heartfelt gratitude to my parents, my brothers, and sisters for whom I am eternally grateful for their love and encouragement. Finally, I would like to thank The Hashemite University for providing the funding which allowed me to undertake this research.

Abstract

Non-orthogonal multiple access (NOMA) has been proposed as a viable multiple access (MA) technique to meet the demanding requirements in fifth-Generation (5G) and beyond wireless networks. Unlike conventional orthogonal multiple access (OMA) techniques, NOMA simultaneously sends signals to multiple users in the same resource block (RB) in time and frequency domains using power-domain superposition coding (SC) at transmitter. Therefore, NOMA has the potential capabilities to serve a large number of devices while significantly improving spectrum efficiency (SE) compared to the conventional MA techniques, which supports massive connectivity of Internet-of-Things (IoT) networks.

To introduce additional degrees of freedom, and hence facilitate implementing NOMA in ultra-dense networks, NOMA has been integrated with different key technologies including multiple antenna techniques and conventional OMA techniques. In particular, the combination between multiple-input single-output (MISO) and NOMA, referred to as MISO-NOMA, is firstly considered in this thesis. In which, different beamforming designs have been proposed for MISO-NOMA system, including global energy efficiency maximization (GEE-Max) design and EE fairness-based designs. In addition, different multi-performance metrics have been also considered in the designs including GEE-SE design and fairness-sum rate design. Due to non-convexity of the formulated optimization problems, different convex relaxation and approximation techniques have been exploited throughout the thesis to approximate the original non-convex problems with convex problems. The performance of the proposed designs has been evaluated through drawing comparisons with that of the existing beamforming designs in the literature.

Secondly, the combination of NOMA with OMA scheme has been investigated, particularly, energy harvesting (EH) capabilities of time division multiple access (TDMA) and NOMA system has been considered. In this hybrid TDMA-NOMA system, simultaneous wireless information and power transfer (SWIPT) technique is integrated such that user has the capability to harvest energy and decode information, simultaneously. Simulation results show that EH capabilities of the TDMA-NOMA system outperform that of the conventional TDMA system.

Table of Contents

List of Figures	viii
List of Tables	x
List of Notations	xii
List of Acronyms	xiii
1 Introduction	1
1.1 Overview	1
1.2 Towards 5G and Beyond	2
1.2.1 5G Requirements	2
1.3 Towards Non-orthogonal Multiple Access	3
1.3.1 Conventional Multiple Access Techniques	3
1.3.2 Non-Orthogonal Multiple Access	5
1.4 Thesis Outline	6
2 Fundamental Concepts and Literature Review of NOMA	10
2.1 NOMA Fundamentals	10
2.1.1 Superposition Coding and Successive Interference Cancellation	11
2.1.2 A Simple SISO NOMA/OMA Scenario	11
2.1.3 Advantages of NOMA	14
2.2 NOMA with other Techniques	15
2.2.1 NOMA with Multiple-Antenna Techniques	15
2.2.2 NOMA with OMA Techniques	18
2.3 Energy-Efficient Strategies	19
2.3.1 Energy-Efficient-Resource Allocation Techniques	19
2.3.2 Simultaneous Wireless Power and Information Transfer	20
2.4 Literature Review	20

2.5	Summary	22
3	Resource Allocations: Performance Metrics and Optimization Techniques	23
3.1	Resource Allocation Techniques	23
3.1.1	Power Minimization Techniques	24
3.1.2	Rate-Aware Techniques	24
3.1.3	Energy Efficiency Aware Techniques	25
3.1.4	Multi-Performance metric Techniques	25
3.2	Single-Objective Optimization Problems	25
3.2.1	Convex Optimization Problems	27
3.2.2	Non-Convex Optimization Problems	28
3.3	Multi-Objective Optimization	29
3.3.1	MOO Framework	29
3.4	General Discussions	31
3.5	Summary	32
4	Energy-Efficient Beamforming Designs	33
4.1	System Model	33
4.2	GEE-Max Design	36
4.2.1	Feasibility check of OP_1	37
4.2.2	Approaches for Solving the GEE-Max Problem	38
4.2.3	Complexity Analysis of the Proposed Schemes	47
4.2.4	Optimality Validation for the SCA Technique	48
4.3	Energy-Efficient Fairness Designs	49
4.3.1	Proposed EE-Fairness Designs	50
4.3.2	The SCA Technique	51
4.4	Simulation Results	55
4.5	Summary	64
5	Multi-Objective based Beamforming Designs	66
5.1	Spectral-Energy Efficiency Trade-off based Beamforming Design	66
5.1.1	Introduction	66
5.1.2	Problem Formulation	68
5.1.3	Feasibility, Proposed Methodology, and Discussions	69
5.1.4	Proposed Methodology	69
5.2	Sum rate Fairness Trade-off-based Design	77
5.2.1	Introduction and Problem Formulation	77

5.3	Simulation Results	80
5.4	Summary	87
6	Energy Harvesting of Hybrid TDMA-NOMA Technique	89
6.1	Introduction	89
6.2	System Model and Problem Formulation	90
6.2.1	System Model	90
6.2.2	Problem Formulation	94
6.3	Proposed Methodology and Discussions	94
6.3.1	Grouping Strategy	95
6.3.2	Proposed Algorithm	95
6.4	Simulation Results	99
6.5	Summary	101
7	Conclusions and Future Work	102
7.1	Conclusions	102
7.2	Future work	104
Appendix A	Proofs for Chapter 4	106
A.1	Proof of Theorem 1	106
A.2	Proof of Lemma 1	107
Appendix B	Proofs for Chapter 5	109
B.1	Proof of Theorem 1	109
B.2	Proof of Lemma 1	110
	References	112

List of Figures

1.1	Key requirements of 5G and beyond wireless networks.	4
1.2	Vision of 5G proposed technique.	7
2.1	Two-users SISO-NOMA with SC and SIC.	12
2.2	Achievable sum-rate for SISO-NOMA and SISO-OMA scenarios.	14
2.3	Hybrid MISO-NOMA configurations: (a) Beamformer-based MISO-NOMA scheme, (b) Cluster-based MISO-NOMA system scheme [1].	17
2.4	An illustration of different MA approaches: (a) TDMA approach, (b) NOMA approach, (c) Hybrid TDMA-NOMA approach.	18
3.1	Recent resource allocation techniques.	26
3.2	Different EE-aware resource allocation techniques.	27
3.3	Illustration of optimization problem types.	30
3.4	Illustration of MOO solving process.	31
4.1	A multiuser, MISO-NOMA system with a multi-antenna base station, and K -single antenna users.	34
4.2	Achieved EE for GEE-Max-based design through Algorithms 1 and 2.	56
4.3	EE for different design criteria.	57
4.4	Achieved sum rates of different beamforming designs against transmit power.	58
4.5	EE of GEE-Max design with different power losses for 5 users scenario.	58
4.6	Required transmit power for different beamforming design criteria.	59
4.7	Achieved EE of GEE-Max design with different power losses.	60
4.8	The achieved EE against different number of transmit antenna N for GEE-Max and SRM designs at TX-SNR =10 dB. The p_{sta} and p_{dyn} are set to be 10 dBm and 5 dBm, respectively.	61
4.9	The convergence of SCA based GEE-Max algorithm for different set of random channels. The TX-SNR and P_{loss} are set to be 20 dB and 40 dBm, respectively.	62

4.10	The performance of the weakest user with different beamforming designs, $\kappa=2, \eta_i^{min} = 10^{-3}$	63
4.11	EE of the system (i.e., GEE) with different EE-based designs, $\kappa=2, \eta_i^{min} = 10^{-3}$	64
5.1	Achieved EE and sum rate against TX-SNR with different weight factors α	81
5.2	Achieved EE and sum rate with different weight factors α	82
5.3	The EE and sum-rate performance of the proposed design versus TX-SNR, with different weight factors. (a) The achieved EE, (b) the achieved sum rate.	83
5.4	Achieved EE and sum rate for the proposed design versus weight factors α , with different SINR thresholds η_{th} , TX-SNR= 20 dB.	83
5.5	Pareto front of SE-EE trade-off-based design for TX-SNR = 24 dB.	84
5.6	Achieved sum rate and FI against the weight factor α , TX-SNR=30 dB.	85
5.7	The weakest user's rate against the available transmit power for different weight factors α	86
5.8	Pareto-front for different TX-SNR thresholds.	87
6.1	Hybrid TDMA-NOMA system; the users are divided among C groups.	91
6.2	Illustration of splitting the received signal at $u_{j,i}$	92
6.3	The required transmit power versus different minimum harvest power requirements P^{min} , with a minimum rate requirement $R^{min} = 10^{-1}$ bit/Hz.	100
6.4	The convergence of the SCA algorithm to solve OP_{10} for different values of the minimum harvest power requirement P^{min} , $R^{min} = 10^{-2}$ bit/Hz.	101

List of Tables

4.1	Parameter values used in the simulations.	56
4.2	Power allocations and the achieved SINRs obtained from solving GEE-Max design using the SCA, TX-SNR= 2dB.	60
4.3	Power allocations for the achieved SINRs In Table 4.2 using the P-Min design.	61
5.1	The impact of the weakest user distance (i.e., d_5) on the sum rate and FI with different weight factors, at TX-SNR=35 dB.	86
6.1	Parameter values used in simulations.	99
6.2	Splitting ratio $\beta_{j,i}$ for all users, with a minimum rate requirement $R^{\min} = 10^{-1}$ bit/Hz	100
6.3	The required transmit power for different minimum rate requirement R^{\min} , with a minimum harvest power requirement $P^{\min} = -30$ dBm.	101

Declaration

I declare that except where specific reference is made to the work of others, the contents of this dissertation are original and have not been submitted in whole or in part for consideration for any other degree or qualification in this, or any other university. Some of the work presented in this thesis have been published in, or planned to submit to conferences, journals and project deliverables, which are listed as follows:

1. **H. Al-Obiedollah**, K. Cumanan, J. Thiyagaligam, A. G. Burr, Z. Ding, and O. A. Dobre, "Sum rate fairness trade-off-based resource allocation technique for MISO NOMA systems," in Proc. IEEE WCNC, 2019.
2. **H. Al-Obiedollah**, K. Cumanan, J. Thiyagaligam, A. G. Burr, Z. Ding, and O. A. Dobre, "Energy efficiency fairness beamforming design for MISO NOMA systems," in Proc. IEEE WCNC, 2019.
3. **H. M. Al-Obiedollah**, K. Cumanan, J. Thiyagaligam, A. G. Burr, Z. Ding, and O. A. Dobre, "Energy Efficient Beamforming Design for MISO Non-Orthogonal Multiple Access Systems", IEEE Trans. Commun., vol. 67, no. 6, pp. 4117–4131, Feb. 2019.
4. **H. Al-Obiedollah**, K. Cumanan, A. G. Burr, J. Tang, Y. Rahulamathavan, Z. Ding, and O. A. Dobre, "On Energy Harvesting of Hybrid TDMA-NOMA Systems," **Accepted at IEEE Globecom, 2019.**
5. **H. Al-Obiedollah**, K. Cumanan, J. Thiyagaligam, J. Tang, A. G. Burr, Z. Ding, and O. A. Dobre, "Spectral-Energy Efficiency Trade-off-based Beamforming Design for MISO Non-Orthogonal Multiple Access Systems", Submitted in IEEE Trans. Wireless Commun., **under major revision.**

Haitham Al-Obiedollah
September 2019

List of Notations

\mathbb{C}^N	N -dimensional complex vectors
\mathbb{R}^N	N -dimensional real vectors
$ x $	Norm of complex number x
\mathbf{x}	Vector \mathbf{x}
\mathbf{X}	Matrix \mathbf{X}
x_i	i^{th} element of a vector \mathbf{x}
∇f	first derivative of f
$\nabla^2 f$	second derivative of f
$(\cdot)^T$	Transpose
$(\cdot)^H$	Transpose conjugate
$\mathbf{X} \succeq \mathbf{0}$	Positive semi-definite matrix
$\mathbf{x} \succeq \mathbf{0}$	Each element in \mathbf{x} is greater than zero
$\text{Tr}(\mathbf{X})$	Trace of the matrix \mathbf{X}
$x^{(n)}$	The approximation of x in the n^{th} iteration
$\Re(x)$	Real part of a complex number x
$\Im(x)$	Imaginary part of a complex number x
$\ \cdot\ _2$	Euclidian vector norm, i.e., $\ \mathbf{x}\ _2 = \sqrt{\mathbf{x}^H \mathbf{x}}$
$\text{dom } f$	Domain of a function f
$\min\{\}$	Minimum of function
$\max\{\}$	Maximum of function

List of Acronyms

1G	First-Generation
2G	Second-Generation
3G	Third-Generation
4G	Forth-Generation
5G	Fifth-Generation
AWGN	Additive White Gaussian Noise
CCA	Convex-Concave Algorithm
CDMA	Code Division Multiple Access
CSI	Channel State Information
EE	Energy Efficiency
EH	Energy Harvesting
FDMA	Frequency Division Multiple Access
FI	Fairness Index
FTPC	Fractional Transmit Power Control

GEE-Max	Global Energy Efficiency Maximization
ICI	Intra-Cluster Interference
ID	Information Decoding
IMT	International Mobile Telecommunications
IoT	Internet-of-Things
ITU-R	International Telecommunication Union-Radio
LTE	Long-Term Evolution
MA	Multiple Access
MCI	Multi-Cluster Interference
MIMO	Multiple-Input Multiple-Output
MISO	Multiple-Input Single-Output
ML	Machine Learning
MMA	Majorization Minimization Algorithm
MMEE	Max-Min Energy Efficiency
MMR	Max-Min Rate
MOO	Multi-Objective Optimization
NOMA	Non-Orthogonal Multiple Access
OFDMA	Orthogonal Frequency Division Multiple Access

PIC	Parallel Interference Cancellation
PF	Proportional Fairness
P-Min	Power minimization
QoS	Quality-of-Service
RB	Resource Block
RF	Radio Frequency
SC	Superposition Coding
SCA	Sequential Convex Approximation
SDMA	Space Division Multiple Access
SDP	Semi-definite Programming
SE	Spectral Efficiency
SE-Max	Spectral Efficiency Maximization
SIC	Successive Interference Cancellation
SINR	Signal-to-interference and Noise Ratio
SISO	Single-Input Single-Output
SOC	Second-Order Cone
SOO	Single-Objective Optimization
SRM	Sum-Rate Maximization

SWIPT	Simultaneous Wireless Information and Power Transfer
TDMA	Time Division Multiple Access
WSRM	Weighted Sum-Rate Maximization
ZFBF	Zero-Forcing Beamforming

Chapter 1

Introduction

1.1 Overview

The first-generation (1G) of commercial cellular networks was launched by 1980s, in which, basic voice services were supported [2]. A decade after, more capacity and digital voice communications services were provided through replacing the 1G with the second-generation (2G) cellular networks. In particular, the higher rates offered by 2G systems are achieved through employing either code division multiple access (CDMA) or time division multiple access (TDMA) [3]. Next, the new set of standards and requirements of mobile communications specified by International Telecommunication Union-Radio (ITU-R) was met by the third-generation (3G)-International Mobile Telecommunications-2000 (IMT-2000). In such 3G networks, the Internet access on mobile devices was possible, which offers different services including video calls, file transmission, and online TV. In particular, various forms of CDMA technologies were used in the deployment of 3G networks, such as wideband CDMA and CDMA2000 [2]. In 2008, the requirements of fourth-generation (4G) were announced by ITU-R [2] which include service speeds of 100 Mbps and 1Gbps for high-mobility and low-mobility communications, respectively. In particular, the two proposed 4G technologies, namely Long-Term Evolution (LTE) and Worldwide Interoperability for Microwave Access (WiMAX), utilize orthogonal frequency division multiple access (OFDMA) technique. By 2011, 4G standards were completed while deploying 4G networks over the world [4]. Considering the ten-year cycle for each generation, the next generation of wireless networks, namely, fifth-generation (5G) is supposed to be rolled out by 2020 [2], [4]. Hence, extensive research efforts have been devoted to meet the increasing and diverse demands of future wireless networks. These demands include offering massive connectivity to billions of smart phones, tablets, and other data-consuming devices, to support a diverse set of wireless communication applications.

1.2 Towards 5G and Beyond

1.2.1 5G Requirements

Due to a considerable impact of future wireless networks in humans' daily activities, 5G networks should be able to support diverse scenarios, including smart homes, e-health, industries, autonomous vehicles, and so on. Obviously, these scenarios demand massive connectivity to connect billions of devices which cannot be supported by already existing 4G networks [2]. In particular, the ITU-R announced its visions and recommendations towards 5G and beyond wireless networks. The key requirements of 5G and beyond wireless networks can be summarized as follows [2]:

1. Connectivity Requirements

In future, Internet of Things (IoT) will become dominant paradigm, where millions of smart devices will be able to communicate with each other and with their neighbours to facilitate day to day activities in human life [5]. Different applications can be supported through this novel IoT paradigm, such as smart homes and intelligent transportation of people. Furthermore, mobile operators are expected to expand their services through offering a wide range of smart mobile applications to their costumers. Based on these predictions, the total number of connected wireless devices is expected to dramatically grow from 25 billion in 2015 to 50 billion by 2020 [6].

2. Capacity Requirements

Both development of new type of smart devices with higher data rate applications and supporting traffic-intensive applications such as video streaming in social networks, will introduce an enormous growth in the volume of mobile data traffic. Compared to the data traffic in 2010, mobile data traffic in 2020 and 2030 will grow by 200 and 2000 times, respectively [4].

3. Data Rate Requirements

The exponential growth in data traffic along with diverse quality-of-service (QoS) requirements demand corresponding improvements in both user-level data rates and system-level throughput. Furthermore, these rate requirements should take into account high mobility environments including high-speed trains. In contrast to the achievable throughput in 4G networks, 5G and beyond wireless networks are expected to achieve 10-fold improvement in peak data rate, such that 1 Gbps throughput should be offered any where any time [2].

4. Latency Requirements

It is expected that 5G will support several real-time applications, including online gaming and self-driving cars [7]. Hence, stringent latency will become a crucial aspect that has to be addressed in future wireless networks to meet the demanding requirements of ultra-reliable low-latency communications. In particular, the latency in 5G networks is expected to be less than 1 millisecond which is one fifth of the latency requirement in 4G networks [8].

5. Energy efficient networks

Triggered by the dramatic growth within the range of connected mobile devices, a corresponding speedy growth within the power consumption is expected, where 3% of world wide power was consumed by the infrastructure of data and communication technology in 2014 [9]. Specifically, this expected rising in power consumption has completely different undesirable impacts on each economical and environmental aspects [10]. Hence, the proposed technologies towards 5G and beyond wireless networks must seriously take the energy efficiency (EE) into consideration, where EE is defined as the ratio between the achievable sum rate and total power consumption [9].

6. Fairness

Generally, fairness is achieved through providing reasonable QoS to all users in wireless networks [11]. In 5G and beyond wireless networks, massive number of devices seek for an affordable QoS anytime, anywhere, and regardless of their channel conditions. Hence, fairness problem should be taken into account. To summarize, the key requirements of 5G and beyond wireless networks are summarized in Fig. 1.1.

1.3 Towards Non-orthogonal Multiple Access

1.3.1 Conventional Multiple Access Techniques

As discussed in previous sections, the demanding requirements of 5G and beyond wireless networks cannot be fulfilled with the existing conventional solutions. Therefore, different novel technologies have been recently explored to meet the demanding requirements of the future wireless networks. These technologies include non-orthogonal multiple access (NOMA) [12], millimeter-wave (mm-wave) communications [13], and massive multiple-input multiple-output [14]. This thesis mainly focuses on NOMA systems in details. However, prior to introducing NOMA, the conventional multiple access techniques, namely orthogonal

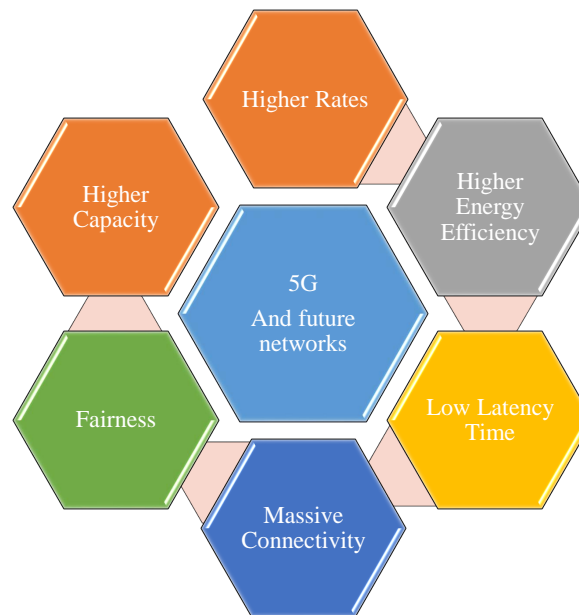


Fig. 1.1 Key requirements of 5G and beyond wireless networks.

multiple access (OMA) and multiple antenna techniques, are presented in the following discussions.

- Orthogonal Multiple Access Techniques

During the last decades, different OMA techniques have been exploited to meet the diverse demands in the preceding wireless network generations [15]. The OMA techniques include TDMA, CDMA, and FDMA techniques. In such OMA techniques, each user is served through allocating an orthogonal resource block (RB) [16]. In spite of mutual interference cancellation offered by orthogonal RB assignment in these OMA techniques, a major concern arises regarding the capabilities of these techniques to support the demanding massive connectivity in 5G and beyond wireless networks.

- Multiple Antennas Technique

Over last two decades, the employment of multiple antennas at transmitter and/or receiver for wireless networks has gained a remarkable interest [17], [18]. These multiple antennas offer additional spatial degrees of freedom due to the multi-paths between the antennas at the transmitter and receiver, as such, these multi-paths support providing reliable wireless communications [19]. In particular, a new domain, named spatial domain, is exploited by making use of multi-paths offered by utilizing multiple antennas. With this new domain in hand, the following performance enhancements

for such multiple antenna techniques over classical single-antenna communication can be achieved:

- Spatial Diversity

With multiple antennas, the same data is transmitted through multi-paths which could experience different fading at the same time. This uncorrelated fading between different paths helps the receiver to choose the best path to decode the signal with better quality which leads to a better performance at the receiver [20]. Note that the diversity gain achieved in a multiple antenna system is $N_t N_r$, where N_t and N_r are the number of antennas at transmitter and receiver, respectively [21].

- Spatial Multiplexing

Unlike the spatial diversity, multiple independent data streams can be transmitted parallelly from the transmitter, which will significantly improve the system throughput by employing spatial multiplexing [22]. In addition, the spatial multiplexing can be achieved through different precoding schemes at the transmitter such as linear and non-linear precoding techniques [23]. In particular, beamforming is a linear precoding scheme in which the signal is steered or guided in certain direction [24], [25]. With multiple antennas at the transmitter or the receiver, the beamforming techniques can be implemented through either by physically steering antennas towards the target [25], or digitally designing beamforming vectors to steer the signal to the intended direction [26].

Obviously, the explosive growth in the connected devices cannot be supported neither by employing the available limited orthogonal RB resources (i.e., OMA techniques) nor the multiple antenna techniques. Hence, developing new multiple access technique stands as one of the key solutions to support this massive connectivity in future wireless networks.

1.3.2 Non-Orthogonal Multiple Access

Recently, NOMA has been envisioned as a promising multiple access technique to meet the unprecedented requirements of 5G and beyond wireless networks [27]. Unlike OMA techniques, multiple users can be served within a same RB using NOMA techniques [28]. In particular, two types of NOMA have been recently adopted, code-domain NOMA and power-domain NOMA [8], where power-domain NOMA will be explored in this thesis. In downlink power-domain NOMA scheme, multiple users can be served at the same RB by

employing the superposition coding (SC), such that different transmit signals are encoded with different power levels [29]. On the other hand, successive interference cancellation (SIC) is utilized at receiver ends by firstly decoding the signals of weaker users prior to decoding the signal intended to the particular user [27]. In fact, NOMA technique is predicted to play a crucial role in the development of future wireless networks due to its potential capability of efficient spectrum utilization and offered massive connectivity which would be able to support the proliferation of IoTs [30], [31], [32].

To enhance the performance of NOMA systems, and to facilitate its practical implementation in ultra-dense networks, NOMA has been tailored to incorporate with different key disruptive technologies, such as multiple antenna techniques and conventional OMA techniques. The combinations of NOMA with different multiple-antenna techniques have been extensively investigated in the literature. For example, those multiple-antenna techniques include multiple-input multiple-output (MIMO) [33] and multiple-input single-output (MISO) [34], referred as MIMO-NOMA and MISO-NOMA systems, respectively. Obviously, the performance enhancement of those systems is achieved by exploiting the power-domain multiplexing offered by NOMA with additional spatial degrees of freedom provided by multiple antennas. Furthermore, the performance of those multiple-antenna NOMA systems is defined based on the employed beamforming designs, which are extensively studied throughout this thesis.

Furthermore, NOMA can also be combined with the existing conventional OMA techniques, as such orthogonal and non-orthogonal domains are jointly exploited to further improve the performance of wireless networks. Different hybrid OMA-NOMA approaches, such as hybrid TDMA-NOMA and OFDMA-NOMA systems have been proposed in the literature [35], [36]. In a hybrid TDMA-NOMA system, users are divided into a number of groups or clusters, and the available time for transmission is shared between these groups through multiple time slots. In particular, a time slot is assigned to serve each group, whereas the users in each group are served based on power-domain NOMA technique. Note that hybrid OFDMA-NOMA is referred to as multi-carrier NOMA in the literature [37], [38].

1.4 Thesis Outline

Due to the demanding requirements of 5G and beyond wireless networks, it is obvious that neither NOMA nor other single techniques can individually meet those diverse requirements, this encourages to further investigate different hybrid systems, especially the combination

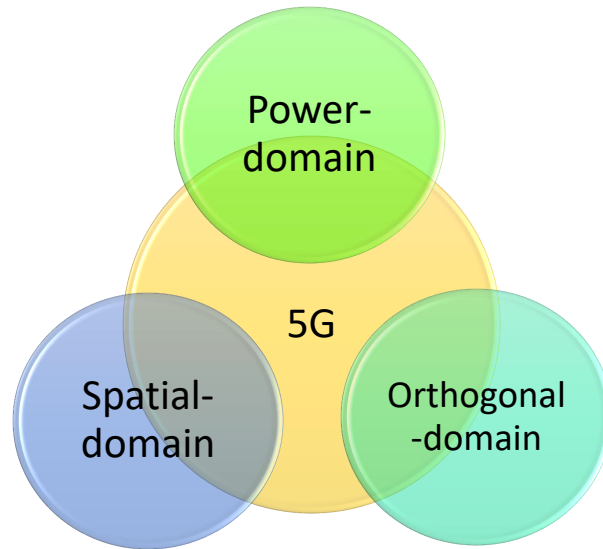


Fig. 1.2 Vision of 5G proposed technique.

of NOMA and other techniques [2]. Furthermore, resource allocation techniques for such hybrid systems play a crucial role in defining their performance. Hence, this thesis focuses on developing several energy efficient resource allocation techniques for different NOMA systems. In the first part of this thesis, different beamforming designs have been proposed for MISO-NOMA systems owing the fact that these systems are expected to play a major role in the development of the future wireless networks. In the second part of this thesis, a hybrid TDMA-NOMA is investigated by incorporating energy harvesting (EH) capabilities. In particular, this thesis consists of seven chapters and the contents of each chapter are summarized as follows:

In Chapter 2, basic principles of NOMA including SIC and SC techniques are provided. Then, an overview of a simple two-user single-input single-output (SISO)-NOMA and OMA techniques is presented, with introducing the advantages of NOMA over conventional OMA techniques. Next, due to the superiority of combining NOMA with other existing techniques, further discussions about such smart combinations are included. In spite of existence of wide range of such hybrid systems, this thesis only focuses on combination of NOMA with multiple antenna and conventional OMA techniques. Furthermore, and with considering the importance of energy consumption in future wireless networks, different energy-efficient strategies are demonstrated. Finally, a detailed overview of related recent resource allocation

techniques for different NOMA approaches developed in literature are provided.

Chapter 3 outlines different resource allocation techniques to optimize crucial performance metrics in future wireless networks including the motivations behind each performance metric are introduced. Next, to mathematically express these resource allocation techniques, detailed discussions on optimization techniques are provided. In the first part of these discussions, some light is shed on the conventional single-objective optimization (SOO) approaches. In the second part, a general non-trivial multi-objective optimization (MOO) framework is presented. Furthermore, a brief procedure to handle any MOO problem is provided. Finally, a discussion on different aspects related to optimization problems is introduced.

In Chapter 4, a beamformer-based MISO-NOMA system model is introduced, where different energy efficient beamforming designs are proposed. In the first design, and motivated by the prominence of EE in future wireless networks, a global energy efficiency maximization (GEE-Max) beamforming design is proposed. In this design, the overall EE of the system is maximized with minimum user rate requirements and transmit power constraints. To solve the non-convex optimization problem of this design, two iterative algorithms are provided, namely sequential convex approximation (SCA) and Dinkelbach's algorithm. The performance of this GEE-Max design is compared with different beamforming designs in the literature including power minimization (P-Min) and sum-rate maximization (SRM) beamforming designs. However, as the performance of weak users might be degraded with the GEE-Max design, other EE fairness designs are proposed for the MISO-NOMA system. In particular, two quantitative fairness-based designs are developed to maintain fairness between the users in terms of achieved EE, i.e., max-min energy efficiency (MMEE) and proportional fairness (PF) designs. While the MMEE-based design aims to maximize the minimum EE of the users in the system, the PF based design aims to seek a good balance between the overall performance of the system and the EE fairness between the users. Detailed simulation results indicate that the proposed designs offer many-fold EE improvements over the existing energy-efficient beamforming designs.

Due to diverse requirements of 5G and beyond wireless networks, different multi-performance beamforming designs are proposed in Chapter 5 for the considered MISO-NOMA system in the previous chapter. In particular, EE and spectral efficiency (SE) are two of the key performance metrics that have to be jointly considered. Therefore, a beamforming design that jointly considers these two conflicting performance metrics for the MISO-NOMA system is firstly proposed in this chapter. This joint SE-EE based design is formulated as a

MOO problem to achieve a good trade-off between these performance metrics. However, this MOO problem is not mathematically tractable and difficult to determine a feasible solution due to the conflicting objectives, where both need to be simultaneously optimized. To overcome this issue, a priori-articulation scheme combined with the weighted sum approach is exploited, as such the original MOO problem is formulated as a conventional SOO problem. Then, an iterative algorithm based on SCA technique is developed to solve this non-convex SOO problem. Simulation results are provided to demonstrate the advantages and effectiveness of the proposed approach over the available beamforming designs. In the second design, a beamforming design that jointly considers the performance metrics of the sum rate and fairness for the MISO-NOMA is also proposed. Unlike the conventional rate-aware beamforming designs, the proposed approach has the flexibility to assign different weights to the objectives (i.e., sum rate and fairness) according to the network requirements and the channel conditions. This design is also formulated as MOO problem and solved using an iterative algorithm. Simulation results are provided to demonstrate the performance and the effectiveness of the proposed approach along with detailed comparisons with conventional rate-aware based beamforming designs.

In Chapter 6, another hybrid NOMA system, namely multi-user SISO TDMA-NOMA system is introduced. In which, the hybrid TDMA-NOMA system model considering EH capability through employing simultaneous wireless information and power transfer (SWIPT) at each user is introduced. Then, the required minimum transmit power at the base station is evaluated to meet a set of QoS requirements including minimum rate and minimum harvested energy requirements. This is achieved through developing an optimization problem which can jointly determine power allocation and power splitting ratios for all users corresponding with minimum transmit power. In particular, this joint optimization framework is non-convex, and hence SCA combined with other relaxations are exploited to handle this non-convexity issues. Finally, the EH capabilities of the introduced hybrid TDMA-NOMA is compared with that of conventional TDMA system using simulation results.

Finally, Chapter 7 concludes the work presented in this thesis. In addition, future research directions related to different NOMA systems are also identified.

Chapter 2

Fundamental Concepts and Literature Review of NOMA

In this chapter, the fundamental concepts of the NOMA systems are introduced. Then, a comparison between NOMA and conventional OMA approaches is presented for a two-user SISO system. Next, the combination of NOMA and other 5G emerging technologies, including multiple antenna techniques and OMA techniques, are discussed. Furthermore, recent energy-efficient strategies for future wireless networks are briefly introduced, in which energy-efficient resource allocation techniques and EH capabilities for NOMA systems are mainly focused. Finally, recent research works related to downlink NOMA in the literature are reviewed briefly.

2.1 NOMA Fundamentals

Motivated by the demanding requirements of 5G and beyond wireless networks and the limitations of the conventional OMA techniques, NOMA has been recently proposed as a promising MA technique for the future wireless networks [28]. Unlike the conventional OMA techniques, NOMA can simultaneously support multiple users within the same RB in frequency and time domains. This can be achieved by exploiting power-domain multiplexing (known as SC in the literature) at the base station [28], [12]. At receiver ends, the multi-user detection technique, namely SIC, can be exploited at stronger users to decode and subtract the signals of the weaker users, prior to decoding their own signals. The basic concepts of SC and SIC are introduced in the following subsections.

2.1.1 Superposition Coding and Successive Interference Cancellation

The fundamental idea of SC is to encode multiple signals intended for different users with different power levels at the transmitter which helps the receiver to successively perform multi-user detection [32], [39], where the concept of SC was firstly introduced in [40]. In downlink NOMA, users with lower channel strengths (i.e., refer to as weaker users) are allocated (i.e., encoded) with higher power levels. On the other hand, users with higher channel strengths (i.e., stronger users) are assigned with lower power levels [8]. At receiver ends, the post-interference cancellation technique, namely SIC is utilized at stronger users to decode the received signals [1]. In particular, the strong user sequentially decodes and subtracts the signals intended for the weaker users. As such, the signal of weakest user is firstly decoded and subtracted from the received signal. Note that the SIC process is carried out sequentially until the signals intended to all weaker users are decoded and finally its own signal is decoded. Two important facts related to SIC should be noted here. First, successful implementation of SIC requires the reception of signals of weaker users with higher power levels compared to the stronger users' signals [1]. Hence, it is important to encode the signals of weaker users with higher power levels. This condition is referred to as SIC condition throughout this thesis. Second, unlike parallel interference cancellation (PIC), SIC is implemented at stronger users with relatively negligible error when the received power levels are different [1], [41]. It is worth mentioning that SIC has been already exploited in different communication systems, including conventional MIMO networks [42].

2.1.2 A Simple SISO NOMA/OMA Scenario

To further demonstrate the key principles of NOMA, a simple two-user SISO system is considered in this subsection, as shown in Fig. 2.1. First, NOMA transmission is presented for this system model, where it is assumed that the first user (UE_1) has the strongest channel condition (i.e., cell-near user) compared to the second user (UE_2). In other words, $|h_1|^2 \geq |h_2|^2$, where h_i is the channel coefficient between UE_i and the base station. Note that both users share the same bandwidth for transmission (W), where W is set to 1 in this example. With employing SC, the signals of the users are encoded with different power levels, as such the transmitted signal from the base station can be written as

$$x = \sqrt{\alpha_1 p} s_1 + \sqrt{\alpha_2 p} s_2, \quad (2.1)$$

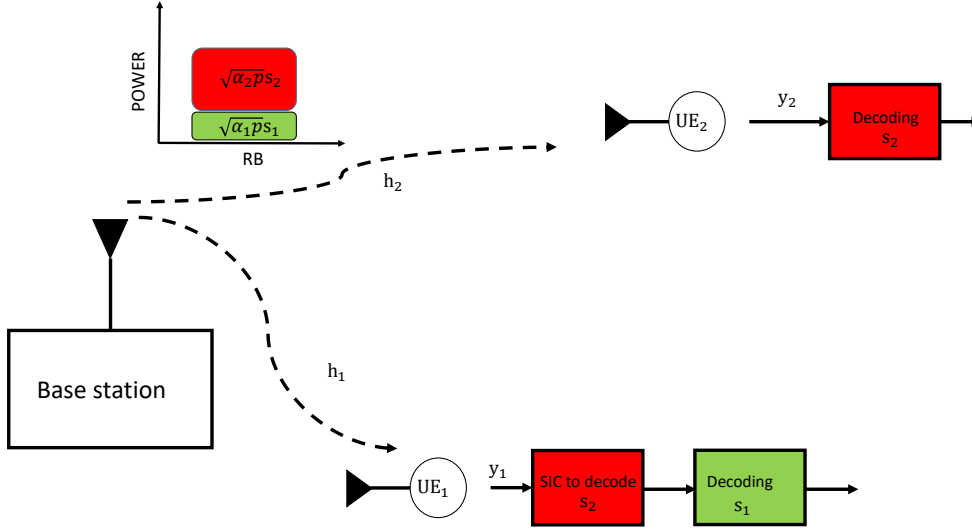


Fig. 2.1 Two-users SISO-NOMA with SC and SIC.

where s_i and $\sqrt{\alpha_i p}$ are the symbol intended for UE $_i$ and the corresponding allocated transmit power, respectively.

Based on the concept of SC technique, the user with the lower channel strength (i.e., UE $_2$) is assigned with a higher power level, i.e., $\alpha_2 \geq \alpha_1$. The superimposed received signals at UE $_i$ can be expressed as

$$y_i = h_i(\sqrt{\alpha_1 p} s_1 + \sqrt{\alpha_2 p} s_2) + n_i, \quad (2.2)$$

where n_i is the additive white Gaussian noise (AWGN) with zero mean and variance σ_i^2 . Based on the users' channel conditions, the strongest user, i.e., UE $_1$, has the capability to perform SIC. Hence, the signal of the weakest user is firstly decoded and subtracted from the received signal with the following signal to noise and interference ratio (SINR) [12]:

$$\text{SINR}_2^{(1)} = \frac{|h_1|^2 \alpha_2 p}{|h_1|^2 \alpha_1 p + \sigma_1^2}, \quad (2.3)$$

where $\text{SINR}_2^{(1)}$ denotes the SINR of decoding the message intended for UE $_2$ at the strongest user UE $_1$. Sequentially, the strongest user decodes its own signal (i.e., s_1) with the following SINR:

$$\text{SINR}_1 = \frac{|h_1|^2 \alpha_1 p}{\sigma_1^2}. \quad (2.4)$$

On the other hand, the weakest user decodes its own signal by treating the signal intended for the strongest user (i.e., UE₁) as interference with SINR defined as,

$$\text{SINR}_2^{(2)} = \frac{|h_2|^2 \alpha_2 p}{|h_2|^2 \alpha_1 p + \sigma_2^2}. \quad (2.5)$$

Due to the fact that the signal of the weakest user will be decoded at both users, the SINR of decoding this signal is defined as [38]

$$\text{SINR}_2 = \min\{\text{SINR}_2^{(1)}, \text{SINR}_2^{(2)}\} = \text{SINR}_2^{(2)}, \quad (2.6)$$

the above equation holds true always when $\sigma_2^2 = \sigma_1^2$. The available rate at the UE_{*i*} $\forall i \in \{1, 2\}$ with this NOMA transmission can be defined as

$$R_i^{\text{NOMA}} = \log_2(1 + \text{SINR}_i), \quad i = 1, 2. \quad (2.7)$$

Next, the OMA transmission scenario, namely OFDMA, is presented. The available bandwidth, W , is divided between the two users, such that W_1 is assigned to UE₁, whereas W_2 is utilized to serve UE₂, where $W_1 + W_2 = 1$. Hence, the achieved rate at each user with this OFDMA transmission can be expressed as

$$R_i^{\text{OMA}} = W_i \log_2 \left(1 + \frac{|h_i|^2 \alpha_i p}{W_i \sigma_i^2} \right), \quad i = 1, 2. \quad (2.8)$$

To illustrate the performance improvement achieved with NOMA against OFDMA approach, the following special scenario is considered. In particular, W is equally divided between UE₁ and UE₂ (i.e., $W_1 = W_2 = 0.5$ Hz). In addition, the noise power is assumed to be one for both users (i.e., $\sigma_2^2 = \sigma_1^2 = 1$). With these assumptions, the achieved sum rate for the both scenarios can be defined as

$$R^{\text{NOMA}} = \log_2(1 + \alpha_1 p |h_1|^2) + \log_2 \left(1 + \frac{\alpha_2 p |h_2|^2}{\alpha_1 p |h_2|^2 + 1} \right) \quad (2.9)$$

and

$$R^{\text{OMA}} = 0.5 \log_2(1 + 2\alpha_1 p |h_1|^2) + 0.5 \log_2(1 + 2\alpha_2 p |h_2|^2) \quad (2.10)$$

With the assumption that $|h_1|^2 = 10|h_2|^2 = 10$, and transmit power being one (i.e., $p = 1$ W), the achieved sum rates for these two scenarios are presented in Fig. 2.2. As it can be seen, the SISO-NOMA outperforms this SISO-OMA in terms of achieved sum rate.

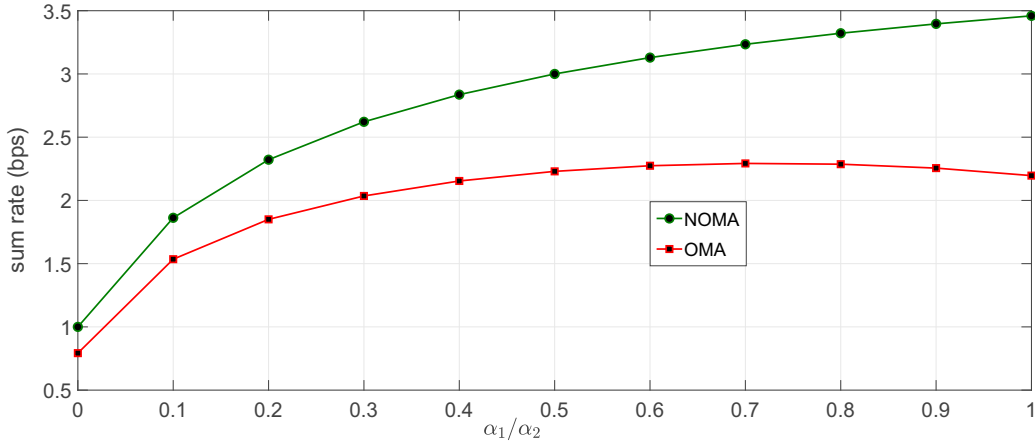


Fig. 2.2 Achievable sum-rate for SISO-NOMA and SISO-OMA scenarios.

Now, a multi-user SISO-NOMA system with K users is considered, at which it is assumed that UE_1 is the strongest user. In this system, UE_i should be able to successively decode and subtract the signals intended for the weaker users $UE_{i+1}, UE_{i+2}, \dots, UE_K$ from the received signal, prior to decode its signal. Therefore, the achievable rate at UE_i for this multi-user SISO-NOMA system can be formulated as [43]

$$R_i^{NOMA} = W \log_2 \left(1 + \frac{|h_i|^2 \alpha_i p}{\sum_{j=1}^{i-1} |h_i|^2 \alpha_j p + W \sigma_i^2} \right). \quad (2.11)$$

The superior performance of NOMA scheme against the conventional OMA scheme in terms of achievable sum rates has been mathematically proven in [43].

2.1.3 Advantages of NOMA

NOMA is expected to play a crucial role in the deployment of future wireless networks due to its different potential benefits. The key advantages that can be offered by NOMA are summarized as follows:

- **Fairness:** The practical implementation of SIC requires to assign more transmit power to the users with poorer channel conditions (i.e., weaker users) [8], [1]. As a result, the performance of these weaker users are expected to be improved considerably in contrast to the conventional resource allocation schemes, which achieves a better user fairness.

- **Compatibility:** From theoretical perspective, NOMA can be easily integrated with existing communication technologies including multiple antenna and OMA techniques. Hence, the schemes developed by combining NOMA with other techniques can offer additional degrees of freedom [44], [45], as evidenced by the recent development of NOMA as an “add-on” technique [1].
- **Massive connectivity:** As multiple users can be served within the same RB by employing power-domain SC, NOMA has the potential capability to offer massive connectivity in proliferation of IoTs. Furthermore, the massive connectivity offered by NOMA improves inefficient utilization of spectral resources in the conventional OMA techniques.
- **Latency:** The potential capability of NOMA to serve multiple users in the same RB meets the demanding delay requirements in ultra reliability low latency communications in future wireless networks [4]. As such, unlike TDMA approaches, multiple users can be simultaneously served in the same time block, which significantly reduces the latency.

2.2 NOMA with other Techniques

To introduce additional degrees of freedom, NOMA has been recently integrated with different technologies such as cognitive radio (CR) [46], mm-wave communication technology [47], [48], multiple antennas techniques [45], [49], and conventional OMA techniques. In this thesis, the combinations of NOMA with spatial multiplexing as well as OMA approaches are explored in details.

2.2.1 NOMA with Multiple-Antenna Techniques

Over the last two decades, multiple antenna techniques have been extensively investigated due to their additional degrees of freedom offered by spatial multiplexing to further improve the overall system performance. This can be achieved by utilizing multiple antennas at the transmitters and/or receivers [50], [51], [52]. In particular, the space division multiple access (SDMA) offered by multiple antennas can be efficiently utilized to multiplex the signals intended for different users within the same RB [53].

Different SDMA schemes have been considered in the literature by employing multiple antennas either at the transmitters or the receivers, such as MISO and MIMO systems. In fact, the combination of NOMA with SDMA can provide more advantages through jointly utilizing both spatial and power domains to meet the demanding requirements in

future wireless networks compared to the conventional stand alone SDMA techniques. In particular, SDMA-NOMA schemes can be classified into two main categories namely, the beamformer-based SDMA-NOMA schemes, and the cluster-based SDMA-NOMA schemes. As this thesis mainly focuses on the developments of the schemes that combine NOMA with MISO, the discussions are narrowed only to MISO-NOMA systems. Note that the multiple access techniques without NOMA are referred as conventional multiple antenna techniques throughout this thesis.

- Beamformer-based MISO-NOMA

Firstly, it is worth to mention that beamforming is a process in which the signal is steered or guided into a certain direction [24]. With multiple antennas at transmitter and/or receiver, the beamforming techniques can be implemented through either by physically steering antennas toward the target [25], or alternatively, steering the signal digitally to the intended user. In particular, the digital beamforming is achieved through designing a complex weights, as such, this vector includes both, the power allocation and the signal direction. In conventional MISO systems, the beamforming vectors are designed to optimize one of the well-known performance metrics, namely P-Min design [54], SRM [55], or GEE-Max design [56]. Note that these designs will be discussed later in this thesis. Similar to the conventional MISO designs, the beamformer-based MISO-NOMA schemes assign an individual beamforming vector to serve each user in the system, as shown in Fig.2.3 (a). For the sake of notation simplicity, the beamformer-based MISO-NOMA system is referred to as MISO-NOMA throughout this thesis.

- Cluster-based MISO-NOMA

Unlike MISO-NOMA (i.e., beamformer-based MISO-NOMA), the users in the cluster-based MISO-NOMA scheme are divided into a number of groups, with a single beamforming vector assigned to serve each cluster, whereas users within each cluster are given access based on NOMA, as shown in Fig.2.3 (b). In particular, users from each cluster suffer from two types of interferences: 1) Inter-cluster interference (ICI), which is produced by another clusters' interference [57], and 2) Intra-cluster interference, that is produced from the users inside each cluster [58]. The main advantage of the cluster-based MISO-NOMA scheme over the beamformer-based MISO-NOMA one is that grouping users significantly reduces the computational complexity associated with employing SIC among all users in the system. As a result, this cluster-based MISO-NOMA can play a crucial role in ultra-dense networks due to its potential capability to support large number of users. However, there are different

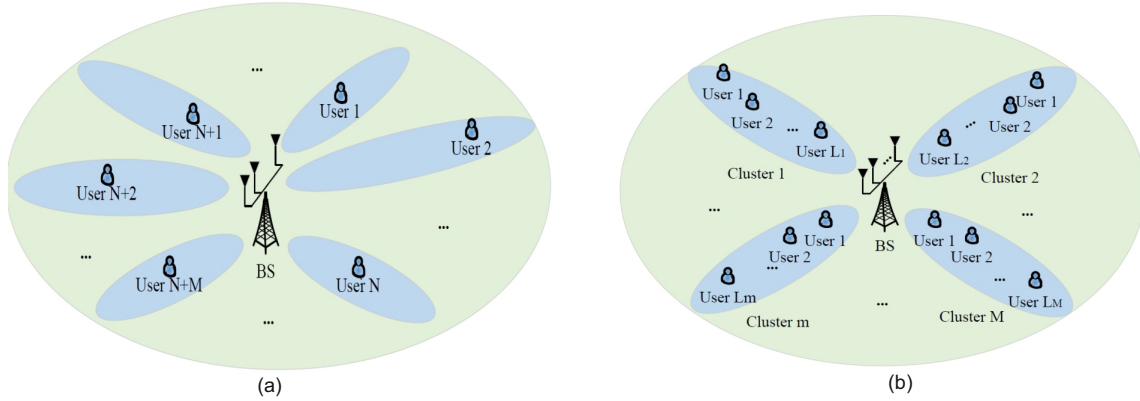


Fig. 2.3 Hybrid MISO-NOMA configurations: (a) Beamformer-based MISO-NOMA scheme, (b) Cluster-based MISO-NOMA system scheme [1].

challenges associated with cluster-based MISO-NOMA, which are provided in the following discussion:

- Clustering algorithms: Choosing an appropriate grouping strategy has a direct impact on the performance of the cluster-based MISO-NOMA scheme, as such the optimal performance can be achieved through determining the optimal clustering sets. However, these optimal clusters can be only determined through exhaustive search [57], which has a very high computational complexity, especially, in ultra-dense networks. To overcome the high complexity associated with the exhaustive search, multiple sub-optimal clustering algorithms have been introduced in the literature [57], [58], [59]. In summary, these clustering algorithms take into account different factors when performing the clustering, including the target of clustering, the number of users, and the channel conditions of the users [58].
- Beamforming design: It is important that the base station determines which channel of the users within each cluster that has to be used to design the beamforming vector. Conventionally, strongest users in the clusters are selected to design beamforming vectors [57], [59]. In addition, different designs can be developed based on the system circumstances and conditions. For example, if the number of clusters is less or equal to the number of transmit antennas at the base station, then, the well-known zero-forcing beamforming (ZFBBF) can be exploited to completely eliminate ICI between clusters.

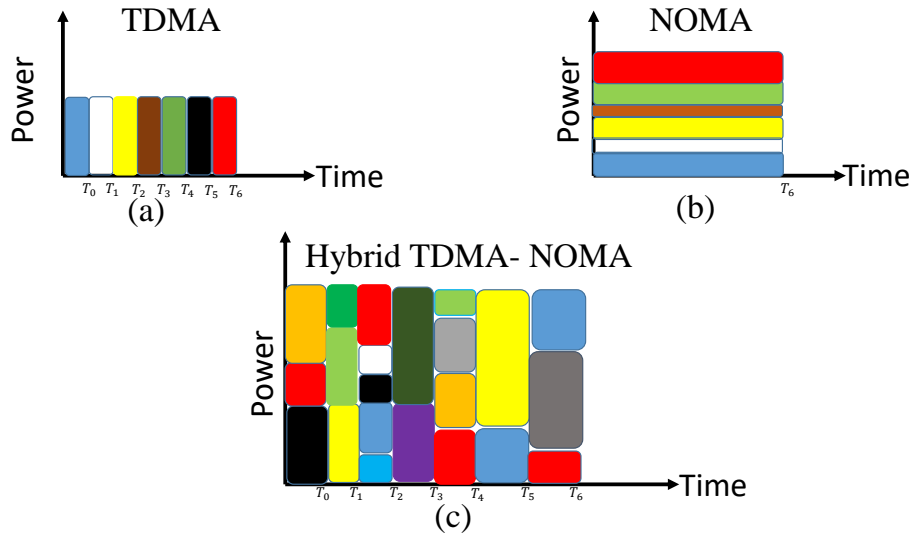


Fig. 2.4 An illustration of different MA approaches: (a) TDMA approach, (b) NOMA approach, (c) Hybrid TDMA-NOMA approach.

- Power allocation technique: As the users within each cluster are served based on NOMA approach, the optimal power allocation should be determined to achieve the best performance, however it introduces a high complexity in the system, which is unaffordable. Hence, to reduce the complexity associated with evaluating the optimal power allocation, different sub-optimal power allocation techniques have been proposed in the literature, such as fractional transmit power control (FTPC), in which the allocated power for each user is inversely proportional to the corresponding channel condition [57].

2.2.2 NOMA with OMA Techniques

In a hybrid OMA-NOMA scheme, users are divided into multiple groups, as such the available RB for transmission (i.e., time or bandwidth) is assigned to serve a group of users. Furthermore, the users in the corresponding group are served based on power-domain NOMA technique [1]. In particular, there are different advantages from such hybrid systems, including the higher RB utilization, and the overhead reduction due to SIC at all users [60]. Different hybrid OMA-NOMA approaches have been considered in the literature, such as OFDMA-NOMA and TDMA-NOMA approaches [39]. In particular, similar to cluster-based MISO-NOMA, different issues have to be considered in the context of hybrid OMA-NOMA

systems, including optimal grouping sets and power allocation techniques within each group [60]. To end with, Fig. 2.4 is presented to illustrate the capabilities of the hybrid TDMA-NOMA approach compared to other MA techniques. As seen, Fig. 2.4 (c) shows that hybrid TDMA-NOMA is capable of serving a larger number of users compared to TDMA and NOMA approaches shown in Figs. 2.4 (a) and 2.4 (b), respectively.

2.3 Energy-Efficient Strategies

With the progressive adoption of 5G and beyond wireless networks, one of the main goals is to achieve a higher spectral efficiency compared to the ones available in contemporary wireless networks. Higher spectral efficiency will enable applications that demand different high data rates and will provide massive connectivity for IoT [2]. With limited available wireless resources, including radio spectrum and transmit power, meeting higher data requirements will only be possible through novel techniques and efficient resource utilizations [61]. Furthermore, the transmit power required to meet the corresponding throughput requirements with the conventional approaches will be significantly high.

The increased power consumption will subsequently induce further issues such as extra CO₂ emission and associated climate changes [56]. In addition, a corresponding increase in the energy bills is also expected, where these bills occupy 30% of the total operational cost of a mobile network operator [61]. With the explosive growth of number of connected devices, and hence increasing the consumed energy, the service providers cannot ignore the expected increase on their operational costs. By considering the fact that NOMA is expected to be employed in future wireless networks including ultra-dense networks, and hence to cope with the problems associated with the explosive growth in power consumption, different energy-efficient strategies have been proposed and investigated. Such as employing green energy resources to feed wireless networks [61], allocating the resources to maximize EE [9], and employing the novel EH technique, namely SWIPT [62].

2.3.1 Energy-Efficient-Resource Allocation Techniques

Recently, energy-efficient-resource allocation is considered as one of the key avenues for addressing the problems associated with the increase in power consumption in the development of future wireless systems [61]. The energy-efficient designs based on the GEE performance metric have become one of the key requirements in the development of future wireless systems. These designs take the EE performance metric into account rather than the achievable rate or transmission power metrics. The GEE performance metric is defined as the

ratio between the achievable sum-rate and total power consumption [9], [56]. Furthermore, the GEE design can be viewed as a multi-objective design problem, which aims to simultaneously optimize two conflicting performance metrics, namely, the sum rate and the required power to achieve this sum rate [9]. In particular, this performance metric efficiently utilizes the available transmit power while striking a good balance between the achievable sum rate and power consumption. Finally, unlike the conventional SRM and P-Min designs, the GEE design incorporates the power losses at the base station as part of the design process [56].

Achieving the massive connectivity offered by NOMA requires a huge amount of transmit power which would only be possible by considering energy efficient designs [29], [12]. In spite the optimal system-level EE achieved through GEE-Max, the individual EE of the weaker users in the system might be degraded. Hence, energy-efficient fairness resource allocation techniques can be considered, such as, PF and MMEE designs [56].

2.3.2 Simultaneous Wireless Power and Information Transfer

In SWIPT, the receiver has the capability to simultaneously harvest energy and decode information [63]. In particular, this could be accomplished by splitting the received radio frequency (RF) signal through either time splitting or power splitting techniques [64]. Despite of the low complexity of the former, this requires a better synchronization between the receiver and the transmitter to precisely perform the splitting [63], and thus, the latter is typically more desirable. In fact, SWIPT is expected to contribute in feeding the power-hungry users, especially in ultra-dense sensor networks, where hundreds of unreachable sensors seek power to extend their life-time [63]. In addition, SWIPT attracts an extraordinary attention in the context of NOMA, as users in NOMA can employ the enormous co-channel interferences by considering the fact that NOMA users share the same time-frequency resources [65].

2.4 Literature Review

Recently, different NOMA techniques have been proposed to cultivate the potential benefits of NOMA in 5G and beyond wireless networks. The fundamental concepts of NOMA are presented in [12], [29], [8], where the advantages of NOMA over classical OMA techniques are provided. The combination of NOMA with multiple antennas techniques was firstly demonstrated in [39] and [45]. In addition, different design criteria have been proposed for the beamformer-based MISO-NOMA schemes. For example, the authors in [49] evaluated the beamforming vectors that minimize the transmit power under QoS constraints for a

two-user MISO-NOMA system. This P-Min problem was solved with perfect channel state information (CSI) assumption at the base station. However, as it is difficult to obtain the perfect CSI at the base station, the work in [49] was extended by [66], where P-Min design is considered for multi-user MISO-NOMA with imperfect CSI. Different relaxations have been exploited to handle the non-convexity of this design, such as semi-definite programming (SDP) approach. Due to the importance of achieved sum rate in 5G and beyond wireless networks, the authors in [67] considered the SRM design for multi-user MISO-NOMA system. As such the minorization maximization algorithm was exploited to handle the non-convexity of the problem through employing the SCA algorithm. Then, the achieved sum rate of the MISO-NOMA system was compared with that of the conventional MISO beamforming design, namely ZFBF, and it was shown that the MISO-NOMA system outperforms ZFBF. However, the SRM design in [67] does not consider the achieved rates of individual users, which might degrade the rates of the users with weaker channel conditions. To overcome this issue, a fairness design in terms of the achieved rates on individual users was considered in [66], in which the minimum achievable rate of the users was maximized for a given total power constraint. In addition, a fairness power allocation technique for multi-user (MU) SISO-NOMA system was considered in [68] through considering weighted-sum rate maximization (WSRM) design. In this WSRM design, the rates of individuals are assigned with different user weights to increase the priorities of the weaker users' rates.

On the other hand, the cluster-based MISO-NOMA schemes have been also investigated in the literature to reduce the complexity of SIC at the receiver ends. For example, the authors in [57] considered the SRM problem for cluster-based MISO-NOMA system, in which each two users with higher difference channel gain are grouped in a cluster. The available power at the base station is divided equally among the clusters, whereas the power assigned for each cluster is further divided among the users based on FTFC. In addition, the beamforming vectors that maximize the sum rate are evaluated through handling the non-convexity of the optimization problem using the difference of convex (DC) technique. Similar to [57], the authors in [58] investigated the cluster-based MISO-NOMA system. However, the beamforming vectors are designed based on the ZFBF approach. Another cluster-based MIMO-NOMA designs are considered in [59], [69]. Furthermore, a hybrid OMA-NOMA approach has been considered in [60], in which a single-antenna base station assigns orthogonal subchannels to serve multiple users, whereas users sharing the same subchannel are served based on NOMA. With assumption of perfect CSI at base station, the authors investigated the energy-efficient subchannel assignment and power allocations within

each subchannel.

The fundamental concepts and future challenges of SWIPT have been provided in different survey articles, including [70], [62], [64], [63], [71]. Furthermore, by considering the application of SWIPT with multiple antenna techniques, different designs have been proposed in the literature. For example, authors in [72] considered the EH capabilities of conventional MU-MISO system, as such each user either harvests energy or decodes information. The target was to design the beamforming vectors that maximize the harvested energy subject to achieve QoS constraints at each user. In addition, authors in [73] considered the same system model of [72], whereas the target was to maximize the minimum harvested energy with the assumption of imperfect CSI. Unlike the assumptions considered in [73] and [72], the authors in [74] and [75] assumed that each user has a power splitter, as such it simultaneously harvests power and decodes information. In particular, the minimum power required to achieve QoS requirements was evaluated in [74] through jointly design the beamforming vectors and the power splitting ratios at each user. Furthermore, the authors in [75] jointly designed the beamforming vectors and the power splitting ratio that maximize the product of rates considering the EH capability at each user. Considering the recent development of NOMA, and by taking into account that users share the same RB, the combination of NOMA and SWIPT has attracted a huge interest [76], [77]. In particular, this combination is classified into two main categories, which are cooperative and non-cooperative SWIPT-NOMA transmissions [32], [65], [78], [79].

2.5 Summary

In this chapter, the basic concepts of NOMA, namely SIC and SC, are presented. In addition, the key features of NOMA compared to the conventional OMA approaches are provided. Furthermore, different SDMA-NOMA approaches are presented and demonstrated. On the other hand, a brief overview about hybrid OMA-NOMA techniques are introduced. Then, different energy-efficient strategies, namely energy-efficient resource allocation techniques and SWIPT are demonstrated. Finally, recent research directions for different NOMA approaches, including MISO-NOMA, OMA-NOMA, and SWIPT techniques, are briefly reviewed.

Chapter 3

Resource Allocations: Performance Metrics and Optimization Techniques

In this chapter, different resource allocation techniques that have been widely developed in the literature to efficiently utilize the available resources are presented. The motivations and the corresponding practical scenarios behind those techniques are discussed. Then, several optimization frameworks that have been exploited to realize low complexity solutions in these resource allocation techniques are investigated. In particular, two main frameworks are introduced to solve resource allocation problem with single and multiple objective functions.

3.1 Resource Allocation Techniques

Over the last few decades, allocating available resources among served users in wireless networks has attracted a great deal of interest due to its various benefits [80], [81]. The communication resources, such as time slots, frequency slots, or power levels, are allocated with an objective of optimizing a certain performance metric. In fact, different performance metrics have been defined in the literature motivated by the unprecedented requirements of wireless networks. However, three of the performance metrics, namely transmit power, achieved sum rate, and EE have recently attracted a considerable attention, as these performance metrics have direct impact on 5G and beyond wireless networks. In particular, selecting a suitable performance metric depends on several factors, including the requirements of users, the service providers' operational circumstances, the channel conditions, and the other emerging requirements of future wireless networks [81]. In the following, the resource allocation techniques that have been considered throughout this thesis are introduced briefly.

3.1.1 Power Minimization Techniques

In emergency scenarios, i.e., earthquakes and flooding, service providers aim to keep their customers connected with minimum transmit power consumptions while satisfying pre-defined QoS requirements. In particular, different QoS requirements, including minimum rate and minimum energy harvesting requirements at each user, can be fulfilled by developing this resource allocation technique, which is referred in the literature as P-Min technique. The fundamental concept of the P-Min technique is to minimize the transmit power consumption under different QoS constraints at each user. This P-Min technique has been considered for different wireless networks in the literature [54], [49], [66]. However, a major drawback of this resource allocation technique is that it cannot meet the demanding rate requirements, which motivates to consider other rate-aware resource allocation techniques.

3.1.2 Rate-Aware Techniques

The performance metrics in terms of throughput are achieved sum rate and rate at each user, these metrics significantly contribute towards the key requirements of spectral efficiency in 5G and beyond wireless networks [4]. In fact, to adapt these demanding rate requirements, several rate-aware resource allocation techniques have been proposed for different wireless networks in the literature, such as SRM and WSRM techniques. In SRM technique, the sum rate is maximized with the available power constraint at the transmitter [67], [82]. In particular, this SRM technique does not take into account the achieved rate of individual users, which might open up naturally the fairness issues among the users, as such the users with weaker channel conditions might achieve unreasonable performance with very lower rates. Furthermore, this fairness problem cannot be ignored, especially in future wireless networks as providing uniform user experience anytime and anywhere is one of the key driving forces in the development of future wireless technologies [11]. Hence, alternative fairness-rate-aware resource allocation techniques have been developed to overcome the issues associated with the SRM technique. For example, the WSRM technique [68], [55], which aims to maximize the sum of weighted achieved users' rates by assigning higher weights to the weaker users. As a result, the fairness between users in such resource allocation technique is enhanced as the rates of weaker users are expected to be improved compared to the SRM technique [83]. However, optimal fairness among users in terms of the individual rates can be only achieved by maximizing the minimum user's rate. In such a maximizing minimum rate (MMR) technique, equal rates will be obtained for all users while satisfying the power constraints [84]. It is worthy mentioning that the selection between these rate-aware techniques is determined based on the requirements of both users and service provider.

3.1.3 Energy Efficiency Aware Techniques

The rate-aware resource allocation techniques, such as SRM and WSRM, consider only the rate requirements of a system while consuming all available power at base station. In fact, with the explosive growth in the number of connected devices in 5G and beyond wireless networks, these rate-aware techniques degrade the EE performance of wireless networks [9], which will subsequently introduce further issues such as extra CO₂ emission and associated climate changes. Therefore, several EE-aware techniques have been developed in the literature as these techniques have the potential capabilities to strike a good balance between the conflicting design metrics, namely the achieved sum rate and the power consumption [9], [61]. For example, GEE-Max technique maximizes the global EE of network without considering the performance of the individuals [9]. Furthermore, PF and MMEE techniques are considered as fairness-EE-aware techniques. More details on these EE-aware techniques are presented throughout this thesis.

3.1.4 Multi-Performance metric Techniques

Inspired by the fact that 5G and beyond wireless networks should be able to fulfill diverse requirements of envisioned applications and services, optimizing multi-performance metric simultaneously arises as a promising solution to meet those unprecedented requirements. In particular, this can be only achieved by developing novel resource allocation techniques that enable base station to take these multi-performance metric into account [85], [86]. Furthermore, with such resource allocation techniques, base station has also a potential capability to strike a good balance between conflicting performance metrics. In this thesis, multi-performance resource allocation techniques are proposed with different constraints: SE-EE trade-off technique and SRM-fairness trade-off technique. Fig. 3.1 illustrates the key resource allocation techniques that are investigated throughout this thesis for NOMA systems.

The aforementioned resource allocation techniques require mathematical representations for developing and solving different classes of optimization problems. In particular, these optimization problems can be mainly classified into two main groups based on the nature of their objective functions, namely SOO and MOO problems.

3.2 Single-Objective Optimization Problems

In SOO problems, such as SRM and GEE-Max resource allocation techniques, a single-performance metric (i.e., objective) is optimized under different constraints. The following

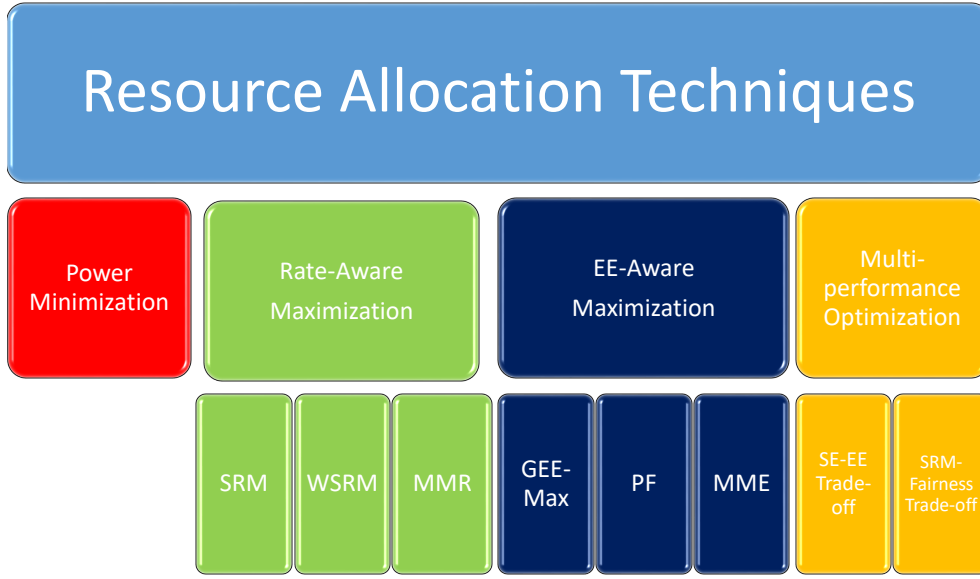


Fig. 3.1 Recent resource allocation techniques.

SOO framework is provided to further demonstrate the relationship between the resource allocation technique and the corresponding optimization problem:

$$\underset{\mathbf{x}}{\text{minimize}} \quad f_0(\mathbf{x}) \quad (3.1a)$$

$$\text{subject to} \quad g_i(\mathbf{x}) \geq 0, i = 1, \dots, K, \quad (3.1b)$$

$$h_j(\mathbf{x}) = 0, j = 1, \dots, N. \quad (3.1c)$$

Firstly, it is worth mentioning that the minimization framework in (3.1) can be transformed into a maximization framework by replacing the objective function by $-f_0(\mathbf{x})$. Furthermore, the vector $\mathbf{x} = [x_1, \dots, x_n]$ contains the optimization variables (i.e., the design parameters regarding the available resources) that need to be determined to allocate resources among users, such as, power allocations, time slots, or bandwidth allocations. In addition, the function $f_0(\mathbf{x})$ is the objective function, which can be sum rate, minimum user rate, EE, or any other performance metric. Finally, the functions $g_i(\mathbf{x})$ and $h_j(\mathbf{x})$ in the inequality and equality constraints, respectively, represent any constraints that define limitations of the available resources or users' requirements in the resource allocation techniques, such as QoS and available power constraints. In the SOO framework provided in (3.1), the resource allocation \mathbf{x}^* is considered to be the global optimal solution if and only if $f_0(\mathbf{x}^*) < f_0(\mathbf{x})$ for all feasible \mathbf{x} [87]. In particular, the global optimal solution can be determined straight forward if the optimization problem is convex in terms of \mathbf{x} [88]. To further understand

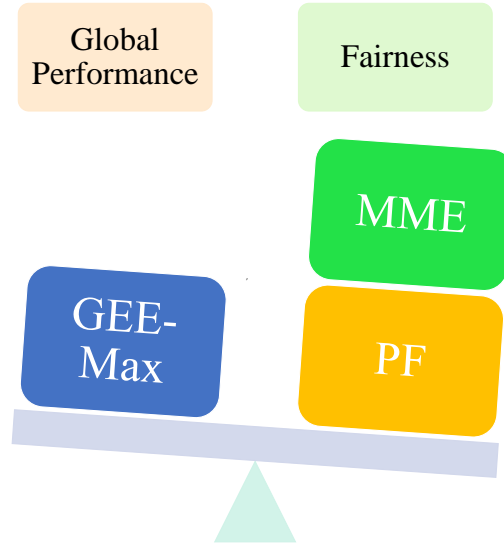


Fig. 3.2 Different EE-aware resource allocation techniques.

the convexity of the optimization problems, a brief overview of the convex optimization problems is introduced in the following subsection.

3.2.1 Convex Optimization Problems

The convexity of the optimization problem guarantees the optimality of the solution which can be determined straightforward by using available different convex optimization toolboxes. In particular, two conditions need to be satisfied for a problem to be a convex optimization problem in (3.1) [87]. Firstly, the objective function $f_0(\mathbf{x})$ should be a convex function, secondly, the domain of the inequality constraints should define a convex set and the equality constraint functions should be affine. The convexity can be defined as follows.

First, a set $\mathcal{S} \in \mathbb{R}^N$ is considered as a convex set if the following condition holds for $\mathbf{x}, \mathbf{y} \in \mathcal{S}$

$$\theta \mathbf{x} + (1 - \theta) \mathbf{y} \in \mathcal{S}, \forall \theta \in [0, 1]. \quad (3.2)$$

Furthermore, a set \mathcal{C} is a convex cone for each $\mathbf{x}, \mathbf{y} \in \mathcal{C}$ if this following condition is satisfied [87]

$$\theta_1 \mathbf{x} + \theta_2 \mathbf{y} \in \mathcal{S}, \forall \theta_1 \geq 0, \forall \theta_2 \geq 0. \quad (3.3)$$

In particular, various convex cones can be defined in engineering applications, however, the second-order cone (SOC) will be widely employed in this thesis, where \mathcal{C} is defined as SOC if $t \geq \|\mathbf{x}\| \forall (t, \mathbf{x}) \in \mathcal{C}$ [87]. The function f is classified as a convex if $\mathbf{dom} f$ is convex

set and if for all $\mathbf{x}, \mathbf{y} \in \mathbf{dom} f$ [87]

$$f(\theta\mathbf{x} + (1 - \theta)\mathbf{y}) \leq \theta f(\mathbf{x}) + (1 - \theta)f(\mathbf{y}). \quad (3.4)$$

In other words, a function is a convex if the line between any two points in this function stands above the graph of it. Furthermore, if f is differentiable, then its convexity can be examined by verifying the following inequity:

$$f(\mathbf{y}) \geq f(\mathbf{x}) + \nabla f(\mathbf{x})^T(\mathbf{y} - \mathbf{x}), \quad (3.5)$$

or

$$\nabla^2 f(\mathbf{x}) \succeq 0. \quad (3.6)$$

Note that the concavity of a function f can be examined by appropriately changing the inequalities in (3.4), (3.5), and (3.6). The following example is provided to investigate the convexity of different simple functions. Let $h_1(x) = x \log x$ and $h_2(x) = \log x$, $\forall x > 0$, the convexity/ concavity of these functions can be examined by evaluating the second derivative for each function. Starting with $h_1(x)$, the second derivative can be defined as $\nabla^2 h_1(x) = \frac{1}{x}$, which is always positive within the positive domain of x (i.e., $x > 0$), this simple verification shows that $h_1(x)$ is convex function in this positive domain. Furthermore, the second derivative of $h_2(x)$ can be defined as $\nabla^2 h_2(x) = -\frac{1}{x^2}$, which is always less than zero. Hence, $h_2(x)$ is a concave function.

In particular, there are several features associated with formulating convex optimization problems. First, convex optimization problems can be analytically solved through several well-know algorithms such as interior-point algorithm with low computational complexity [89]. In addition, there are different softwares and toolboxes which are available to efficiently solve the convex optimization problems, including CVX software [90] and Yalmip [91]. Secondly, the solution of convex optimization problem ensures that every local optimal solution is also a global one [87]. Based on these key benefits, formulating resource allocation techniques as convex optimization problems is very useful to find the optimal solution with low complex algorithms.

3.2.2 Non-Convex Optimization Problems

The optimization problems that do not fulfill the definition of a convex problem provided in (3.1) will be classified as non-convex optimization problems. In general, it is difficult to determine the optimal solution of a non-convex problem and the available convex optimization

software and toolboxes cannot be directly exploited to determine the solutions of such non-convex problems. This introduces additional complexity to the solutions. To overcome those non-convexity issues, different mathematical techniques have been considered in the literature. For example, these techniques include SCA [92], convex-concave approach (CCA)[93], and majorization minimization algorithm (MMA) [94]. Furthermore, Dinkelbach's algorithm [95] has been proposed to efficiently handle the optimization problems with fractional objective functions. These techniques are used in the proposed resource allocation techniques in this thesis.

3.3 Multi-Objective Optimization

Multi-performance metric techniques can be handled through developing MOO problems. In these MOO problems, unlike the conventional SOO problems, the aim is to optimize multi-objective functions simultaneously. Further details on MOO problems are provided in the following subsection.

3.3.1 MOO Framework

In general, MOO problems cannot be solved directly using the conventional optimization approaches due to their structures. Hence, a brief introduction on the procedures of dealing with such MOO problems are provided in this section. Firstly, a general MOO framework is defined as follows:

$$\underset{\mathbf{x}}{\text{minimize}} \quad f_1(\mathbf{x}), f_2(\mathbf{x}), \dots, f_I(\mathbf{x}) \quad (3.7a)$$

$$\text{subject to} \quad g_i(\mathbf{x}) \geq 0, i = 1, \dots, K, \quad (3.7b)$$

$$h_j(\mathbf{x}) = 0, j = 1, \dots, N. \quad (3.7c)$$

Note that the MOO problem in (3.7) contains I objective functions. In general, $\{f_i\}_{i=1}^I$ represent conflicting performance metrics which could be sum rate, transmit power, and fairness. Therefore, there is no unique global optimal solution that can minimize all objective functions simultaneously [96]. Therefore, designers look for the best trade-off solutions, which are referred as Pareto-optimal solutions [96], [97]. The definition of Pareto-optimality is provided below with the assumption that the vector $\mathbf{f}(\mathbf{x})$ is defined as $\mathbf{f}(\mathbf{x}) = [f_1(\mathbf{x}), f_2(\mathbf{x}), \dots, f_I(\mathbf{x})]$.

Definition 1. [97], [98] A feasible solution \mathbf{x}^* is defined as a Pareto-optimal solution if there exists no other feasible solution \mathbf{x}^+ such that $\mathbf{f}(\mathbf{x}^+) \preceq \mathbf{f}(\mathbf{x}^*)$. The set of all Pareto-

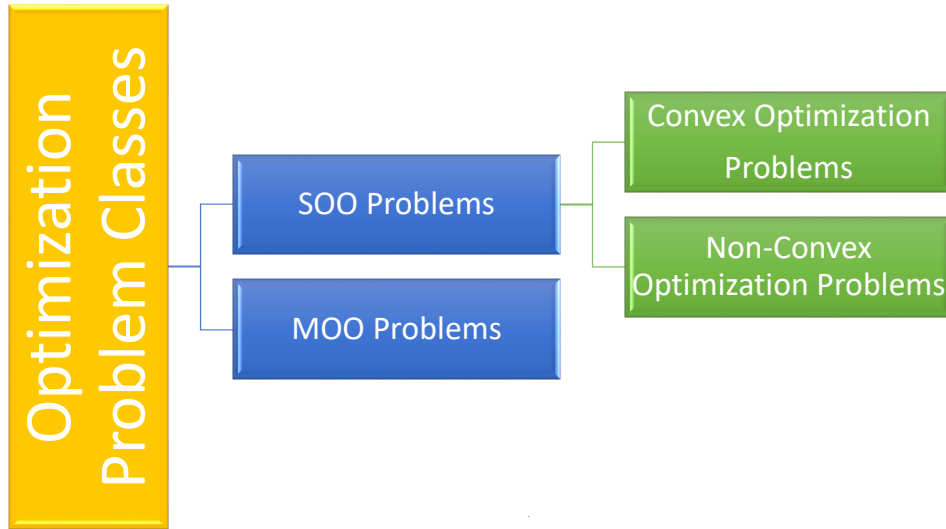


Fig. 3.3 Illustration of optimization problem types.

optimal solutions are collectively defined as the Pareto front in the literature [97].

Obviously, finding the Pareto-optimal solutions for MOO framework is not a straightforward task. Therefore, a brief review is presented below to handle any MOO problem, including the framework defined in (3.7). In particular, the procedure consists of three steps; firstly, weights articulation, then SOO transformation, and finally solving the SOO problem via the conventional approaches. The details of these steps are provided in the following discussions.

- Weights articulation:** It is obvious that the solutions of the MOO framework in (3.7) depend directly on the relative priority (importance) of each objective in the overall problem. Therefore, it is crucial to determine the priority (i.e., weight) of each objective and this process is referred as weights articulation [99]. In particular, two articulation schemes have been defined in the literature: priori-articulations and posteriori-articulations [99]. With the priori-articulation scheme, the relative importance of the i^{th} objective (α_i) is determined prior to solving the problem such that $\sum_{i=1}^I \alpha_i = 1$. On the other hand, with the posteriori-articulations, a solution can be picked up from the set of Pareto-optimal solutions [97]. In other words, the designer can determine the importance of the objectives once he has full information on the all available solutions.

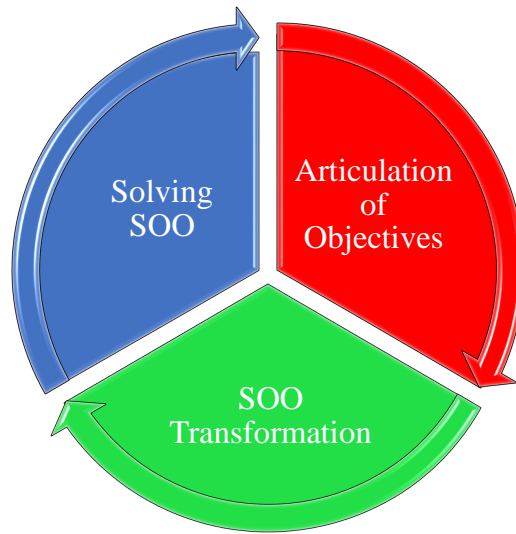


Fig. 3.4 Illustration of MOO solving process.

- **SOO transformation:** Due to the complexity associated with handling the multiple objective function in (3.7), converting it into a single-objective function is crucial step to make the problem tractable, and hence solvable. This can be achieved by replacing the multi-objective function by a single-objective function which is referred as utility function [96]. In particular, many utility functions have been considered in the literature, for example, weighted-sum function, weighted-product function, and max-min function [97], [98]. It is worthy pointing out that the multi-objective problems in (3.7) consist of different objective functions with different units and ranges. Hence, these objectives have to be scaled (i.e., normalized) prior to collecting them together in a utility function.
- **Solving the SOO problem:** As the MOO problem is formulated into a SOO form, the classical optimization techniques can be now utilized to efficiently solve the SOO problem. The steps involved with these solution approaches are summarized in Fig. 3.4.

3.4 General Discussions

When dealing with different types of optimization problems, several considerations need to be taken into account. These considerations mainly depend on a number of factors, including the convexity of the optimization problem and the developed solution approach. Therefore, a

brief overview on these considerations are provided in the following discussion. However, further details on these issues can be found in the following chapters of this thesis.

- **Feasibility Check:** Generally, several constraints are included in the formulations of the original optimization problems and examining the feasibility of the problem is a crucial step that needs to be carried out prior to solving it. In fact, in some scenarios, an optimization problem cannot be solved due to infeasibility of the constraints, i.e., there no solution exists to satisfy those constraints and therefore the original problem can be classified as an infeasible problem. For example, with minimum rate and power budget constraints at base station, a GEE-Max problem might become infeasible when these minimum rate requirements cannot be satisfied under the available power budget. Therefore, it is important to examine the feasibility of the optimization problem prior to devising a solution approach.
- **Optimality Check:** Unlike the convex optimization problems, different approximations and relaxations are exploited to solve non-convex optimization problems. Hence, to validate the performance of the obtained solutions, an optimality check needs to be carried out, in which, the solutions are determined whether they are optimal or not.
- **Convergence Check:** When exploiting SCA technique, optimization problems are solved via iterative algorithms. Hence, those iterative algorithms need be inspected whether they converge to the solution within a finite number of iterations or not. It is worth pointing out that the convergence of the iterative algorithms depends on a number of different factors, including the nature of the approximated functions and selection criterion of initial conditions.

3.5 Summary

In this chapter, different performance metrics and the corresponding resource allocation techniques to efficiently optimize these metrics are presented. Furthermore, two classes of optimization problems are discussed: SOO and MOO optimization problems. Then, a brief review on the recent techniques that have been utilized to handle these types of optimization problems is provided. Finally, general discussions on solving any types of optimization problems are discussed.

Chapter 4

Energy-Efficient Beamforming Designs

In this chapter, different EE-aware beamforming designs are developed for MISO-NOMA system. First, GEE-Max design is proposed, for which the target is to maximize the overall EE of the system. Two algorithms are developed to handle the non-convexity of this design, namely SCA and Dinkelbach's algorithm. Then, to overcome the unfairness associated with the GEE-Max design, two energy-efficient fairness beamforming designs are considered, namely PF and MMEE designs. The performance evaluations of these designs are introduced through comparing them with other existing beamforming designs using simulation results.

4.1 System Model

In this chapter, a downlink transmission of a MISO-NOMA system is considered, as shown in Figure 4.1, where a single base station equipped with N antennas (i.e., $N > 1$) simultaneously transmits information to K single-antenna users. The signal transmitted from the base station can be expressed as

$$\mathbf{x} = \sum_{i=1}^K \mathbf{w}_i s_i, \quad (4.1)$$

where s_i and $\mathbf{w}_i \in \mathbb{C}^{N \times 1}$ denote the signal intended for the i^{th} user (U_i) and the corresponding beamforming vector, respectively, as such \mathbf{w}_i digitally steers s_i towards U_i . Furthermore, it is assumed that all s_i are uncorrelated and have the power of one, i.e., $E(|s_i|^2) = 1$. The received signal at U_i can be expressed as:

$$y_i = \mathbf{h}_i^H \mathbf{w}_i s_i + \sum_{j=1, j \neq i}^K \mathbf{h}_i^H \mathbf{w}_j s_j + n_i, \quad (4.2)$$

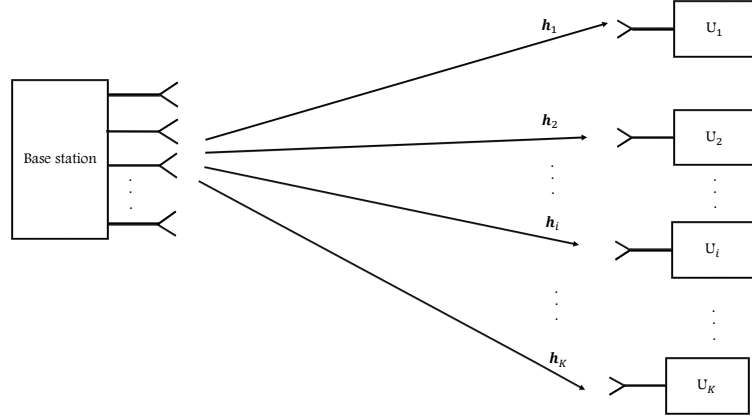


Fig. 4.1 A multiuser, MISO-NOMA system with a multi-antenna base station, and K -single antenna users.

where $\mathbf{h}_i \in \mathbb{C}^{N \times 1}$ represents the channel coefficients between the base station and U_i , and n_i represents the zero-mean AWGN with variance σ_i^2 . Furthermore, the channel vector \mathbf{h}_i is defined such that $\mathbf{h}_i = \sqrt{d_i^{-\kappa}} \mathbf{g}_i$, where κ , d_i and \mathbf{g}_i denote the path loss exponent, the distance between U_i and the base station, and the small scale fading, respectively. Throughout this thesis, it is assumed that the base station has the perfect CSI for each user.

In downlink NOMA, user ordering plays a crucial role in implementing the SIC at the users, and in fact, determines the overall performance of the system. However, determining the optimal user ordering is an NP-hard problem, which can only be solved through exhaustive search [12], [100]. Throughout this thesis, and for the reasons of simplicity, the users are ordered based on their respective channel strengths. As such, the first user (i.e., U_1) has the strongest channel strength while the channel strength of U_K has the weakest. In other words, the channels can equivalently be ordered as follows:

$$\|\mathbf{h}_1\|^2 \geq \|\mathbf{h}_2\|^2 \geq \dots \geq \|\mathbf{h}_K\|^2. \quad (4.3)$$

Based on this user ordering, to ensure that the power allocated to each user in the system is inversely proportional to its channel gain, and to successfully implement SIC at the stronger users [67], the following conditions should be satisfied with the beamforming design [101]:

$$|\mathbf{h}_i^H \mathbf{w}_K|^2 \geq \dots \geq |\mathbf{h}_i^H \mathbf{w}_1|^2, \forall i \in \mathcal{K} \triangleq \{1, \dots, K\}. \quad (4.4)$$

The constraint expressed in (4.4) is referred to as the SIC constraint in the rest of this thesis. The received signal at U_i after performing SIC is written as

$$y_i^* = \underbrace{\mathbf{h}_i^H \mathbf{w}_i s_i}_{\text{Intended signal}} + \underbrace{\sum_{j=1}^{i-1} \mathbf{h}_i^H \mathbf{w}_j s_j}_{\text{Interference}} + \underbrace{n_i}_{\text{Noise}}, \forall i \in \mathcal{K}. \quad (4.5)$$

Note that the interference caused by U_{i+1}, \dots, U_K is removed through SIC. Furthermore, U_k has the capability to decode the message of U_i ($k \leq i$) with SINR that can be written as

$$\text{SINR}_i^{(k)} = \frac{|\mathbf{h}_k^H \mathbf{w}_i|^2}{\sum_{j=1}^{i-1} |\mathbf{h}_k^H \mathbf{w}_j|^2 + \sigma_k^2}, \forall i \in \mathcal{K}, k \leq i. \quad (4.6)$$

Now, with the assumption that s_i is only decodable provided its SINR is higher than a threshold γ^{th} , this explicitly requires that decoding of s_i at other stronger users should be also higher than this threshold [67], i.e., $\text{SINR}_i^{(k)} \geq \gamma^{th}, \forall k = 1, 2, \dots, i$. Based on this argument, the definition of SINR_i should take into account the decoding of s_i at the stronger users in order to align with the basic principle of NOMA, namely SIC. Based on this requirement, the achievable SINR can be defined as follows:

$$\text{SINR}_i = \min(\text{SINR}_i^{(1)}, \text{SINR}_i^{(2)}, \dots, \text{SINR}_i^{(i)}), \forall i \in \mathcal{K}. \quad (4.7)$$

For notational simplicity, SINR_i and $\text{SINR}_i^{(k)}$ are denoted by γ_i and γ_i^k , respectively. Based on the above discussion, the achieved rate at U_i can be defined as [67]

$$R_i = \min(R_i^{(1)}, R_i^{(2)}, R_i^{(3)}, \dots, R_i^{(i)}), \forall i \in \mathcal{K}. \quad (4.8)$$

Note that $R_k^{(i)}$ is the rate of decoding s_i at U_k , and it is given as

$$R_i^{(k)} = B_w \log_2 \left(1 + \frac{|\mathbf{h}_k^H \mathbf{w}_i|^2}{\sum_{j=1}^{i-1} |\mathbf{h}_k^H \mathbf{w}_j|^2 + \sigma_k^2} \right), \forall i \in \mathcal{K}, k \leq i, \quad (4.9)$$

where B_w is the available bandwidth, set to be one in this analysis. For the MISO-NOMA system defined above, different energy-efficient designs are considered in the remaining of this chapter.

4.2 GEE-Max Design

The GEE of the system is defined as the ratio between the total achievable sum rate and the total power consumption [9],

$$GEE = \frac{\sum_{i=1}^K R_i}{P_{total}}, \quad (4.10)$$

where P_{total} stands for the total power consumption at the base station which accounts for both the transmit power allocated for data transmission and the power losses. As for the required transmit power (P_{tr}), it should satisfy the available power budget (P_{ava}) at the base station, which can be mathematically formulated as the following constraint:

$$P_{tr} = \sum_{i=1}^K \|\mathbf{w}_i\|_2^2 \leq P_{ava}. \quad (4.11)$$

On the other hand, the power losses at the base station are denoted by P_{loss} , and it accounts for both, the dynamic power (p_{dyn}) and static power (p_{sta}). The former one primarily (i.e., p_{dyn}) depends on the number of transmit antennas N , whereas the latter one is intended to account for the power required to maintain the system, such as through cooling and conditioning. Therefore, the total power losses can be defined as [9]

$$P_{loss} = p_{sta} + Np_{dyn}. \quad (4.12)$$

Based on that, the power consumption at the base station can be formulated as

$$P_{total} = \frac{1}{\epsilon_0} P_{tr} + P_{loss}, \quad (4.13)$$

where $0 < \epsilon_0 \leq 1$ is the efficiency of the power amplifier. With these definitions in place, the beamforming design that maximizes the GEE in the defined MISO-NOMA system with the K users can be formulated into the following optimization framework:

$$OP_1: \underset{\{\mathbf{w}_i\}_{i=1}^K}{\text{maximize}} \quad \frac{\sum_{i=1}^K \log(1 + \gamma_i)}{\frac{1}{\epsilon_0} \sum_{i=1}^K \|\mathbf{w}_i\|_2^2 + P_{loss}} \quad (4.14a)$$

$$\text{subject to} \quad R_i \geq R_i^{\min}, \forall i \in \mathcal{K}, \quad (4.14b)$$

$$\sum_{i=1}^K \|\mathbf{w}_i\|_2^2 \leq P_{ava}, \quad (4.14c)$$

$$|\mathbf{h}_i^H \mathbf{w}_K|^2 \geq |\mathbf{h}_i^H \mathbf{w}_{K-1}|^2 \geq \dots \geq |\mathbf{h}_i^H \mathbf{w}_1|^2, i \in \mathcal{K}, \quad (4.14d)$$

where R_i^{\min} is the minimum rate requirement for the user U_i , and (4.14d) ensures the successful implementation of the SIC for all users while maintaining the rate fairness between them. Clearly, the optimization problem OP_1 is non-convex as the objective function, the constraint in (4.14b), and the constraint in (4.14d) are non-convex. To cope the non-convexity issues in this problem, two algorithms are provided. In addition, the feasibility of OP_1 will be firstly investigated prior to solving it. Finally, the convergence of the proposed algorithms will be investigated.

4.2.1 Feasibility check of OP_1

The optimization problem OP_1 defined in (4.14) is worth solving only when it is feasible to solve for a given set of constraints. For instance, the OP_1 problem may not be solvable because of insufficient available power budget at the base station, or higher user data rate requirements. As such, it is first worth verifying the feasibility conditions prior to attempting to solve the GEE-Max problem. An approach for verifying the feasibility conditions is outlined using the following P-Min problem:

$$OP_2: P^* = \underset{\{\mathbf{w}_i\}_{i=1}^K}{\text{minimize}} \quad \sum_{i=1}^K \|\mathbf{w}_i\|_2^2 \quad (4.15a)$$

$$\text{subject to} \quad R_i \geq R_i^{\min}, \forall i \in \mathcal{K}, \quad (4.15b)$$

$$|\mathbf{h}_i^H \mathbf{w}_K|^2 \geq \dots \geq |\mathbf{h}_i^H \mathbf{w}_1|^2, \forall i \in \mathcal{K}, \quad (4.15c)$$

where P^* denotes the minimum power required to achieve the minimum rate and satisfy the SIC constraints. The above optimization problem, OP_2 , has been solved in [49] by handling the non-convex constraints through a set of convex approximation techniques, which are detailed in the next section. If $P^* > P_{ava}$, then the optimization problem in OP_1 can be classified as an infeasible problem. To overcome this infeasibility issue, the following SRM problem is considered, where the achievable sum-rate is maximized with transmit power constraint and SIC constraints. This SRM problem can be formulated as in [67]

$$OP_3: \underset{\{\mathbf{w}_i\}_{i=1}^K}{\text{maximize}} \quad \sum_{i=1}^K \log(1 + \gamma_i) \quad (4.16a)$$

$$\text{subject to} \quad \sum_{i=1}^K \|\mathbf{w}_i\|_2^2 \leq P_{ava}, \quad (4.16b)$$

$$|\mathbf{h}_i^H \mathbf{w}_K|^2 \geq \dots \geq |\mathbf{h}_i^H \mathbf{w}_1|^2, \forall i \in \mathcal{K}. \quad (4.16c)$$

The solution of the optimization problem OP_3 can be reached throughout this section, however, full details can be found in [67].

It is worth to explore an efficient method to solve the original GEE-Max problem in OP_1 , provided that the problem is feasible. In the following discussion, two iterative algorithms are developed to determine a solution with the assumption that the minimum data requirements and the SIC constraints can be met within the available power budget P_{ava} .

4.2.2 Approaches for Solving the GEE-Max Problem

As it is just mentioned, the GEE-Max problem defined in (4.14) is a non-convex problem due to non-convex objective function and constraints. Hence, it is challenging to obtain the solution. To overcome these non-convexity issues, two iterative algorithms are developed to determine the beamforming vectors that maximize the GEE of the system while satisfying the respective constraints. These algorithms are proposed by approximating the non-convex objective function and constraints to convex ones based on the SCA and Dinkelbach's algorithms. The details of the algorithms are provided in the following two subsections.

Approach based on the Sequential Convex Approximation

The SCA technique is one of the well-known techniques that has been widely adopted to approximate and transform non-convex problems into convex problems [92]. The basic idea of SCA is to approximate the non-convex functions in an optimization problem with lower convex approximations, such that the approximated convex optimization problem is solved iteratively. In the GEE-Max design, and by introducing a slack variable α , the original optimization problem OP_1 can be reformulated in the following form:

$$\underset{\alpha, \{\mathbf{w}_i\}_{i=1}^K}{\text{maximize}} \quad \alpha \quad (4.17a)$$

$$\text{subject to} \quad \frac{\sum_{i=1}^K \log(1 + \gamma_i)}{\frac{1}{\epsilon_0} \sum_{i=1}^K \|\mathbf{w}_i\|_2^2 + P_{loss}} \geq \sqrt{\alpha}, \quad (4.17b)$$

$$R_i \geq R_i^{\min}, \forall i \in \mathcal{K}, \quad (4.17c)$$

$$\sum_{i=1}^K \|\mathbf{w}_i\|_2^2 \leq P_{ava}, \quad (4.17d)$$

$$|\mathbf{h}_i^H \mathbf{w}_K|^2 \geq \dots \geq |\mathbf{h}_i^H \mathbf{w}_1|^2, \forall i \in \mathcal{K}, \quad (4.17e)$$

where the objective function in the original problem (4.14) is replaced by $\sqrt{\alpha}$ (or equivalently α). Without loss of generality, by introducing the slack variable β , the non-convex constraint

in (4.17b) can be equivalently decomposed into the following two constraints:

$$\sum_{i=1}^K \log(1 + \gamma_i) \geq \sqrt{\alpha\beta}, \quad (4.18a)$$

$$\frac{1}{\epsilon_0} \sum_{i=1}^K \|\mathbf{w}_i\|_2^2 + P_{loss} \leq \sqrt{\beta}. \quad (4.18b)$$

By incorporating the definition of SINR_i (i.e., γ_i) in (4.7), the constraint in (4.18a) can be represented as follows:

$$\sum_{i=1}^K \log(1 + \min(\gamma_i^1, \gamma_i^2, \dots, \gamma_i^k, \dots, \gamma_i^i)) \geq \sqrt{\alpha\beta}. \quad (4.19)$$

To handle the non-convexity of (4.19), a set of new slack variables is firstly introduced such that:

$$\log(1 + \min(\gamma_i^1, \gamma_i^2, \dots, \gamma_i^k, \dots, \gamma_i^i)) \geq \delta_i, \forall i \in \mathcal{K}, \quad (4.20a)$$

$$(1 + \min(\gamma_i^1, \gamma_i^2, \dots, \gamma_i^k, \dots, \gamma_i^i)) \geq \zeta_i, \forall i \in \mathcal{K}. \quad (4.20b)$$

Based on these new slack variables, the constraint in (4.20a) can equivalently be represented by the following set of constraints:

$$(4.20a) \Leftrightarrow \begin{cases} \sum_{i=1}^K \delta_i \geq \sqrt{\alpha\beta}, \\ \zeta_i \geq 2^{\delta_i}, \quad \forall i \in \mathcal{K}. \end{cases} \quad (4.21a)$$

$$(4.21b)$$

However, the constraint in (4.21a) still remains non-convex. In order to relax this, the first-order Taylor series is exploited, providing approximations around the values of $(\alpha^{(n-1)}, \beta^{(n-1)})$. With this,

$$\sum_{i=1}^K \delta_i \geq \sqrt{\alpha^{(n-1)}\beta^{(n-1)}} + 0.5\sqrt{\frac{\alpha^{(n-1)}}{\beta^{(n-1)}}}(\beta^{(n)} - \beta^{(n-1)}) + 0.5\sqrt{\frac{\beta^{(n-1)}}{\alpha^{(n-1)}}}(\alpha^{(n)} - \alpha^{(n-1)}). \quad (4.22)$$

To handle the constraint expressed in (4.20b), another slack variable, $\theta_{k,i} \in \mathbb{R}_+^1$ ($\forall i \in \mathcal{K}, k \leq i$) is introduced, and the constraint in (4.20b) is reformulated into the following set of

equivalent constraints, with $\forall i \in \mathcal{K}$ and $k \leq i$,

$$|\mathbf{h}_k^H \mathbf{w}_i|^2 \geq (\zeta_i - 1)\theta_{k,i}, \quad (4.23a)$$

$$\sum_{j=1}^{i-1} |\mathbf{h}_k^H \mathbf{w}_j|^2 + \sigma_i^2 \leq \theta_{k,i}. \quad (4.23b)$$

To handle the non-convexity issues in the constraint (4.23a), the left-hand side of the inequality is approximated as follows:

$$|\mathbf{h}_k^H \mathbf{w}_i|^2 \geq (\Re(\mathbf{h}_k^H \mathbf{w}_i))^2, \forall k, \forall i. \quad (4.24)$$

Note that the approximation in (4.24) always holds for any set of channel coefficients and beamforming vectors and thus not required to be included in the optimization problem. By taking the square-root of both sides of the inequality in (4.23a) after incorporating the new approximation in (4.24), the constraint in (4.23) can be equivalently formulated as follows:

$$\Re(\mathbf{h}_k^H \mathbf{w}_i) \geq \sqrt{(\zeta_i - 1)\theta_{k,i}}. \quad (4.25)$$

Now, the right-hand side of the above inequality can be approximated using the first-order Taylor series expansion. Therefore, the non-convex inequality in (4.25) can be written in the following convex form:

$$\begin{aligned} \Re(\mathbf{h}_k^H \mathbf{w}_i) \geq & \sqrt{(\zeta_i^{(n-1)} - 1)\theta_{k,i}^{(n-1)}} + 0.5 \sqrt{\frac{(\zeta_i^{(n-1)} - 1)}{\theta_{k,i}^{(n-1)}}} (\theta_{k,i}^{(n)} - \theta_{k,i}^{(n-1)}) \\ & + 0.5 \sqrt{\frac{\theta_{k,i}^{(n-1)}}{(\zeta_i^{(n-1)} - 1)}} (\zeta_i^{(n)} - \zeta_i^{(n-1)}). \end{aligned} \quad (4.26)$$

On the other hand, the non-convex constraint in (4.23b) can be formulated into a SOC as in [66]:

$$\frac{\theta_{k,i}^{(n)} - \sigma_i^2 + 1}{2} \geq \|\mathbf{v}_k^{(n)}\|_2, \quad (4.27)$$

where

$$\mathbf{v}_k^{(n)} = \left[\mathbf{h}_k^H \mathbf{w}_1^{(n)} \dots \mathbf{h}_k^H \mathbf{w}_{i-1}^{(n)} \phi_{i,k}^{(n)} \right]^T \quad (4.28)$$

and

$$\phi_{i,k}^n = \frac{(\theta_{k,i}^{(n)} - \sigma_i^2) - 1}{2}. \quad (4.29)$$

The non-convexity of the constraint in (4.18b) can be handled by introducing new slack variable β_β and expressed into multiple constraints as follows:

$$\sqrt{\beta} \geq \beta_\beta, \quad (4.30a)$$

$$\beta_\beta \geq \frac{1}{\epsilon_0} \sum_{i=1}^K \|\mathbf{w}_i\|_2^2 + P_{loss}. \quad (4.30b)$$

This can further be formulated into the following SOC constraints [87]:

$$\frac{\beta + 1}{2} \geq \left\| \begin{bmatrix} \frac{\beta - 1}{2} & \beta_\beta \end{bmatrix}^T \right\|_2, \quad (4.31a)$$

$$\frac{(\beta_\beta - P_{loss}) + 1}{2} \geq \left\| \begin{bmatrix} w_0 & \frac{\mathbf{w}_1}{\sqrt{\epsilon_0}} & \dots & \frac{\mathbf{w}_K}{\sqrt{\epsilon_0}} \end{bmatrix}^T \right\|_2, \quad (4.31b)$$

where:

$$w_0 = \frac{(\beta_\beta - P_{loss}) - 1}{2}. \quad (4.32)$$

Having approximated the original non-convex objective function in (4.14a) by introducing a number of slack variables, the final form of the objective function is same as:

$$(4.14a) \Leftrightarrow \begin{cases} \text{maximize} & \alpha \\ \text{subject to} & (4.21b), (4.22), (4.26), \\ & (4.27), (4.31a), (4.31b). \end{cases}$$

With this, other non-convex constraints are handled in the original GEE-Max problem expressed by OP_1 . Without the loss of generality, the minimum rate constraint in (4.14b) can be expressed as:

$$\gamma_i^{(k)} \geq \gamma_i^{\min}, \forall i \in \mathcal{K}, k \leq i, \quad (4.34)$$

where $\gamma_i^{\min} = 2^{R_i^{\min}} - 1$. Furthermore, this SINR constraint can be formulated into an SOC by employing the slack variable incorporation in (4.24) and with $\forall i \in \mathcal{K}, k \leq i$

$$\frac{1}{\sqrt{\gamma_i^{\min}}} \Re(\mathbf{h}_k^H \mathbf{w}_i) \geq \left\| \begin{bmatrix} \mathbf{h}_k^H \mathbf{w}_1 & \dots & \mathbf{h}_k^H \mathbf{w}_{i-1} & \sigma_k \end{bmatrix}^T \right\|_2. \quad (4.35)$$

The non-convexity of the constraint in (4.14d) can be approximated to a convex constraint by applying the first-order Taylor series approximation. However, instead of applying the Taylor series expansion to the original equation, a new proxy function $f(\psi_{i,j})$ is defined by stacking

the real and imaginary parts of the product $\mathbf{h}_i^H \mathbf{w}_j$ as follows:

$$|\mathbf{h}_i^H \mathbf{w}_j|^2 = \|[\Re(\mathbf{h}_i^H \mathbf{w}_j) \Im(\mathbf{h}_i^H \mathbf{w}_j)]^T\|^2 \geq f(\psi_{i,j}), \quad (4.36)$$

where $\psi_{i,j} = [\Re(\mathbf{h}_i^H \mathbf{w}_j), \Im(\mathbf{h}_i^H \mathbf{w}_j)]$. Then the first-order Taylor series expansion is applied to this proxy function $f(\psi_{i,j})$, such as

$$f(\psi_{i,j}) \cong f(\psi_{i,j}^{(n-1)}) + 2(\psi_{i,j}^{(n-1)})^T(\psi_{i,j}^{(n)} - \psi_{i,j}^{(n-1)}). \quad (4.37)$$

With this approximation in place, the non-convex constraint in (4.14d) can be replaced with the following convex one:

$$f(\psi_{i,K}) \geq f(\psi_{i,K-1}) \geq \cdots \geq f(\psi_{i,1}), \forall i \in \mathcal{K}. \quad (4.38)$$

By incorporating all of these approximations, the original GEE-Max problem in (4.14) can be formulated into the following approximated problem:

$$\underset{\Lambda}{\text{maximize}} \alpha \quad (4.39a)$$

$$\text{subject to } (4.14d), (4.20b), (4.26), (4.27), (4.35), \quad (4.39b)$$

$$(4.22), (4.31a), (4.31b), (4.14c), (4.38). \quad (4.39c)$$

Note that the expression

$$\Lambda^{(n)} \triangleq \{\mathbf{w}_i^{(n)}, \alpha^{(n)}, \beta^{(n)}, \beta_\beta^{(n)}, \theta_{k,i}^{(n)}, \zeta_i^{(n)}, \delta_i^{(n)}\}_{i=1}^K$$

indicates the n^{th} iteration of the optimization parameters. In particular, the original GEE-Max problem is iteratively solved using the approximated convex problem in (4.39). As such, the optimization parameter is initialized with $\Lambda^{(0)}$. In particular, the selection of $\Lambda^{(0)}$ determines both the feasibility and the convergence of (4.39). Hence, $\Lambda^{(0)}$ is initialized by firstly evaluating the beamforming vectors that satisfy the constraints specified by the optimization problem in (4.15), where the initial slack variables $\alpha^{(0)}, \beta^{(0)}, \beta_\beta^{(0)}, \theta_{k,i}^{(0)}, \zeta_i^{(0)}$ and $\delta_i^{(0)}$ are found by substituting these initial beamforming vectors in (4.18a), (4.18b), (4.30a), (4.23b), (4.23a), and (4.20b), respectively. The algorithm developed to determine the solution of the original GEE-Max problem is summarized in Algorithm 1. The algorithm is terminated when the absolute difference between two sequential optimal values is less than a pre-defined threshold ε (i.e., $|\alpha^{(n)} - \alpha^{(n-1)}| < \varepsilon$).

Algorithm 1 GEE-Max using SCA

Step 1: Initialization of $\Lambda^{(0)}$

Step 2: Repeat

1. Solve the optimization problem in (4.39).
2. Update $\Lambda^{(n)}$.

Step 3: Until required accuracy is achieved.

Approach based on the Dinkelbach's Algorithm

Now, another approach based on the Dinkelbach's algorithm is developed to solve the same GEE-Max problem in OP_1 . In addition to offering an alternative, this approach also helps to compare and validate the performance of the SCA-based algorithm. Furthermore, although the SCA-based algorithm was useful in transforming the non-convex constraints into convex ones, the fractional nature of the objective function in OP_1 still remains untouched. This issue is addressed using the Dinkelbach's algorithm [95], in which an additional non-negative variable is introduced to represent the objective function by a parametrized, yet equivalent, non-fractional function. In particular, the non-negative variable, named χ , is introduced to parametrize the objective function of the original optimization problem OP_1 as follows:

$$OP_5: \text{maximize} \left(\sum_{i=1}^K \log(1 + \gamma_i) - \chi \left(\frac{1}{\epsilon_0} \sum_{i=1}^K \|\mathbf{w}_i\|_2^2 + P_{loss} \right) \right) \quad (4.40a)$$

$$\text{subject to } R_i \geq R_i^{\min}, \forall i \in \mathcal{K}, k \leq i, \quad (4.40b)$$

$$\sum_{i=1}^K \|\mathbf{w}_i\|_2^2 \leq P_{ava}, \quad (4.40c)$$

$$(4.4). \quad (4.40d)$$

For the reasons of notational simplicity, the numerator and the denominator of the objective function in OP_1 are denoted by f_1 and f_2 , respectively, such that

$$f_1(\{\mathbf{w}_i\}_{i=1}^K) = \sum_{i=1}^K \log(1 + \gamma_i), \quad (4.41a)$$

$$f_2(\{\mathbf{w}_i\}_{i=1}^K) = \frac{1}{\epsilon_0} \sum_{i=1}^K \|\mathbf{w}_i\|_2^2 + P_{loss}. \quad (4.41b)$$

In order to realize the relationship between OP_1 and OP_5 , the following theorem [95] is presented:

Theorem 1 *A necessary and sufficient condition for*

$$\chi^* = \underset{\{\mathbf{w}_i\}_{i=1}^K}{\text{maximize}} \frac{f_1(\{\mathbf{w}_i\}_{i=1}^K)}{f_2(\{\mathbf{w}_i\}_{i=1}^K)} = \frac{f_1(\{\mathbf{w}_i^*\}_{i=1}^K)}{f_2(\{\mathbf{w}_i^*\}_{i=1}^K)}, \quad (4.42)$$

is

$$F(\{\mathbf{w}_i\}_{i=1}^K, \chi^*) = \underset{\{\mathbf{w}_i\}_{i=1}^K}{\text{maximize}} \left(f_1(\{\mathbf{w}_i\}_{i=1}^K) - \chi^* f_2(\{\mathbf{w}_i\}_{i=1}^K) \right) = f_1(\{\mathbf{w}_i^*\}_{i=1}^K) - \chi^* f_2(\{\mathbf{w}_i^*\}_{i=1}^K) = 0, \quad (4.43)$$

where $\{\mathbf{w}_i^*\}_{i=1}^K$ is the solution of the original GEE-Max problem.

Proof: Please refer to Appendix A.1.

Theorem 1 confirms that obtaining the beamforming vectors that maximize the GEE in the original problem OP_1 is the same as solving the parametrized optimization problem OP_5 . However, the precondition is that the non-negative parameter χ is a solution of (4.43) [95]. In this approach, the design variables χ and $\{\mathbf{w}_i\}_{i=1}^K$ in OP_5 are iteratively optimized by exploiting the Dinkelbach's algorithm. First, the parameter χ is initialized with zero and the parametrized optimization problem in (4.40) can be solved using convex approximation techniques [87]. For a given set of beamformers, the design parameter in the n^{th} iteration $\chi^{(n)}$ is updated as follows:

$$\chi^{(n)} = \frac{f_1(\{\mathbf{w}_i^{(n-1)}\}_{i=1}^K)}{f_2(\{\mathbf{w}_i^{(n-1)}\}_{i=1}^K)}. \quad (4.44)$$

In particular, the beamforming vectors in the n^{th} iteration ($\{\mathbf{w}_i^{(n)}\}_{i=1}^K$) can be found by solving the following optimization problem:

$$\underset{\{\mathbf{w}_i^{(n)}\}_{i=1}^K}{\text{maximize}} \left(\sum_{i=1}^K \log(1 + \gamma_i) - \chi^{(n-1)} \left(\frac{1}{\epsilon_0} \sum_{i=1}^K \|\mathbf{w}_i^{(n)}\|_2^2 + P_{\text{loss}} \right) \right) \quad (4.45a)$$

$$\text{subject to } R_i \geq R_i^{\min}, \forall i \in \mathcal{K}, k \leq i, \quad (4.45b)$$

$$\sum_{i=1}^K \|\mathbf{w}_i^{(n)}\|_2^2 \leq P_{\text{ava}}, \quad (4.45c)$$

$$(4.4). \quad (4.45d)$$

Due to the non-convex objective function and the non-convex constraints of the optimization problem in (4.45), an iterative algorithm is developed using the SCA approach. It is obvious that $(\frac{1}{c_0} \sum_{i=1}^K \|\mathbf{w}_i^{(n)}\|_2^2 + P_{loss})$ is convex. Hence, without any loss of generality, multiplying it with $-\chi^{(n)}$ will ensure the concavity of this part. On the other hand, the first part of the objective function (i.e., $\sum_{i=1}^K \log(1 + \gamma_i)$) requires some relaxations to convert it to a concave form. To this end, a new slack variable is introduced such that:

$$\sum_{i=1}^K \log(1 + \gamma_i) \geq \nu, \quad (4.46)$$

where the left side of the inequality in (4.46) can be approximated by incorporating new slack variables z_i and q_i , such that

$$1 + \gamma_i \geq z_i, \forall i \in \mathcal{K}, \quad (4.47a)$$

$$z_i \geq 2^{q_i}, \forall i \in \mathcal{K}. \quad (4.47b)$$

Hence, the non-convex constraint in (4.46) can be equivalently rewritten as

$$\sum_{i=1}^K q_i \geq \nu. \quad (4.47c)$$

Without any loss of generality, the non-convexity of the constraint in (4.47a) can be addressed by following the same approach that has been developed to approximate the constraint in (4.20b) in the previous subsection. In particular, ζ_i and $\theta_{k,i}$ in (4.23a) and (4.23b) are replaced by z_i and $\rho_{k,i}$, respectively. The constraint in (4.47a) can be equivalently re-written as a set of the following convex constraints:

$$\begin{aligned} \Re(\mathbf{h}_k^H \mathbf{w}_i) &\geq \sqrt{(z_i^{(n-1)} - 1)\rho_{k,i}^{(n-1)}} + 0.5 \sqrt{\frac{(z_i^{(n-1)} - 1)}{\rho_{k,i}^{(n-1)}}} (\rho_{k,i}^{(n)} - \rho_{k,i}^{(n-1)}) \\ &\quad + 0.5 \sqrt{\frac{\rho_{k,i}^{(n-1)}}{(z_i^{(n-1)} - 1)}} (z_i^{(n)} - z_i^{(n-1)}), \forall i \in \mathcal{K}, k \leq i, \end{aligned} \quad (4.48)$$

$$\frac{(\rho_{k,i}^{(n)} - \sigma_i^2) + 1}{2} \geq \|\mathbf{h}_k^H \mathbf{w}_1^{(n)} \mathbf{h}_k^H \mathbf{w}_2^{(n)} \dots \mathbf{h}_k^H \mathbf{w}_{i-1}^{(n)} \frac{(\rho_{k,i}^{(n)} - \sigma_i^2) - 1}{2}\|_2, \forall i \in \mathcal{K}, k \leq i. \quad (4.49)$$

So far, the first part of the objective function in OP_5 has been transformed into a concave form. As both the optimization problems have the same constraints, the approaches that have been used to handle the constraints of OP_1 will be exploited to handle the constraints of OP_5 . Based on these new transformations, the GEE-Max problem based on the parametrized objective function can be expressed as follows:

$$\underset{\Upsilon^{(n)}}{\text{maximize}} \nu^{(n)} - \chi^{(n-1)} \left(\frac{1}{\epsilon_0} \sum_{i=1}^K \|\mathbf{w}_i^{(n)}\|_2^2 + P_{loss} \right) \quad (4.50a)$$

$$\text{subject to (4.48), (4.49), (4.35), (4.14d), } \forall i \in \mathcal{K}, k \leq i, \quad (4.50b)$$

$$(4.47b), \forall i \in \mathcal{K}, \quad (4.50c)$$

$$(4.45c), (4.47c), (4.38). \quad (4.50d)$$

Furthermore, the parameters Υ obtained through the n^{th} iteration for the new relaxed optimization problem in (4.50) are denoted by $\Upsilon^{(n)}$, such as

$$\Upsilon^{(n)} = \{\nu^{(n)}, z_i^{(n)}, \rho_{k,i}^{(n)}, \mathbf{w}_i^{(n)}\}_{i=1}^K.$$

In this Dinkelbach's-based iterative algorithm, there are two steps that have to be carried out to determine the solution of the original GEE-Max problem, OP_1 . These steps involve iteratively determining the optimal beamforming vectors that would solve the optimization (4.50) for different values of χ until the required accuracy thresholds (i.e., ε and ς) are achieved. The overall process is outlined in Algorithm 2. To conclude, the Dinkelbach's algorithm provided in the previous discussion offers an alternative approach to solve the original GEE-Max problem OP_1 . However, due to the non-concavity of the original objective function in OP_1 , the parametrization carried out in the Dinkelbach's algorithm doesn't simplify the problem, instead, this new algorithm is provided to validate and compare the results obtained through the SCA technique.

This iterative algorithm for obtaining the solution terminates when the absolute difference between two consecutive solutions of the parameter is less than a predefined threshold of ε . Furthermore, the following Lemma is introduced to confirm the convergence of the proposed Dinkelbach's algorithm.

Lemma 1 *The GEE-Max using the Dinkelbach's Algorithm converges to the solution after finite iterations.*

That is

$$\lim_{n \rightarrow \infty} F(\{\mathbf{w}_i^{(n)}\}_{i=1}^K, \chi^{(n)}) \rightarrow 0.$$

Algorithm 2 GEE-Max using Dinkelbach's Algorithm.

Step 1: Initialize $\chi^{(0)} = 0$, choose feasible values for $\rho_{k,i}^{(0)}$, $\nu^{(0)}$ and z_i^0 .

Step 2: Repeat

Step 3: Repeat

1. Solve the optimization problem in (4.50).
2. Update $\Upsilon^{(n)}$.

Step 4: Until required accuracy is achieved.

Step 5: Update $\chi^{(n)} = \frac{\nu^{(n-1)}}{\frac{1}{\epsilon_0} \sum_{i=1}^K \|\mathbf{w}_i^{(n-1)}\|_2^2 + P_{loss}}$.

Step 6: Until required accuracy is achieved.

Proof: Please refer to Appendix A.2.

It is worth making two important observations regarding the solution of the original GEE-Max problem OP_1 here. First, unlike the sum-rate (i.e., $\sum_{i=1}^K \log(1 + \gamma_i)$) in OP_3 , GEE is not monotonically increasing with the available power. However, the maximum GEE in OP_1 is achieved within certain available power budget, which is referred to as the *green power*. In particular, the GEE remains constant for any available power that is higher than the green power. Secondly, the GEE-Max problem OP_1 and SRM problem OP_3 provide similar or same set of solutions (i.e., beamforming vectors and GEE) for any available power budget that is less than the green power.

4.2.3 Complexity Analysis of the Proposed Schemes

The computational complexities of the proposed algorithms to solve the GEE-Max optimization problem are defined as follows:

The SCA Technique

An iterative algorithm is developed to solve the original GEE-Max optimization problem OP_1 by exploiting the SCA technique in which an approximated optimization problem is solved in each iteration and the approximated terms are updated in the next iteration. In particular, a standard second-order cone programme (SOCP) is solved with a number of SOC and linear constraints. Hence, the worst-case complexity of the SCA technique can be examined through defining the complexity of this SOCP, which is solved through the interior-point methods [88], [102]. Furthermore, the total number of constraints associated with this problem is $(2.5K^2 + 5.5K + 6 + q_c)$, where q_c is a constant related to the number of constraints that

arise due to the relaxation of the exponential constraints in interior-point methods [103]. Hence, the total number of iterations that are required to converge to the solution is bounded by $\mathcal{O}(\sqrt{2.5K^2 + 5.5K + 6 + q_c} \log(\frac{1}{\epsilon}))$, where ϵ is the required accuracy. On the other hand, at each iteration, the work required to achieve the solution is at most $\mathcal{O}(\mathcal{N}^2 \mathcal{M})$ [102], where \mathcal{N} and \mathcal{M} denote the number of optimization variables and the total dimensions of the optimization problems, respectively. For the developed SCA based algorithm, \mathcal{N} and \mathcal{M} are estimated as $(1.5K^2 + 3.5K + 2NK + 3 + q_c)$ and $(5.5K^2 + 4K + 2NK + 4 + q_c)$, respectively.

The Dinkelbach's Algorithm

Now, the computational complexity of the proposed Dinkelbach's algorithm is defined in which the convex parametrized problem provided in (4.50) is iteratively solved at each iteration for each non-negative parameter χ . In particular, similar to the SCA technique, a standard SOCP with a set of SOC constraints is solved through the interior-point methods. Furthermore, this SOCP mainly determines the computational complexity of the algorithm. Note that the number of constraints in the SCA technique and the Dinkelbach's algorithm are approximately the same. Hence, the estimated work to determine the solution at each iteration is approximately similar to that required in the SCA based algorithm. However, due to the parametrization required in the Dinkelbach's algorithm, an additional iterative algorithm is required to obtain the optimal χ , as shown in Algorithm 2. The total maximum number of required iterations can be defined by $\mathcal{O}(\sqrt{4K^2 + 4K + 4 + q_c} \log(\frac{1}{\epsilon}) \log(\frac{1}{\zeta}))$, which is higher than that required in the SCA based algorithm.

4.2.4 Optimality Validation for the SCA Technique

In the previous subsections, the original GEE-Max problem OP_1 is solved through the SCA technique, which is developed by approximating non-convex functions. However, it is important to validate the optimality of the corresponding solutions and evaluate their performances by comparing them with the optimal results. In order to do this, the optimality validation procedure is summarized as the following:

- First, the solution of the GEE-Max problem is evaluated using the SCA technique. The achieved SINR and rate at i^{th} user are denoted as γ_i^* and R_i^* , $\forall i \in \mathcal{K}$, respectively.
- Then, the achieved rate R_i^* $\forall i \in \mathcal{K}$ are set as the minimum rate requirements in power minimization (i.e., P-Min) problem OP_2 . Note that due to the non-convexity of the

constraints (4.15b) and (4.15c), P-Min is not convex, and hence, the optimality of the evaluated solution cannot be guaranteed.

- However, based on [54], P-Min can be cast as a convex SDP through introducing the matrix \mathbf{W}_i , such as $\mathbf{W}_i = \mathbf{w}_i \mathbf{w}_i^H$, with pre-assumption that \mathbf{W}_i is rank-one matrix. Note that the SDP relaxation of P-Min can be formulated as the following [54]:

$$\tilde{OP}_2: P^* = \underset{\{\mathbf{W}_i\}_{i=1}^K}{\text{minimize}} \sum_{i=1}^K \text{Tr}[\mathbf{W}_i] \quad (4.51a)$$

$$\text{subject to } \text{Tr}[\mathbf{H}_k \mathbf{W}_i] - \gamma_i^* \sum_{j=1}^{i-1} \text{Tr}[\mathbf{H}_k \mathbf{W}_j] \geq \gamma_i^* \sigma_k^2, \forall i \in \mathcal{K}, k \leq i, \quad (4.51b)$$

$$\text{Tr}[\mathbf{H}_i \mathbf{W}_1] \leq \text{Tr}[\mathbf{H}_i \mathbf{W}_2] \leq \dots \leq \text{Tr}[\mathbf{H}_i \mathbf{W}_K], \forall i \in \mathcal{K}, \quad (4.51c)$$

$$\mathbf{W}_i = \mathbf{W}_i^H, \mathbf{W}_i \succeq 0, \forall i \in \mathcal{K}. \quad (4.51d)$$

The above problem \tilde{OP}_2 is a standard SDP problem and therefore, it leads to an optimal solution [54]. Note that, the corresponding beamforming vectors which solve \tilde{OP}_2 (i.e., \mathbf{w}_i) can be determined by extracting the eigenvector corresponding to the maximum eigenvalue of this rank-one matrix.

- Hence, if the obtained solutions and the corresponding beamforming vectors evaluated through solving the SDP relaxation of P-Min (i.e., \tilde{OP}_2) are similar to those obtained through solving GEE-Max using the SCA algorithm, then, it can be stated that the SCA technique provides the optimal solution of the GEE-Max problem.

As it is discussed in the simulation results section, this SDP problem always provides rank-one solutions that same to the solutions to the GEE-Max problem. This confirms the optimality of the solutions obtained through the proposed SCA algorithm. Note that the P-Min design for the OP_2 cannot be directly employed to solve the original GEE-Max problem without knowing the achieved SINRs (i.e., γ_i^*) that maximize the GEE of the system.

4.3 Energy-Efficient Fairness Designs

As it has been already presented, the GEE-Max-based design in OP_1 considers the overall EE of the system without taking the performance of the individual users into account. Hence, the users with weaker channel conditions (i.e., cell-edge users) might achieve relatively low EE compared to those users with stronger channel conditions (near users) [104]. To overcome

such unfairness issue among the users, the transmitter should be able to incorporate the performance of the individual users in the design rather than optimizing the GEE of the system to maintain fairness between users. In particular, considering individual EE at each user has a direct impact on the achieved rate at that user and the corresponding transmit power. Therefore, several fairness resource allocation techniques have been developed for wireless networks including [105], [106], [107]. In fact, there is no unique definition for fairness, however, this could be generally defined in terms of allocating the resources between the users to provide a reasonable QoS at all of them [11].

In this section, two fairness-based beamforming designs for the introduced MISO-NOMA system are proposed, namely MMEE and PF designs. In these designs, the achieved EE at each user is considered. As such the achieved EE at the i^{th} user (i.e., EE_i) is defined as the ratio between the achieved rate at U_i and the consumed power at the base station to achieve this rate [9], which can be expressed as

$$EE_i = \frac{R_i}{\frac{1}{\epsilon_0} P_i + P_{loss}}, \forall i \in \mathcal{K}, \quad (4.52)$$

where P_i denotes the transmit power allocated to U_i .

4.3.1 Proposed EE-Fairness Designs

MMEE Design

Firstly, MMEE design is considered as the bottleneck fairness design [108]. As such, MMEE is achieved if any performance increment in the EE of the i^{th} user (i.e., EE_i) causes a deterioration of the EE of the j^{th} user (i.e., EE_j) which already has lower performance [84]. This MMEE design can be achieved through solving the following optimization problem:

$$OP_6 \underset{\{\mathbf{w}_i\}_{i=1}^K}{\text{maximize}} \quad \min \{EE_1, EE_2, \dots, EE_K\} \quad (4.53a)$$

$$\text{subject to} \quad (4.14b), (4.14c), (4.14d). \quad (4.53b)$$

This max-min problem is not convex due to the non-convex objective function in (4.53a), the SIC constraint in (4.14d), and the minimum rate requirement in (4.14b). Therefore, the solution to the problem OP_6 cannot easily be determined through existing convex optimization techniques [90].

Proportional Fairness (PF) Design

Despite the fact that the MMEE design aims to achieve the same EE for all users by maximizing the minimum EE of a user, the fairness in that design comes at the cost of GEE degradation. Therefore, another approach, namely the PF-based design is developed, which has the capability to finding a good balance between GEE and achieved EE for each user [108]. Assume that a design achieves EE_i by allocating an amount of Γ_i resources, then, the resource allocation $\{\Gamma_i^*\}_{i=1}^K$ is considered to be a *proportionally fair* if the following condition holds for any other feasible resource allocation $\{\Gamma_i\}_{i=1}^K$ [11]:

$$\sum_{i=1}^K \frac{EE_i - EE_i^*}{EE_i^*} \leq 0, \quad (4.54)$$

where EE_i^* corresponds to Γ_i^* . It is worth mentioning that the condition in (4.54) can be satisfied through determining the feasible set $\{\Gamma_i^*\}_{i=1}^K$ that maximizes $\sum_{i=1}^K \log(EE_i)$ [109]. Based on these definitions, the PF design for the MISO-NOMA system can be defined into the following optimization framework [11]:

$$OP_7 \text{ maximize } \sum_{i=1}^K \log(EE_i) \quad (4.55a)$$

$$\text{subject to } (4.14b), (4.14c), (4.14d). \quad (4.55b)$$

The solutions for the non-convex problems OP_6 and OP_7 are presented in the following discussion.

4.3.2 The SCA Technique

Now, the SCA technique is exploited to convert the original non-convex functions in OP_6 and OP_7 to convex ones. First, the non-convex constraints in OP_6 and OP_7 are similar to those in the GEE-Max design in OP_1 . Therefore, the same approximations that have been developed to handle the non-convexity of these constraints are used to handle the constraints in OP_6 and OP_7 . In particular, the non-convex constraint in (4.14b) is replaced with the convex one in (4.35), whereas, the non-convexity of the SIC constraint in (4.14d) is handled by replacing it with the approximated convex constraint (4.38). Next, the SCA technique is used again to handle the non-convex objective functions of OP_6 and OP_7 .

MMEE Design

In the following, the original non-convex objective function of the MMEE design in OP_6 is transformed by introducing a new slack variable τ as

$$\min \{EE_1, EE_2, \dots, EE_K\} \geq \tau.$$

Without loss of generality, the optimization problem in OP_6 can be equivalently written as

$$\tilde{OP}_6: \underset{\{\mathbf{w}_i\}_{i=1}^K}{\text{maximize}} \quad \tau \quad (4.56a)$$

$$\text{subject to} \quad (4.14b), (4.14c), (4.14d), \quad (4.56b)$$

$$EE_i \geq \tau, i \in \mathcal{K}. \quad (4.56c)$$

Then, the slack variable named β_i is introduced to handle the non-convexity of the constraint in (4.56c), as such

$$R_i \geq \tau \beta_i^2, \forall i \in \mathcal{K}, k \leq i, \quad (4.57a)$$

$$\frac{1}{\epsilon_0} \|\mathbf{w}_i\|_2^2 + P_{loss} \leq \beta_i^2, \forall i \in \mathcal{K}. \quad (4.57b)$$

Following a similar formulation as in (4.31b), the constraint in (4.57b) can be cast as the following standard convex SOC:

$$\beta_i \geq \left\| \left[\frac{\mathbf{w}_i}{\sqrt{\epsilon_0}} \sqrt{P_{loss}} \right]^T \right\|_2, \quad \forall i \in \mathcal{K}. \quad (4.58)$$

Furthermore, a new set of slack variables π_i and t_i is incorporated to approximate the non-convex constraint in (4.57a) as

$$\log(1 + \text{SINR}_i^{(k)}) \geq \pi_i, \forall i \in \mathcal{K}, k \leq i, \quad (4.59a)$$

$$(1 + \text{SINR}_i^{(k)}) \geq t_i, \forall i \in \mathcal{K}, k \leq i, \quad (4.59b)$$

which can be equivalently represented as the following set of constraints:

$$(4.57a) \Leftrightarrow \begin{cases} \frac{|\mathbf{h}_k^H \mathbf{w}_i|^2}{\sum_{j=1}^{i-1} |\mathbf{h}_k^H \mathbf{w}_j|^2 + \sigma_k^2} \geq t_i - 1, k \leq i, & (4.60a) \\ t_i \geq 2^{\pi_i}, \quad \forall i \in \mathcal{K} & (4.60b) \\ \pi_i \geq \tau \beta_i^2, i \in \mathcal{K}. & (4.60c) \end{cases}$$

The non-convexity of the constraint in (4.60a) is handled by incorporating a new slack variable $r_{i,k}^2$ and splitting it into the following two sets of constraints:

$$|\mathbf{h}_k^H \mathbf{w}_i|^2 \geq (t_i - 1)r_{i,k}^2, \forall i \in \mathcal{K}, k \leq i, \quad (4.61a)$$

$$r_{i,k}^2 \geq \sum_{j=1}^{i-1} |\mathbf{h}_k^H \mathbf{w}_j|^2 + \sigma_k^2, \forall i \in \mathcal{K}, k \leq i. \quad (4.61b)$$

Following the same approach in (4.31b), the constraint in (4.61b) can be transformed into a standard convex SOC constraint as

$$r_{i,k} \geq \|[\mathbf{h}_k^H \mathbf{w}_1 \quad \mathbf{h}_k^H \mathbf{w}_2 \quad \cdots \quad \mathbf{h}_k^H \mathbf{w}_{i-1} \quad \sigma_k]^T \|_2, \forall i \in \mathcal{K}, k \leq i. \quad (4.62)$$

Furthermore, using the approximation that has been introduced in (4.24), the constraint in (4.61a) can be represented as the following convex constraint:

$$\Re(\mathbf{h}_k^H \mathbf{w}_i) \geq \sqrt{(t_i^{(n)} - 1)} r_{i,k}^{(n)} + 0.5 \frac{1}{\sqrt{(t_i^{(n)} - 1)}} r_{i,k}^{(n)} (t_i - t_i^{(n)}) + \sqrt{(t_i^{(n)} - 1)} (r_{i,k} - r_{i,k}^{(n)}),$$

$$\forall i \in \mathcal{K}, k \leq i. \quad (4.63)$$

Finally, the first-order Taylor series expansion is employed to approximate the right hand-side of (4.60c) as follows:

$$\pi_i \geq \tau^{(n)} (\beta_i^2)^{(n)} + (\beta_i^2)^{(n)} (\tau - \alpha^{(n)}) + 2\beta_i^{(n)} \tau^{(n)} (\beta_i - \beta_i^{(n)}), \quad i \in \mathcal{K}. \quad (4.64)$$

After introducing these multiple slack variables, the original non-convex MMEE optimization problem OP_6 is approximated as the following optimization problem:

$$OP_6^{\approx}: \underset{\Psi}{\text{maximize}} \quad \tau \quad (4.65a)$$

$$\text{subject to} \quad (4.34), (4.14c), (4.14d) \quad (4.65b)$$

$$(4.58), (4.60b), (4.62), (4.63), (4.64), (4.38), \quad (4.65c)$$

where Ψ includes all the optimization variables involved in the MMEE problem: $\Psi \triangleq \{\mathbf{w}_k, r_{i,k}, t_i, \beta_i, \pi_i, \tau\}_{i=1}^K$. The developed technique to determine the solution of OP_6 is summarized Algorithm 3.

Algorithm 3 MMEE design using SCA.

Step 1: Initialization of $\Psi^{(0)}$

Step 2: Repeat

1. Solve the optimization problem \tilde{OP}_6 in (4.65).
2. Update $\Psi^{(n)}$.

Step 3: Until required accuracy is achieved.

PF Design

Now, the PF problem OP_7 is considered. In particular, the non-convexity of the objective function in OP_7 can be tackled by introducing new slack variables μ_i and ς_i as

$$\log EE_i \geq \varsigma_i, \forall i \in \mathcal{K}, \quad (4.66a)$$

$$EE_i \geq \mu_i, \forall i \in \mathcal{K}. \quad (4.66b)$$

With these new slack variables, OP_7 can be equivalently expressed as

$$\tilde{OP}_7: \begin{array}{ll} \text{maximize} & \sum_{i=1}^K \varsigma_i \\ \text{subject to} & \end{array} \quad (4.67a)$$

$$\mu_i \geq 2^{\varsigma_i}, i \in \mathcal{K}, \quad (4.67b)$$

$$EE_i \geq \mu_i, i \in \mathcal{K}, \quad (4.67c)$$

$$(4.34), (4.14c), (4.14d). \quad (4.67d)$$

Without loss of generality, the non-convex constraint in (4.67c) can be converted to a convex one by using the same approach as in (4.56c). This could be implemented by replacing τ in (4.56c) by μ_i , and then applying the corresponding approximations. Hence, the problem \tilde{OP}_7 can be written in a convex form as

$$\tilde{OP}_7: \begin{array}{ll} \text{maximize} & \sum_{i=1}^K \varsigma_i \\ \text{subject to} & \end{array} \quad (4.68a)$$

$$(4.56b), \quad (4.68b)$$

$$\mu_i \geq 2^{\varsigma_i}, i \in \mathcal{K}, \quad (4.68c)$$

$$(4.65c), (4.38), \quad (4.68d)$$

where φ consists of all the optimization variables: $\varphi \triangleq \{\varsigma_i, \mathbf{w}_i, \rho_{i,k}, \tau_i, \beta_i, \pi_i, \mu_i\}_{i=1}^K$. Note that τ is replaced by μ_i at all constraints in (4.68d).

It is worth noting that the solutions of \tilde{OP}_6 and \tilde{OP}_7 depend on several factors including the appropriate selection of the initial parameters: $\Psi^{(0)}$ and $\varphi^{(0)}$. These initial parameters are chosen by determining the beamforming vectors ($\{\mathbf{w}_i^{(0)}\}_{i=1}^K$) that minimize the total transmit power (i.e., $P = \sum_{i=1}^K \|\mathbf{w}_i\|_2^2$) subject to the minimum rate constraint in (4.14b) and the SIC constraint in (4.14d). Then, all initial parameters (i.e., $\Psi^{(0)}$ and $\varphi^{(0)}$) are evaluated by replacing the inequality with equality at each constraint. On the other hand, it is obvious that the solutions of \tilde{OP}_6 and \tilde{OP}_7 are iteratively obtained. This iterative approach can be terminated by comparing the difference of the objective values at two successive iterations against a predefined threshold ε . The developed algorithms to determine the solutions of the original PF design is summarized in Algorithm 4.

Algorithm 4 PF design using SCA.

Step 1: Initialization of $\varphi^{(0)}$

Step 2: Repeat

1. Solve the optimization problem \tilde{OP}_7 in (4.68).
2. Update $\varphi^{(n)}$.

Step 3: Until required accuracy is achieved.

4.4 Simulation Results

In this section, simulation results are provided to demonstrate the effectiveness of the proposed EE-aware designs. In particular, the performance of the developed algorithms to solve the GEE-Max problem is firstly investigated. Afterwards, the GEE-Max design is compared with other beamforming designs available in literature. In addition, the performance of the different EE-aware designs is also provided. Table 4.1 shows different parameters that are adopted in the simulations. The performance of the designs is evaluated in terms of the achieved EE against different normalized transmit powers. This is defined by TX-SNR in dB as follows:

$$\text{TX-SNR (dB)} = 10 \log_{10} \frac{P_{ava}}{\sigma^2}.$$

Table 4.1 Parameter values used in the simulations.

Parameter	Value(s)
Transmit Antennas (N)	3
User Distances (m)	[1.0, 5.5, 10.0]
Path Loss Factor (κ)	1.0
Noise Variance of Users (σ^2)	2.0
Threshold for Algorithm 1 (ϵ)	0.01
Threshold for Algorithm 2 (ς)	0.01
Power-Amp Efficiencies (ϵ_0)	0.65
User SINR Thresholds for OP_1	10^{-2}
Bandwidth B_w (MHz)	1
Small scale fading \mathbf{g}_i	Rayleigh fading

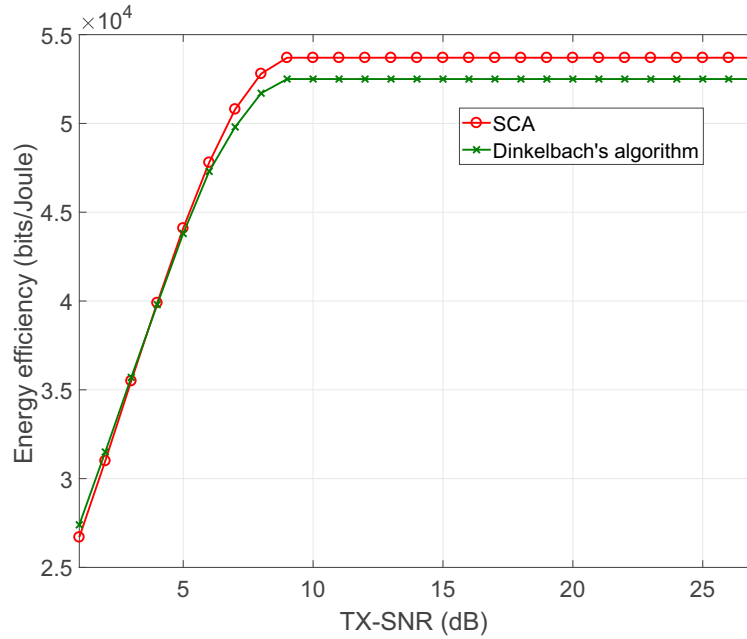


Fig. 4.2 Achieved EE for GEE-Max-based design through Algorithms 1 and 2.

Figure 4.2 shows the achieved EE for the GEE-Max-based design with different TX-SNR using the algorithms developed through the SCA and Dinkelbach's techniques. The performance gap between these two approaches is not significant in terms of the achieved EE. However, the design based on the SCA approach outperforms the latter due to the parametrization of the objective function in the latter. As seen in Figure 4.2, the achieved EE increases with the available transmit power until it reaches the corresponding maximum

green power, where it saturates. It is worth to mention that the feasibility check provided in the previous sections is proceeded prior to solve OP_1 , if it is infeasible, OP_3 is solved alternatively.

In order to demonstrate the advantages of the proposed GEE-Max-based design, the EE of the proposed GEE-Max design is compared with the existing conventional beamforming designs in the literature, namely, beamforming design for SRM in MISO-NOMA system [67], and maximizing the sum rate in MISO-OMA based on the ZFBF design [110], [111]. As evidenced by results in Figure 4.3, the GEE-Max based design outperforms the other designs in terms of achieved EE. On the other hand, the EE of the SRM-based designs declines dramatically when the transmit power exceeds the green power. This is particularly the case for the SRM-based designs for both NOMA and OMA (i.e., ZFBF), where these designs consume all available power for maximizing the achieved sum rate, as it is seen below.

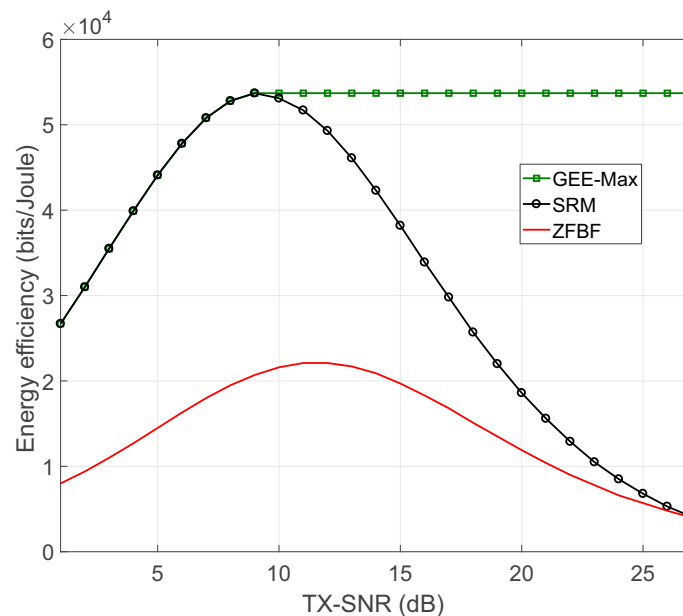


Fig. 4.3 EE for different design criteria.

In order to demonstrate the trade-off between the achieved EE and the sum-rate across different beamforming designs, the performance of the proposed scheme is evaluated in terms of the achieved sum-rate of the overall system. Figure 4.4 illustrates the achieved sum-rates of different designs against a range of transmit powers. As expected, the SRM-based design shows the same performance as the GEE-Max design up to the green power, and outperforms the GEE-Max scheme when the available transmit power exceeds the green power. The sum-rate of the GEE-Max-based scheme remains constant in this region, where it achieves

the maximum EE as shown in Figure 4.3. On the other hand, the achieved sum rates of both SRM and ZFBF schemes increases with the available transmit power while decreasing their EE performance (Figure 4.3).

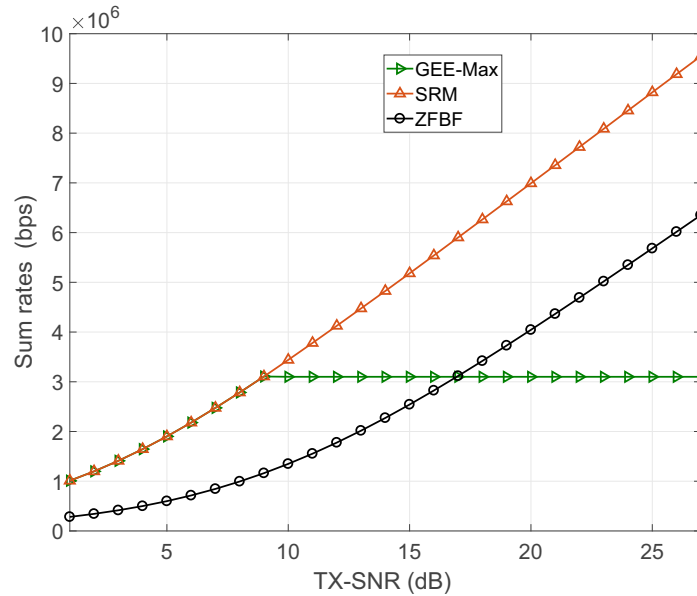


Fig. 4.4 Achieved sum rates of different beamforming designs against transmit power.

Next, a 5 users scenario is considered, in which, the users are located at 1.0, 5.5, 10.0, 15, and 20 meters from the base station. As seen in Figure 4.5, increasing the number of users has a direct impact on the green power.

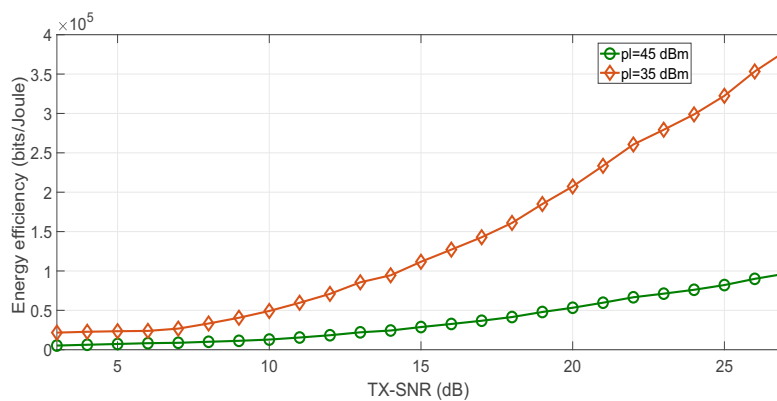


Fig. 4.5 EE of GEE-Max design with different power losses for 5 users scenario.

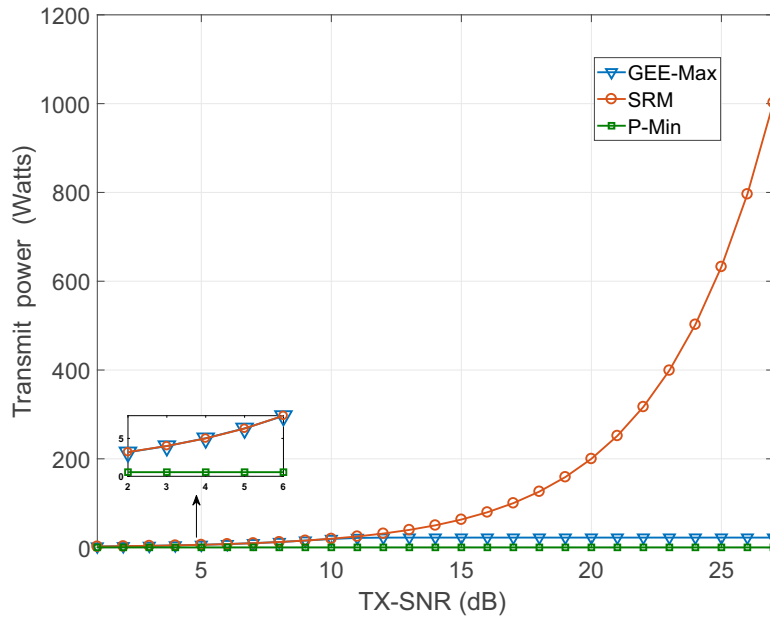


Fig. 4.6 Required transmit power for different beamforming design criteria.

To evaluate the transmit power consumption (i.e., P_{tr}), the transmit power requirements for different NOMA beamforming designs are introduced in Figure 4.6. As it can be seen, the P-Min beamforming design [49] outperforms the SRM- and GEE-Max-based designs. This is because the P-Min-based beamforming design uses the transmit power to satisfy the required SINR constraints. On the other hand, the SRM-based scheme makes use of all the available transmit power to achieve the maximum sum rate, while the GEE-Max-based scheme consumes a certain amount of transmit power (i.e., green power) to maximize the GEE of the system. From these observations, the GEE-Max-based design can be considered as the scheme that strikes a good balance between the SRM and P-Min-based designs.

Furthermore, the impact of the power losses on the performance of the proposed GEE-Max design is evaluated in Figure 4.7, at which the achieved EE against different power losses is shown. There are two key observations to be drawn from Figure 4.7. Firstly, the achievable EE decreases as the power loss increases. Secondly, the green power that achieves the maximum EE increases as the power losses increase.

Next, the target is to validate the optimality of the proposed SCA-based GEE-Max algorithm. Therefore, the achieved SINRs and power allocations of the proposed scheme are compared with the P-Min-based scheme, which assumes to use the same SINR targets obtained in the GEE-Max-based scheme. The power allocations and the achieved SINRs using the proposed SCA-based GEE-Max algorithm are given for five different random channels in Table 4.2. For the same set of channels used in Table 4.2, the power allocations

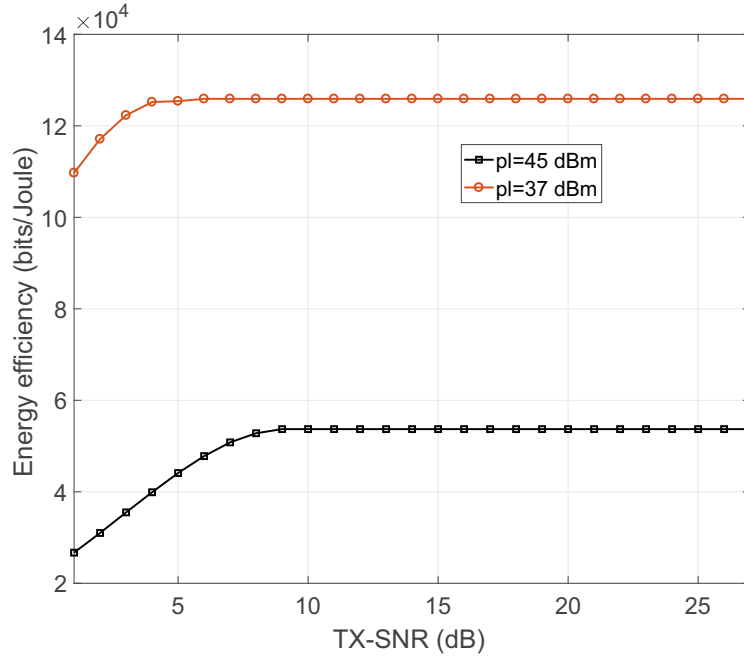


Fig. 4.7 Achieved EE of GEE-Max design with different power losses.

obtained through solving the P-Min $\tilde{O}P_2$ are given in Table 4.3 where the achieved SINRs in Table 4.2 have been set as the target SINRs in $\tilde{O}P_2$. By comparing the results provided in Tables 4.2 and 4.3, it can be concluded that both problems provide the same solutions in terms of power allocation. It can also be noticed that the beamforming vectors obtained in both cases are the same, and they are not presented here for the reasons of brevity. Therefore, it can be confirmed that the SCA algorithm yields the optimal solution to the original GEE-Max problem. In addition, Figure 4.8 illustrates the impact of increasing the number of transmit antennas N on the achieved EE for the proposed GEE-Max design and the SRM design. Considering the GEE-Max design, in spite of the increase of the achieved rate offered with

Table 4.2 Power allocations and the achieved SINRs obtained from solving GEE-Max design using the SCA, TX-SNR= 2dB.

Channels	User 1		User 2		User 3	
	γ_1^*	P_1 (W)	γ_2^*	P_2 (W)	γ_3^*	P_3 (W)
Channel 1	1.2468	0.9095	0.1848	0.9095	0.1482	1.3507
Channel 2	0.9975	0.8660	0.1535	0.8660	0.1381	1.4378
Channel 3	1.3353	0.9115	0.1789	0.9115	0.1512	1.3082
Channel 4	1.8190	0.9815	0.2485	0.9815	0.1640	1.2068
Channel 5	1.4606	0.9400	0.2098	0.9400	0.1551	1.2898

Table 4.3 Power allocations for the achieved SINRs In Table 4.2 using the P-Min design.

Channels	$P_i = \text{Tr}[\mathbf{W}_i]$		
	P_1 (W)	P_2 (W)	P_3 (W)
Channel 1	0.9094	0.9095	1.3508
Channel 2	0.8660	0.8660	1.4379
Channel 3	0.9113	0.9115	1.3082
Channel 4	0.9815	0.9815	1.2068
Channel 5	0.9400	0.9400	1.2897

the increase of the transmit antennas N , the achieved EE tends to have different behaviour. Specifically, this behaviour can be divided into two regions. In the first region, the rate enhancements offered with increasing N overcomes the increase of the power consumption. Hence, EE increases gradually until it achieves its maximum value when $N = 3$. Afterwards, the increase of the transmit antennas causes a considerable increment on P_{loss} , which causes the total power consumption to be folded compared to the expected sum-rate enhancement. Therefore, EE decays exponentially just after achieving its maximum. On the other hand, same behaviour can be noticed for the SRM design. However, the EE achieved through the GEE-Max design outperforms that obtained for the SRM design.

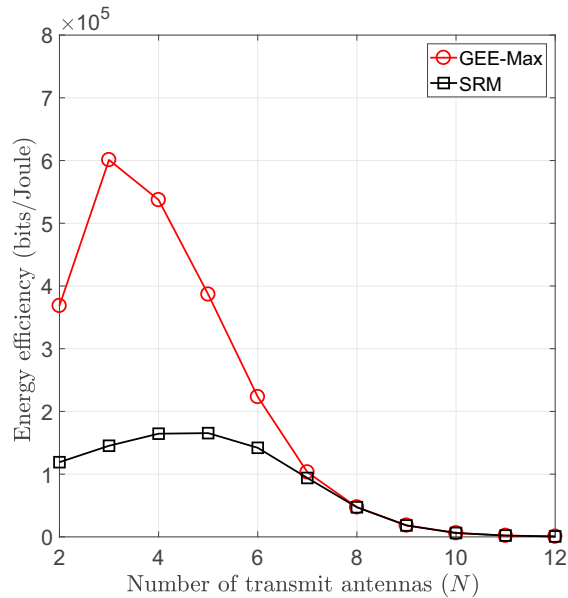


Fig. 4.8 The achieved EE against different number of transmit antenna N for GEE-Max and SRM designs at TX-SNR = 10 dB. The p_{sta} and p_{dyn} are set to be 10 dBm and 5 dBm, respectively.

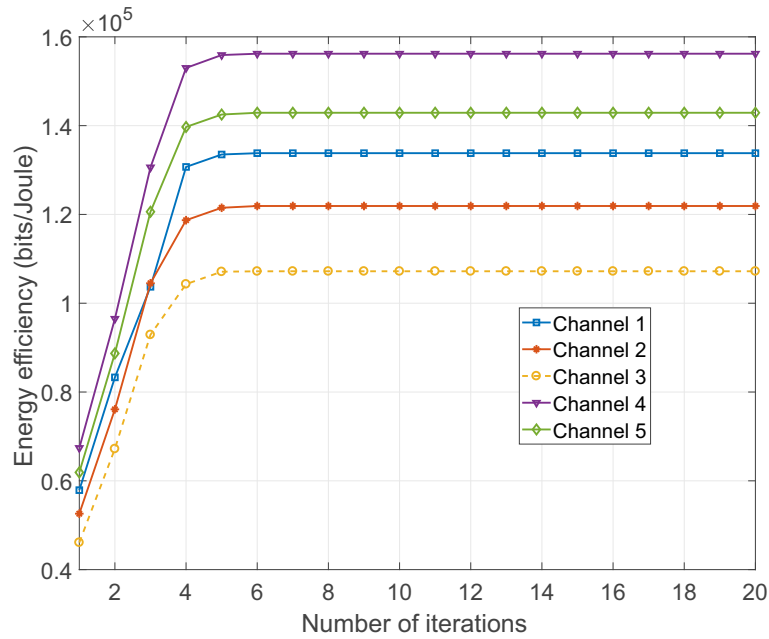


Fig. 4.9 The convergence of SCA based GEE-Max algorithm for different set of random channels. The TX-SNR and P_{loss} are set to be 20 dB and 40 dBm, respectively.

Furthermore, the number of iterations required for the convergence of the proposed SCA-based GEE-Max algorithm is introduced. Figure 4.9 depicts the convergence of the proposed SCA algorithm with a set of channels. The threshold (ε in Algorithm 1) to terminate the algorithm has been set to 0.01. As seen in Figure 4.9, the algorithm converges within a few iterations.

Now, to demonstrate the effectiveness of the proposed EE-fairness designs, namely the MMEE and PF designs, a set of detailed simulations is provided. In the following simulations, the first and second user remain at the same distances, whereas the weakest user is re-located at distance of 25 meters from the base station. In fact, the GEE-Max-based design is used as baseline.

In Fig. 4.10, the achieved EE of the weakest user in the system with different beamforming designs, namely GEE-Max, PF, and MMEE designs, is presented. As can be seen in Fig. 4.10, the performance of the weakest user is significantly improved in terms of EE when considering the MMEE and PF-based designs compared to the conventional GEE-Max-based design. For example, at TX-SNR=20 dB, the weakest user experiences an EE of around 2800 bits/Joule with the MMEE design, which is almost five times that of the EE that can be achieved with the GEE-Max-based design. Similarly, the PF-based design outperforms the GEE-Max-based design in terms of the performance for the weakest user. However, MMEE achieves the best EE for the weakest user compared to the other two designs. This is because

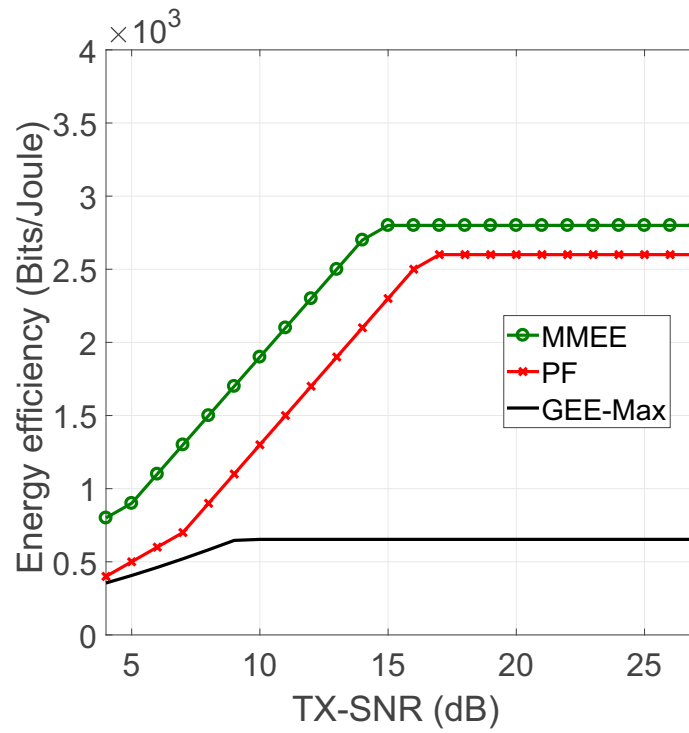


Fig. 4.10 The performance of the weakest user with different beamforming designs, $\kappa=2$, $\eta_i^{min} = 10^{-3}$.

MMEE maximizes the minimum achievable EE between all the users and attains the same EE for all users.

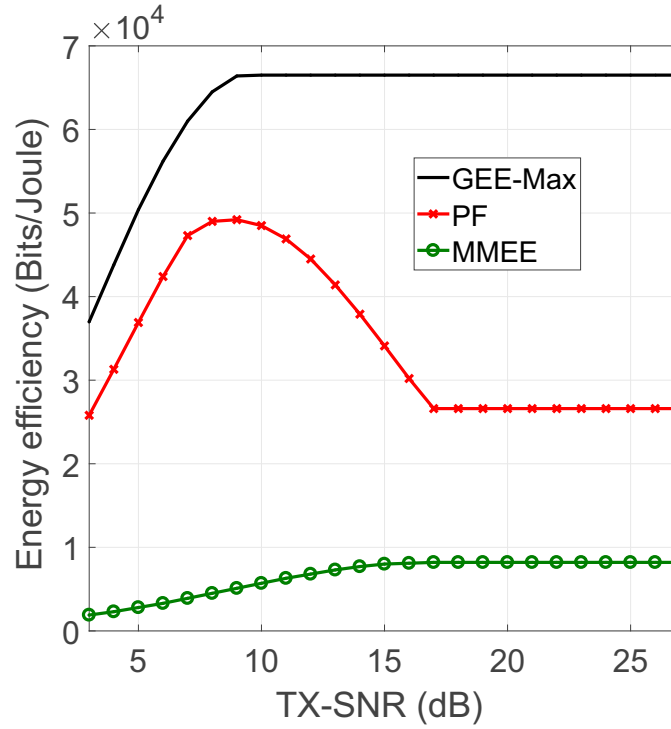


Fig. 4.11 EE of the system (i.e., GEE) with different EE-based designs, $\kappa=2$, $\eta_i^{\min} = 10^{-3}$.

Next, the achieved EE of the system (i.e., GEE) for different designs is introduced and compared in Fig. 4.11. As expected, the GEE-Max design outperforms the other fairness-based designs in terms of the EE of the system, whereas the MMEE-based design shows the worst GEE performance between the three schemes presented in Fig. 4.11. However, the PF-based design attains a good balance between the EE at the system level and the achieved individual EE for each user. In other words, the PF-based design shows a better GEE compared to that of the MMEE-based design. The same design significantly improves EE of the weakest user compared to that of the GEE-Max-based design.

4.5 Summary

In this chapter, different EE-aware beamforming designs are proposed for a MISO-NOMA system. First, the GEE-Max is proposed to maximize the overall EE of the system subject to the system requirements (i.e., constraints). The non-convexity of this design is handled by proposing two different algorithms, namely SCA and Dinkelbach's algorithms. In particular, this GEE-Max design achieves the maximum EE of the system at the cost of the EE degradation of the users with lower channel conditions. Hence, two fairness EE designs are proposed and presented, which are the MMEE and PF designs. In MMEE design, the

target is to achieve equal EE among all users. In fact, this design achieves optimal fairness among users. However, this fairness enhancement is achieved at the cost of the overall EE degradation. To cope with the problems associated with the GEE-Max and MMEE designs, the PF design is developed. In particular, as it was shown in the simulation results, the PF design strikes a good balance between the GEE-Max and MMEE designs in terms of the conflicting design metrics, named the overall EE and EE of the weakest user. On the other hand, due to the non-convexity of the optimization problems associated with these designs, different approximations and relaxations have been developed to overcome these non-convexity issues. In particular, SCA technique was used to handle these non-convexity issues, at which each non-convex term is approximated by lower linear approximation (i.e., convex-concave). It was shown in simulation results that SCA technique can obtain the optimal solution with few number of iterations.

Chapter 5

Multi-Objective based Beamforming Designs

As previously mentioned, future wireless networks are expected to optimize different performance metrics, simultaneously, such as sum rate, EE, and fairness. Therefore, two multi-objective based beamforming designs for MISO-NOMA systems are proposed in this chapter. In the first beamforming design, both performance metrics, namely sum rate (i.e., SE) and EE, are maximized, simultaneously. Then, the sum rate and the fairness among users in terms of achieved rates of the MISO-NOMA system are both considered. In particular, these designs are formulated as MOO problems, which are hard and challenging to solve. Therefore, weighted-sum approach combined with priori-articulation techniques is utilized to obtain solutions of these problem. The performance of the proposed designs are compared with other existing beamforming designs in the literature.

5.1 Spectral-Energy Efficiency Trade-off based Beamforming Design

5.1.1 Introduction

Motivated by the importance of both the key performance metrics SE and EE in 5G and beyond wireless networks [4], [2], and to overcome the limitations associated with conventional GEE-Max and SRM designs [101], [67], a SE-EE trade-off based design for a MISO-NOMA system is proposed in this chapter. Unlike the conventional designs, this SE-EE design optimizes SE and EE simultaneously to strike a good balance between these conflicting performance metrics. Furthermore, this joint SE-EE design provides a flexibility

to the base station to adapt the beamforming design by taking into account the instantaneous transmission conditions and the different requirements of the system. In particular, the practical applications of the proposed SE-EE trade-off design can be summarized as follows:

- Base stations with hybrid power resources are expected to play a crucial role in the deployments of 5G and beyond wireless networks [112]. These hybrid base stations are powered by either non-renewable energy resources such as diesel generators, or renewable energy resources such as photovoltaic panels and wind turbines to provide the different network services [113]. For such hybrid base stations, the priority to choose either of EE or SE depends on the available energy resources, i.e., if the base station utilizes a renewable energy resource, then the importance of EE becomes less than that of the SE, and vice-versa for non-renewable energy resources. Hence, a SE-EE trade-off based design offers a flexibility for the base station to switch between different design criteria based on the available energy resources.
- Furthermore, some resource allocation techniques aim to maximize EE with a SE constraint [114]. However, this design limits the performance of either SE or EE due to its inflexibility [85]. Hence, the SE-EE trade-off based design has a potential capability to strike a good balance between these conflicting performance metrics, especially in some practical applications where both SE and EE become with a similar importance.

The key contributions in this design can be summarized as follows:

- Unlike the conventional designs in [67], [66], [101], and [49], the proposed SE-EE design is formulated into a MOO problem, which is challenging and difficult to realize a feasible solution directly. In particular, conventional optimization techniques employed in the context of SOO problem cannot be directly applied to solve this MOO problem. Furthermore, the proposed SE-EE design can be considered as a general framework as the GEE max and SE maximization (i.e., SRM) designs will become the special cases of it by setting appropriate weight factors.
- Hence, a step-by-step algorithm is provided to handle this non-trivial MOO problem. This algorithm utilizes priori-articulation method combined with weighted-sum utility function to recast the MOO problem into a form of a SOO problem [96], [97], [98].
- In addition, it is proven that solving the SOO problem provides the Pareto-optimal solution to the original MOO problem. In particular, the SCA technique is exploited in the context of handling the non-convexity of the SOO problem.

- Furthermore, simulation results are provided to validate the effectiveness of the proposed design by drawing comparisons with the conventional designs. In particular, these results confirm that this SE-EE trade-off design has a potential capability to strike a balance between SE and EE through choosing an appropriate weight factor. In addition, unlike the conventional design criteria, the base station has the flexibility to switch between different designs by only choosing an appropriate weight factor α .

5.1.2 Problem Formulation

In this chapter, the downlink MISO-NOMA system introduced in the previous chapter is considered. Furthermore, and for notation simplicity, SE and EE (i.e., GEE) are represented by the functions $f_1(\{\mathbf{w}_i\}_{i=1}^K)$ and $f_2(\{\mathbf{w}_i\}_{i=1}^K)$, respectively. Such that,

$$f_1(\{\mathbf{w}_i\}_{i=1}^K) = \sum_{i=1}^K R_i,$$

$$f_2(\{\mathbf{w}_i\}_{i=1}^K) = \frac{\sum_{i=1}^K R_i}{P_{total}}.$$

In particular, the aim is to develop a beamforming design that can *jointly* maximize these conflicting performance metrics (i.e., $\max f_1(\{\mathbf{w}_i\}_{i=1}^K)$ and $f_2(\{\mathbf{w}_i\}_{i=1}^K)$) with a given set of constraints. Therefore, the beamforming vectors that can achieve a trade-off between the conflicting SE and EE metrics in the MISO-NOMA system can be formulated into the following MOO problem:

$$OP_8: \underset{\{\mathbf{w}_i\}_{i=1}^K}{\text{maximize}} \mathbf{f}(\{\mathbf{w}_i\}_{i=1}^K) = [f_1(\{\mathbf{w}_i\}_{i=1}^K), f_2(\{\mathbf{w}_i\}_{i=1}^K)] \quad (5.2a)$$

$$\text{subject to} \quad \sum_{i=1}^K \|\mathbf{w}_i\|_2^2 \leq P_{ava}, \quad (5.2b)$$

$$R_i \geq R_i^{\min}, \forall i \in \mathcal{K}, \quad (5.2c)$$

$$|\mathbf{h}_i^H \mathbf{w}_K|^2 \geq |\mathbf{h}_i^H \mathbf{w}_{K-1}|^2 \geq \dots \geq |\mathbf{h}_i^H \mathbf{w}_1|^2, i \in \mathcal{K}. \quad (5.2d)$$

Note that the objective vector $\mathbf{f}(\{\mathbf{w}_i\}_{i=1}^K)$ consists of the conflicting SE and GEE functions. It is obvious that there is no global optimal solution that maximizes these conflicting objectives in OP_8 [96]. However, the MOO problem OP_8 looks for all possible best trade-off solutions, which are known as the Pareto-optimal solutions in the literature [98]. Therefore, the aim is to find the set of the feasible solutions that satisfy the Pareto-optimality condition for this

MOO problem. However, due to the fact that the original OP_8 problem might be infeasible with certain P_{ava} , a feasibility check for OP_8 has to be carried out prior to solving it. The feasibility check and the proposed methodology to solve the problem OP_8 are provided in the next subsection.

5.1.3 Feasibility, Proposed Methodology, and Discussions

Firstly, a feasibility condition is examined prior to solving the optimization problem OP_8 . For infeasible problems, another alternative beamforming design is proposed. The feasible OP_8 is then solved by reformulating it as SOO problem using a priori articulation technique combined with the weighted-sum approach. Then, the SCA technique is exploited to handle the non-convexity issue of the SOO problem. At the end of this section, some discussions on the convergence and the performance evaluation of the proposed SCA algorithm to solve OP_8 are provided.

Feasibility Check

Firstly, it is worthy to mention that the original optimization problem OP_8 turns out to be infeasible when the minimum rate requirements (i.e., R_i^{min}) at each user cannot be met with the available power budget at the base station (i.e., P_{ava}). Therefore, it is important to investigate the feasibility of the original problem OP_8 prior to solving it. Similar to the feasibility check developed for the GEE-Max optimization problem OP_1 in the previous chapter, the feasibility check for OP_8 can be performed through evaluating the required minimum transmit power, referred as P^* , that is required to satisfy the minimum rate and SIC constraints, in (5.2c) and (5.2d), respectively. This P^* can be determined through solving the corresponding P-Min optimization problem OP_2 in the previous chapter. Note that the original problem OP_8 can only be solved provided that $P^* \leq P_{ava}$, and is infeasible when P^* is higher than the available power at the base station (i.e., P_{ava}). To overcome this infeasibility, an alternative beamforming design can be considered to maximize the sum rate with available power budget, as in OP_3 defined in the previous chapter.

5.1.4 Proposed Methodology

To solve the MOO problem OP_8 , it has to be firstly reformulated into a SOO form. Then, the SCA technique is exploited to solve the developed SOO problem. More details are provided in the following discussions.

Single Objective Transformation

First, a priori articulation scheme is used to assign a weight factor for each objective, as such the base station determines the relative importance of each objective function prior to determining the beamforming vectors based on the design requirements. In particular, the weight factor α_i is assigned to the i^{th} objective function (i.e., $f_i(\{\mathbf{w}_i\}_{i=1}^K)$) to reflect its relative importance on the overall design, such that $\sum_{i=1}^2 \alpha_i = 1$, $\alpha_i \in [0, 1]$. Then, the vector containing the objective functions in the original MOO problem OP_8 is replaced with a single objective function known as the utility function in the literature. Note that the utility function is a single-objective function that can alternatively represent the original multi-objective function based on the importance of each objective function [96]. There are several utility functions available in the literature [96], [97], [98]; however, the weighted sum approach is chosen here as it provides the Pareto-optimal solution to the original problem, as stated in Theorem 1.

Theorem 2 *The solutions of the weighted-sum SOO problem in \tilde{OP}_8 provide the Pareto-optimal solutions for the original MOO OP_8 problem.*

Proof: Please refer to Appendix B.1. ■

Based on the previous discussion, the SOO framework that represents the original MOO problem OP_8 can be formulated as follows:

$$\tilde{OP}_8: \underset{\{\mathbf{w}_i\}_{i=1}^K}{\text{maximize}} \quad f_{EE-SE}(\{\mathbf{w}_i\}_{i=1}^K) \quad (5.3a)$$

$$\text{subject to} \quad \sum_{i=1}^K \|\mathbf{w}_i\|_2^2 \leq P_{ava}, \quad (5.3b)$$

$$R_i \geq R_i^{\min}, \forall i \in \mathcal{K}, \quad (5.3c)$$

$$(5.2d), \quad (5.3d)$$

where $f_{EE-SE}(\{\mathbf{w}_i\}_{i=1}^K) = \sum_{l=1}^2 \alpha_l f_l^{Norm}(\{\mathbf{w}_i\}_{i=1}^K)$. Note that $f_1^{Norm}(\{\mathbf{w}_i\}_{i=1}^K)$ and $f_2^{Norm}(\{\mathbf{w}_i\}_{i=1}^K)$ represent the unit-less normalized version of $f_1(\{\mathbf{w}_i\}_{i=1}^K)$ and $f_2(\{\mathbf{w}_i\}_{i=1}^K)$, respectively, which can be defined as

$$f_1^{Norm}(\{\mathbf{w}_i\}_{i=1}^K) = \frac{f_1(\{\mathbf{w}_i\}_{i=1}^K)}{f_1^*}, \quad (5.4a)$$

$$f_2^{Norm}(\{\mathbf{w}_i\}_{i=1}^K) = \frac{f_2(\{\mathbf{w}_i\}_{i=1}^K)}{f_2^*}, \quad (5.4b)$$

where f_1^* and f_2^* are the maximum values of SE and GEE, respectively. In particular, f_1^* and f_2^* can be determined through solving OP_3 and OP_1 , respectively. Note that the normalization of the objectives in (5.4) is an important step in the context of solving the original MOO problem OP_8 due to several reasons. Firstly, it is obvious that the performance metrics GEE and SE have different units. Therefore, adding such functions without normalization is not allowed and does not define any meaningful performance metric. Secondly, as these two functions have completely different ranges, combining them in a weighted-sum utility function will certainly degrade the achievable objective value of the function with lower range [96]. Therefore, to treat both objective functions in a fair manner, a unitless normalization is employed by dividing each objective function with its corresponding optimal value. With such a normalization, a non-dimensional objective function is obtained with an upper bound of one. Note that different normalization (i.e., transformations) methods have been widely considered for MOO problems in the literature [85], [96], [98]. For notation simplicity, it is assumed that $\alpha_2 = \alpha$ and $\alpha_1 = 1 - \alpha$. It is obvious that \tilde{OP}_8 turns out to be SE-Max (i.e., SRM and SE-Max carry the same meaning in this thesis) when $\alpha = 0$. Furthermore, the problem becomes GEE-Max with $\alpha = 1$.

However, a good balance between the conflicting SE and EE performance metrics can be achieved through choosing an appropriate α between 0 and 1. To this end, the original MOO problem OP_8 has been transformed into a form of a SOO problem \tilde{OP}_8 . However, the optimization problem \tilde{OP}_8 cannot be directly solved due to the non-convexity nature of the objective function and the corresponding constraints. To circumvent this non-convexity issue, SCA is developed.

Sequential Convex Approximation

Similar to iterative approach that developed to handle the GEE-Max design problem OP_1 in the previous chapter, the SCA technique is exploited to solve the \tilde{OP}_8 problem by approximating each non-convex term with a convex one. In particular, each term of the objective function is replaced by the lower slack variables Γ_1 and Γ_2 , such that

$$(1 - \alpha)f_1^{Norm}(\{\mathbf{w}_i\}_{i=1}^K) \geq \Gamma_1, \quad (5.5a)$$

$$\alpha f_2^{Norm}(\{\mathbf{w}_i\}_{i=1}^K) \geq \Gamma_2. \quad (5.5b)$$

Based on these slack variables, the original \tilde{OP}_8 problem can be equivalently written as

$$\tilde{OP}_8 : \underset{\Gamma_1, \Gamma_2, \{\mathbf{w}_i\}_{i=1}^K}{\text{maximize}} \quad \Gamma_1 + \Gamma_2 \quad (5.6a)$$

$$\text{subject to} \quad \sum_{i=1}^K \|\mathbf{w}_i\|_2^2 \leq P_{ava}, \quad (5.6b)$$

$$R_i \geq R_{\min}, \forall i \in \mathcal{K}, \quad (5.6c)$$

$$(5.2d), \quad (5.6d)$$

$$(1 - \alpha) f_1^{Norm}(\{\mathbf{w}_i\}_{i=1}^K) \geq \Gamma_1, \quad (5.6e)$$

$$\alpha f_2^{Norm}(\{\mathbf{w}_i\}_{i=1}^K) \geq \Gamma_2, \quad (5.6f)$$

It is obvious that the objective function in \tilde{OP}_8 is a linear function in terms of Γ_1 and Γ_2 . However, the constraints are not, and hence, the convexity issues of these constraints can be handled in the following discussion. First, the non-convex constraint in (5.6e) can be reformulated as

$$\sum_{i=1}^K \log_2(1 + \text{SINR}_i) \geq \frac{f_1^*}{(1 - \alpha)} \Gamma_1. \quad (5.7)$$

The non-convexity issue of this constraint can be handled by introducing new slack variables z_i, ρ_i , such that

$$\log_2(1 + \text{SINR}_i^{(k)}) \geq \rho_i, \forall i \in \mathcal{K}, k \leq i, \quad (5.8a)$$

$$1 + \text{SINR}_i^{(k)} \geq z_i, \forall i \in \mathcal{K}, k \leq i. \quad (5.8b)$$

Based on these multiple slack variables, the constraint in (5.7) can be equivalently written as the following set of constraints:

$$(5.7) \Leftrightarrow \begin{cases} \sum_{i=1}^K \rho_i \geq \frac{f_1^*}{(1 - \alpha)} \Gamma_1, & (5.9a) \\ z_i \geq 2^{\rho_i}, \quad \forall i \in \mathcal{K}, & (5.9b) \\ (5.8b). & (5.9c) \end{cases}$$

It is obvious that the inequalities (5.9a) and (5.9b) are convex constraints, whereas the constraint in (5.9c) remains still non-convex. Furthermore, another slack variable $a_{i,k}$ is

introduced to convert it into a convex one as follows:

$$|\mathbf{h}_k^H \mathbf{w}_i|^2 \geq (z_i - 1)a_{i,k}^2, \forall i \in \mathcal{K}, k \leq i, \quad (5.10a)$$

$$a_{i,k}^2 \geq \sum_{j=1}^{i-1} |\mathbf{h}_k^H \mathbf{w}_j|^2 + \sigma_k^2, \forall i \in \mathcal{K}, k \leq i. \quad (5.10b)$$

By incorporating the approximation that developed in the previous chapter, i.e., $|\mathbf{h}_k^H \mathbf{w}_i|^2 \geq (\Re(\mathbf{h}_k^H \mathbf{w}_i))^2$, $\forall k, \forall i$, the constraint in (5.10a) can be written in the following approximated convex form:

$$\begin{aligned} \Re(\mathbf{h}_k^H \mathbf{w}_i) \geq & \sqrt{(z_i^{(n)} - 1)} a_{i,k}^{(n)} + 0.5 a_{i,k}^{(n)} \frac{1}{\sqrt{(z_i^{(n)} - 1)}} (z_i - z_i^{(n)}) \\ & + \sqrt{(z_i^{(n)} - 1)} (a_{i,k} - a_{i,k}^{(n)}), \forall i \in \mathcal{K}, k \leq i, \end{aligned} \quad (5.11)$$

where $a_{i,k}^{(n)}$ and $z_i^{(n)}$ represent the approximations of $a_{i,k}$ and z_i in the n^{th} iteration, respectively. However, the constraint in (5.10b) can be reformulated into the following second-order cone (SOC) [87]:

$$a_{i,k} \geq \left\| \left[\mathbf{h}_k^H \mathbf{w}_{i-1} \cdots \mathbf{h}_k^H \mathbf{w}_1 \sigma_k \right]^T \right\|_2, \forall i \in \mathcal{K}, k \leq i. \quad (5.12)$$

Next, the non-convexity of the constraint in (5.6f) is tackled by introducing a new slack variable b such that

$$\frac{\sum_{j=1}^K R_j}{\frac{1}{\epsilon_0} P_t + P_{loss}} \geq \frac{f_2^* \Gamma_2 b^2}{\alpha b^2}. \quad (5.13)$$

Note that R_i is already approximated with ρ_i . The constraint in (5.6f) can be split into the following two constraints:

$$\sum_{j=1}^K R_j \geq \frac{f_2^*}{\alpha} \Gamma_2 b^2, \quad (5.14a)$$

$$b^2 \geq \frac{1}{\epsilon_0} \sum_{i=1}^K \|\mathbf{w}_i\|_2^2 + P_{loss}. \quad (5.14b)$$

Now, the non-convexity of (5.14a) is handled by approximating the right-hand side with first-order Taylor approximation, as follows:

$$\sum_{j=1}^K \rho_j \geq \frac{f_2^*}{\alpha} \left(\Gamma_2^{(n)} b^{2(n)} + 2b^{(n)} \Gamma_2^{(n)} (b - b^{(n)}) + b^{2(n)} (\Gamma_2 - \Gamma_2^{(n)}) \right). \quad (5.15)$$

Similar to the constraint in (5.10b), the constraint in (5.14b) can be cast as the following SOC constraint:

$$b \geq \frac{1}{\sqrt{\epsilon_0}} \left\| \left[\|\mathbf{w}_1\|_2 \|\mathbf{w}_2\|_2 \cdots \|\mathbf{w}_K\|_2 \sqrt{P_l} \right]^T \right\|_2. \quad (5.16)$$

Next, the non-convexity of the constraint in (5.6d) is handled in [67] by using minorization-maximization approximation (MMA). In this technique, each term of the inequality in (5.6d) is approximated by a linear term using the first-order Taylor series expansion:

$$\begin{aligned} |\mathbf{h}_k^H \mathbf{w}_i|^2 \geq & \left\| \left[\Re(\mathbf{h}_k^H \mathbf{w}_i^{(n)}) \Im(\mathbf{h}_k^H \mathbf{w}_i^{(n)}) \right]^T \right\|^2 + 2 \left[\Re(\mathbf{h}_k^H \mathbf{w}_i^{(n)}) \Im(\mathbf{h}_k^H \mathbf{w}_i^{(n)}) \right] \\ & \left[(\Re(\mathbf{h}_k^H \mathbf{w}_i) - \Re(\mathbf{h}_k^H \mathbf{w}_i^{(n)})) (\Im(\mathbf{h}_k^H \mathbf{w}_i) - \Im(\mathbf{h}_k^H \mathbf{w}_i^{(n)})) \right]^T. \end{aligned} \quad (5.17)$$

Note that the right-hand side of the inequality in (5.17) is linear in terms of \mathbf{w}_i . Hence, each term in the constraint in (5.6d) is replaced by the right-side of (5.17). Finally, the constraint in (5.6c) can now be equivalently written as

$$\frac{|\mathbf{h}_k^H \mathbf{w}_i|^2}{\sum_{j=1}^{i-1} |\mathbf{h}_k^H \mathbf{w}_j|^2 + \sigma_k^2} \geq \eta_i^{th}, \forall i \in \mathcal{K}, k \leq i, \quad (5.18)$$

where $\eta_i^{th} = 2^{R_i^{\min}} - 1$. Furthermore, the constraint in (5.18) can be reformulated as the following SOC constraint:

$$\frac{1}{\sqrt{\eta_i^{th}}} \Re(\mathbf{h}_k^H \mathbf{w}_i) \geq \left\| \left[\mathbf{h}_k^H \mathbf{w}_1 \cdots \mathbf{h}_k^H \mathbf{w}_{i-1} \sigma_k \right]^T \right\|_2, \forall i \in \mathcal{K}, k \leq i. \quad (5.19)$$

Based on these approximations, the original non-convex optimization problem \tilde{OP}_8 can be reformulated as

$$\tilde{OP}_8 : \underset{\Psi}{\text{maximize}} \quad \Gamma_1 + \Gamma_2 \quad (5.20a)$$

$$\text{subject to} \quad (5.2b), (5.6d)^2, (5.9a), (5.9b), (5.11), \quad (5.20b)$$

$$(5.12), (5.15), (5.16), (5.19), \quad (5.20c)$$

where Ψ consists of all the variables involved in this design, which can be expressed as

$$\Psi = \{\mathbf{w}_i, r_i, b, \Gamma_1, \Gamma_2, z_i, \xi_{i,k}, a_{i,k}, \rho_i\}_{i=1}^K.$$

Note that the relationship between SE and EE basically shows two different trends with the available power. In the first trend, both SE and EE increase with the available power and

²Replace (5.17) instead of each term in the inequality.

this trend continues until the available power reaches the green power. Once the available power exceeds the green power, both SE and EE show the conflicting nature with the available power, which leads to the second trend. In order to provide further insights on these trends, we provide the following lemma:

Lemma 2 *The SE-EE optimization problem \tilde{OP}_8 provides the same solution with different weight factors $\{\alpha_l\}_{l=1}^2$ when the available power P_{ava} is less than the green power (i.e., $P_{ava} \leq \text{green power}$).*

Proof: Please refer to Appendix B.2. ■

It is worth mentioning that the solution of \tilde{OP}_8 requires an appropriate selection of the initial parameters (i.e., $\Psi^{(0)}$). As this is an iterative approach, it is important to provide discussion on the initial conditions and the convergence of the proposed algorithm, which are presented in the following subsection.

Initial Conditions

Firstly, it is crucial to choose an appropriate set $\Psi^{(0)}$ to ensure the feasibility of the problem in the first iteration of the algorithm. In particular, a set of feasible beamforming vectors to satisfy all the constraints in the approximated problem \tilde{OP}_8 is chosen. Then, all required slack variables in \tilde{OP}_8 are determined based on chosen initial beamforming vectors. The proposed algorithm to solve the original OP_8 is summarized in Algorithm 5.

Algorithm 5 SE-EE trade-off maximization using SCA.

Step 1: Check the feasibility of the problem

Step 2: Initialization of $\Psi^{(0)}$

Step 3: Repeat

1. Solve the optimization problem in (5.20)
2. Update $\Psi^{(n+1)}$

Step 4: Until required accuracy is achieved.

Convergence Analysis

By making use of the analysis presented in [92], a convergence analysis is provided for the proposed algorithm. Note that the optimization parameters at the n^{th} iteration (i.e., $\Psi^{(n)}$) are

updated based on the solution obtained by solving the approximated optimization problem in (5.20). To ensure the convergence of this algorithm, three key conditions need to be satisfied. Firstly, appropriate initial conditions are chosen to ensure the feasibility of the approximated problem \hat{OP} at the first iteration of Algorithm 5. This provides a feasible solution to update the parameters in the next iteration. It is worthy mentioning that the feasible solution to the approximated problem can always ensure the satisfaction of the original constraint. In order to provide additional insights on this feasibility issue, the following lemma is required:

Lemma 3 *Suppose that the feasible solution set of the optimization problem OP_8 is denoted by χ , then the feasible region of the approximated convex optimization problem Ψ^n falls within the same feasible region of the original non-convex problem, i.e., $\Psi^n \subseteq \chi, \forall n$.*

Proof: To prove this lemma, it is firstly important to point out that the approximated optimization problem \hat{OP}_8 is solved iteratively. As such, at each iteration, the solution of \hat{OP}_8 is provided for the given set of convex constraints in (5.20). Using the first-order Taylor series expansion, these constraints in the original problem OP_8 are approximated with their lower bounds. This implies that the solution that also lies within the same feasible region Ψ^n also satisfies all the constraints in the original problem [92], i.e., $\Psi^n \subseteq \chi$, which completes the proof of Lemma 3.

Secondly, a new lemma is now presented to support that the objective function in \hat{OP}_8 is non-decreasing with each iteration.

Lemma 4 *The objective function in \hat{OP}_8 is non-decreasing in terms of Ψ^n , i.e., $\Upsilon(\Psi^{(n+1)}) \geq \Upsilon(\Psi^{(n)})$, where $\Upsilon(\Psi^{(n)}) = \Gamma_1(\Psi^{(n)}) + \Gamma_2(\Psi^{(n)})$.*

Proof: To prove this lemma, it is important to point out that the solution of \hat{OP}_8 at the n^{th} iteration is a feasible solution to \hat{OP}_8 in the subsequent iteration. This inherently means the objective function value of in the n^{th} iteration $\Upsilon(\Psi^{(n)})$, is less than or equal to that obtained in the next iteration, i.e., $\Upsilon(\Psi^{(n+1)})$, which means that $\Upsilon(\Psi)$ is a non-decreasing function [92]. This completes the proof of Lemma 4.

Therefore, the objective value at each iteration will either increase or remain the same as in the previous iteration. Finally, the power constraint in (5.2b) ensures that the objective function of \hat{OP} provides an upper bound due to the fact that $P_{ava} \ll \infty$. In particular, the satisfaction of these three conditions ensures that the developed SCA technique converges to a solution with a finite number of iterations.

5.2 Sum rate Fairness Trade-off-based Design

5.2.1 Introduction and Problem Formulation

Considering the expected diverse users channel conditions in ultra-dense networks, future wireless networks should not only aim to maximize the sum rate of all users, however, the fairness in terms of the achieved rate at each user has also to be guaranteed [2]. The fairness index (FI) has been used to measure the fairness between users in terms of their achievable rates [115]. In particular, the FI of the system with K users is defined as follows [11]:

$$\text{FI} = \frac{(\sum_{i=1}^K R_i)^2}{K \sum_{i=1}^K R_i^2}. \quad (5.21)$$

The best fairness can be achieved with an FI of one. Note that the FI and sum rate are conflicting performance metrics, which means that maximizing the sum rate will degrade the FI, and vice versa, especially with users that have significantly different channel strengths. Motivated by this discussion, a novel beamforming design is proposed in this section to jointly optimize the conflicting performance metrics, i.e., the sum rate and fairness for the MISO-NOMA system. In this multi-performance metric based design, the base station decides the importance of each performance metric (i.e., sum rate and FI) through assigning a weight factor for each objective based on the service requirements and the channel conditions of the users. For instance, the base station will consider the fairness with a higher weight when the channel strengths of the users are significantly different and the users expect to achieve the same QoS in terms of their achievable throughput. On the other hand, a higher weight will be assigned for the sum rate when the users have similar channel conditions. Furthermore, this design has the capability to strike a good balance between the sum rate and fairness through assigning appropriate weights to each performance metric. In particular, similar to spectral-energy efficiency trade-off design introduced in the previous section, this trade-off-based design can be formulated as a MOO problem, as such the same techniques developed to handle the MOO problem OP_8 are exploited to solve this problem.

For the sake of notation simplicity, the sum rate is denoted by $g_1(\{\mathbf{w}_i\}_{i=1}^K)$, whereas FI is represented by $g_2(\{\mathbf{w}_i\}_{i=1}^K)$ (i.e., $g_2(\{\mathbf{w}_i\}_{i=1}^K) = \text{FI}$). In this design, the target is to jointly maximize the conflicting objectives (i.e., maximize $g_1(\{\mathbf{w}_i\}_{i=1}^K)$ and $g_2(\{\mathbf{w}_i\}_{i=1}^K)$) subject to SIC and total transmit power constraints, which can be formulated as the following MOO

problem:

$$OP_9 : \underset{\{\mathbf{w}_i\}_{i=1}^K}{\text{maximize}} \quad \mathbf{g}(\{\mathbf{w}_i\}_{i=1}^K) \quad (5.22a)$$

$$\text{subject to} \quad \sum_{i=1}^K \|\mathbf{w}_i\|_2^2 \leq P_{ava}, \quad (5.22b)$$

$$|\mathbf{h}_i^H \mathbf{w}_K|^2 \geq |\mathbf{h}_i^H \mathbf{w}_{K-1}|^2 \geq \cdots \geq |\mathbf{h}_i^H \mathbf{w}_1|^2, i \in \mathcal{K}. \quad (5.22c)$$

where $\mathbf{g}(\{\mathbf{w}_i\}_{i=1}^K)$ denotes the vector which consists of the both objective functions (i.e., $\mathbf{g}(\{\mathbf{w}_i\}_{i=1}^K) = [g_1(\{\mathbf{w}_i\}_{i=1}^K) \ g_2(\{\mathbf{w}_i\}_{i=1}^K)]^T$). In fact, there exists no single global optimal solution that simultaneously maximizes $g_1(\{\mathbf{w}_i\}_{i=1}^K)$ and $g_2(\{\mathbf{w}_i\}_{i=1}^K)$ together. Therefore, to handle such a problem, the designers search for the Pareto optimal solution (i.e., best trade-off solutions). In particular, similar to the SE-EE optimization problem OP_8 , the sum-weight approach combined with a priori-articulation are exploited to reformulate OP_9 into the following SOO form:

$$\tilde{OP}_9 : \underset{\{\mathbf{w}_i\}_{i=1}^K}{\text{max}} \quad \alpha_1 g_1^{Norm}(\{\mathbf{w}_i\}_{i=1}^K) + \alpha_2 g_2^{Norm}(\{\mathbf{w}_i\}_{i=1}^K) \quad (5.23a)$$

$$\text{s.t.} \quad (5.22b), (5.22c), \quad (5.23b)$$

where $g_i^{Norm}(\{\mathbf{w}_i\}_{i=1}^K)$ is the normalized objective function of $g_i(\{\mathbf{w}_i\}_{i=1}^K)$, which can be written as [116]

$$g_i^{Norm}(\{\mathbf{w}_i\}_{i=1}^K) = \frac{g_i(\{\mathbf{w}_i\}_{i=1}^K)}{g_i^*}, \quad (5.24)$$

where g_i^* represents the maximum value of $g_i(\{\mathbf{w}_i\}_{i=1}^K)$. In particular, the maximum value of the FI is one (i.e., $g_2^* = 1$). It is worth to mention that \tilde{OP}_9 turns out to be the conventional SRM problem when $\alpha_1 = 1$. However, when $\alpha_2 = 1$, the problem \tilde{OP}_9 becomes MMR optimization problem. In particular, the MMR solution achieves the same rate (i.e., a unity FI) for all the users in the system [117]. However, the WSRM and PF problems could be formulated from the original optimization problem \tilde{OP}_9 through appropriately scaling the weight factor between zero and one.

Note that \tilde{OP}_9 is non-convex. Hence, the SCA technique is again exploited to handle the non-convexity issues of this problem. Note that the non-convexity of the constraint (5.22c) is already handled in the previous section. To handle the objective function of \tilde{OP}_9 , multiple

slack variables (ξ_1, ξ_2, ξ) are introduced to represent the single objective function as follows:

$$\alpha_1 g_1^{Norm}(\{\mathbf{w}_i\}_{i=1}^K) \geq \xi_1, \quad (5.25a)$$

$$\alpha_2 g_2^{Norm}(\{\mathbf{w}_i\}_{i=1}^K) \geq \xi_2, \quad (5.25b)$$

$$\xi_1 + \xi_2 \geq \xi. \quad (5.25c)$$

Based on these new slack variables, the optimization problem in (5.23) can be rewritten as

$$\tilde{OP}_9 : \underset{\xi_1, \xi_2, \xi, \{\mathbf{w}_i\}_{i=1}^K}{\text{maximize}} \quad \xi \quad (5.26a)$$

$$\text{subject to} \quad \xi_1 + \xi_2 \geq \xi, \quad (5.26b)$$

$$(1 - \alpha) g_1^{Norm}(\{\mathbf{w}_i\}_{i=1}^K) \geq \xi_1, \quad (5.26c)$$

$$\alpha g_2^{Norm}(\{\mathbf{w}_i\}_{i=1}^K) \geq \xi_2, \quad (5.26d)$$

$$(5.22b), (5.22c), \quad (5.26e)$$

where $\alpha_2 = \alpha$ and $\alpha_1 = 1 - \alpha$. Note that the non-convex constraint in (5.26c) is similar to the constraint in (5.6e) as $f_1^{Norm} = g_1^{Norm}$. Hence, and without loss of generality, the same approximations done to approximate (5.6e) will be exploited to handle (5.26c), with only replacing Γ_1 by ξ_1 . On the other hand, the non-convexity of the constraint in (5.26d) will be tackled by employing the same approximations techniques that have been already implemented to handle (5.26c) (i.e., (5.6e)). Firstly, this constraint can be equivalently rewritten as

$$\frac{(\sum_{i=1}^K \rho_i)^2}{K \sum_{i=1}^K \rho_i^2} \geq \frac{\xi_2}{\alpha}, \quad (5.27)$$

The constraint in (5.27) is approximated by introducing the following new slack variables γ, β such that

$$(5.27) \Leftrightarrow \begin{cases} (\sum_{i=1}^K \rho_i)^2 \geq \gamma \beta^2, & (5.28a) \\ K \sum_{i=1}^K \rho_i^2 \leq \beta^2, & (5.28b) \\ \gamma \geq \frac{\xi_2}{\alpha}. & (5.28c) \end{cases}$$

The square root of both sides in the inequality in (5.28a) is taken, then, the non-convex right-hand side of this inequality is tackled by approximating it with the first-order Taylor

series approximation, as follows:

$$\sum_{i=1}^K \rho_i \geq \sqrt{\gamma^{(n-1)}} \beta^{(n-1)} + 0.5 \frac{1}{\sqrt{\gamma^{(n-1)}}} \beta^{(n-1)} (\gamma - \gamma^{(n-1)}) + \sqrt{\gamma^{(n-1)}} (\beta - \beta^{(n-1)}). \quad (5.29)$$

Similarly, the constraint in (5.28b) can be written as the following SOC constraint:

$$\beta \geq \sqrt{K} \|[\rho_1 \ \rho_2 \ \cdots \ \rho_K]^T \|_2. \quad (5.30)$$

Hence, the non-convex constraint in (5.26d) can be now reformulated as the following convex constraints:

$$(5.26d) \Leftrightarrow (5.28c), (5.29), (5.30). \quad (5.31)$$

Through including these approximations, the original optimization problem \tilde{OP}_9 can be reformulated as follows:

$$\underset{\chi}{\text{maximize}} \quad \xi \quad (5.32a)$$

$$\text{subject to} \quad (5.9a), (5.9b), (5.11), (5.12), (5.22b), \quad (5.32b)$$

$$(5.22c), (5.26b), (5.28c), (5.29), (5.30), \quad (5.32c)$$

where χ includes all the optimization parameters such that

$$\chi \triangleq \{ \mathbf{w}_i, \xi, \xi_1, \xi_2, \beta, \gamma, \rho_i, a_{i,k}, z_i \}_{i=1}^K.$$

It is obvious that solving the optimization problem in (5.32) requires to initialize the parameters $\chi^{(0)}$ and these parameters can be obtained by choosing a feasible beamforming vectors $\{ \mathbf{w}_i^{(0)} \}_{i=1}^K$. Furthermore, the other slack variables can be determined through substituting $\{ \mathbf{w}_i^{(0)} \}_{i=1}^K$ in the inequalities. The optimization problem in (5.32) is iteratively solved until the required accuracy is achieved such that $|\xi^{(n)} - \xi^{(n-1)}|$ is less than a pre-defined threshold.

5.3 Simulation Results

In this section, simulation results are provided to support the effectiveness of the proposed multi-objective beamforming designs of the downlink MISO-NOMA system over other conventional beamforming designs. In simulations, a base station equipped with three transmit antennas (i.e., $N = 3$) is considered, which simultaneously transmits to five single-

antenna users that are located at a distance of 1, 2, 3, 4, and 50 meters from the base station, respectively. The small-scale fading is chosen to be Rayleigh fading, while the path loss exponent κ and the noise variance of all users σ^2 are both set to be 1. In addition, the minimum SINR thresholds are set to be 10^{-2} for all the users, i.e., $\eta_{th} = 10^{-2}$. The amplifier gain ϵ_0 is set to 0.65, whereas the power loss at the base station are assumed to be 40 dBm (i.e., $P_{loss} = 40$ dBm). Furthermore, the available power at the base station by TX-SNR in dB is defined such that TX-SNR (dB) = $10 \log_{10} \frac{P_{ava}}{\sigma^2}$. In addition, the available bandwidth of transmission is assumed to be 1 MHz, i.e., $B_w = 1$ MHz. Furthermore, the algorithm terminates when the difference between two consequent outputs is less than 0.001 (i.e., $\varepsilon \leq 0.001$).

SE-EE Trade-off Beamforming Design

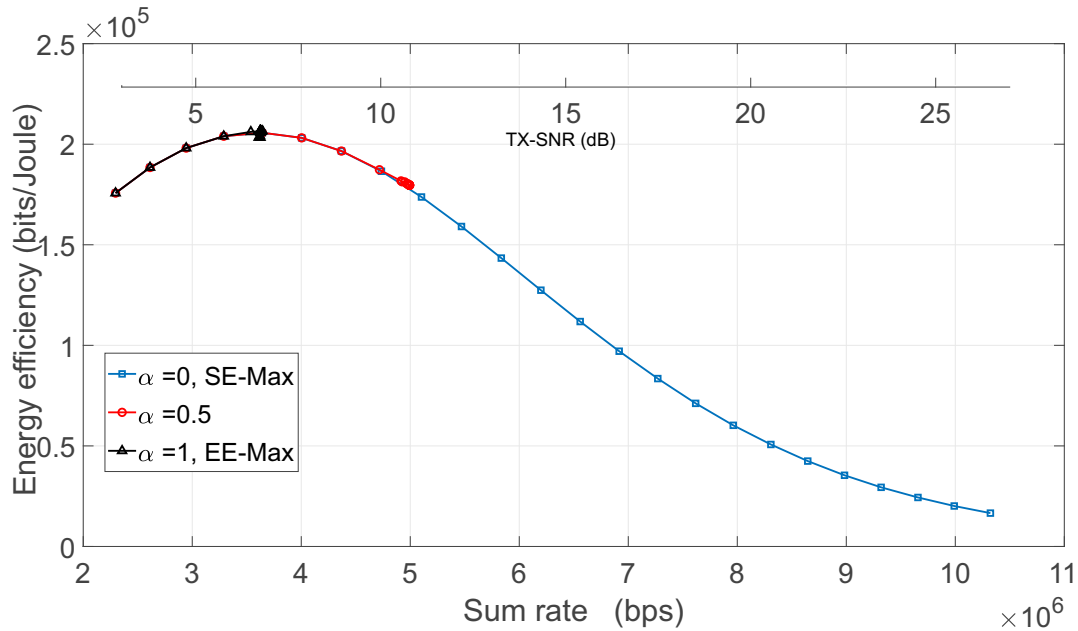


Fig. 5.1 Achieved EE and sum rate against TX-SNR with different weight factors α .

Fig. 5.1 illustrates the achieved EE and sum rate versus different TX-SNR and for different weight factors α . As seen in Fig. 5.1, the SE-EE trade-off design considered in $\tilde{O}P_8$ turns out to be SE-Max with $\alpha = 0$. Furthermore, $\tilde{O}P_8$ keeps maximizing the sum rate as TX-SNR increases at the cost of EE degradation. This is due to the fact that the GEE (i.e.,

EE) has been assigned with zero weight (i.e., $\alpha = 0$) in the MOO problem. However, with $\alpha = 1$, the problem is transformed into a GEE-Max design; as a result, the maximum EE is achieved with certain power threshold, referred as green power in the literature. Beyond this green power, no further enhancement is achieved either in the EE or in the sum rate. Furthermore, this design has the flexibility to strike a good balance between EE and the sum rate by setting the weight factor α between 0 and 1. For example, when $\alpha = 0.5$, an increment in the sum rate is attained compared to that obtained with $\alpha = 1$, as seen in Fig. 5.1. However, this sum rate enhancement is attained at the cost of EE degradation.

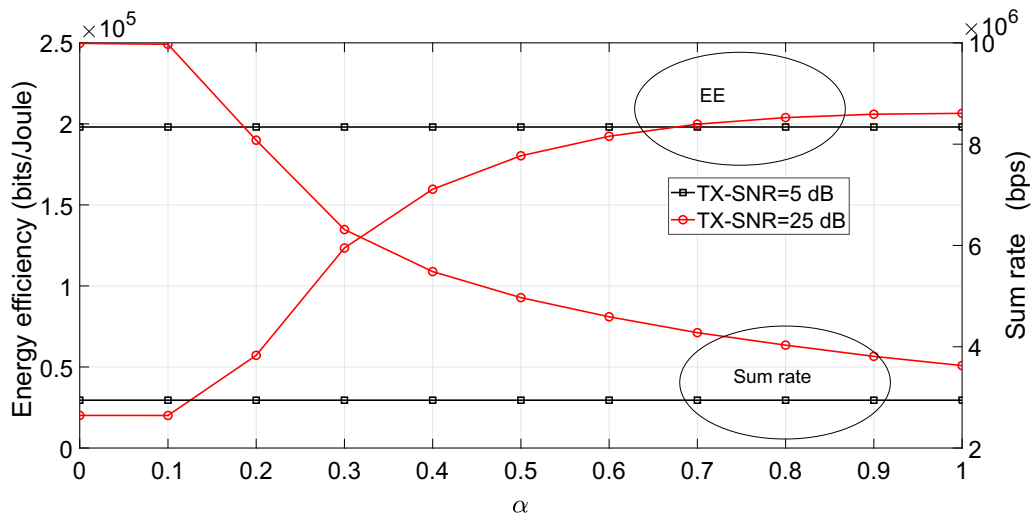


Fig. 5.2 Achieved EE and sum rate with different weight factors α .

Fig. 5.2 presents the achieved EE and sum rate with different weight factors for 5 and 25 dB TX-SNR thresholds. In particular, Fig. 5.2 shows two different behaviours. First, both performance metrics (i.e., sum rate and EE) remain constant with the available power lower than the green power for different weight factors α , which supports the validation of Lemma 2. However, as TX-SNR exceeds the green power, for example with TX-SNR= 25 dB, the trade-off between EE and sum rate can be realized by varying the weight factor. In particular, at this TX-SNR threshold, the achieved rate and EE show a performance in the range of 10-3.5 Mbps and 0.02-0.2 Mbits/Joule, respectively. This performance range is achieved with different weight factors α , as presented in Fig. 5.2.

Furthermore, Figs. 5.3a and 5.3b show the achieved EE and sum rate versus TX-SNR for different weight factors α , respectively. It can be clearly understood the impacts of the weight factors on the achieved EE and sum rate of the system. For example, at TX-SNR = 20 dB, EE declines from 2.2×10^5 bits/Joule to 0.5×10^5 bits/Joule by changing the weight factor from $\alpha = 1$ to $\alpha = 0$. However, the sum rate (i.e., SE) shows a different behavior.

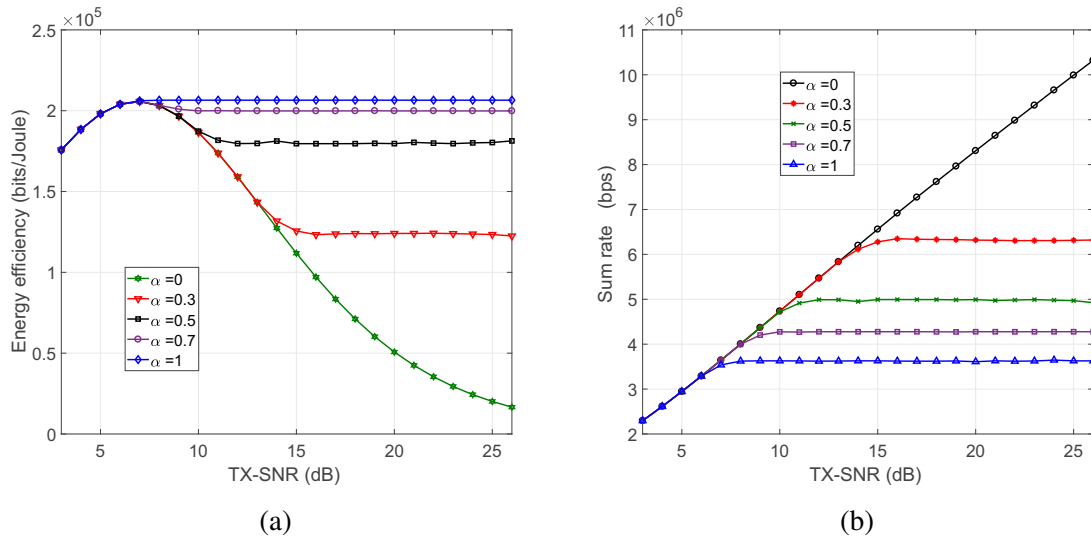


Fig. 5.3 The EE and sum-rate performance of the proposed design versus TX-SNR, with different weight factors. (a) The achieved EE, (b) the achieved sum rate.

With TX-SNR = 20 dB, this increases from 3.6×10^6 bps to 8.2×10^6 bps by changing the weight factor α from 1 to 0. Therefore, the proposed EE-SE trade-off design offers the flexibility to the base station to choose an appropriate weight factor based on the favorable conditions and system requirements to determine the desired performance metric.

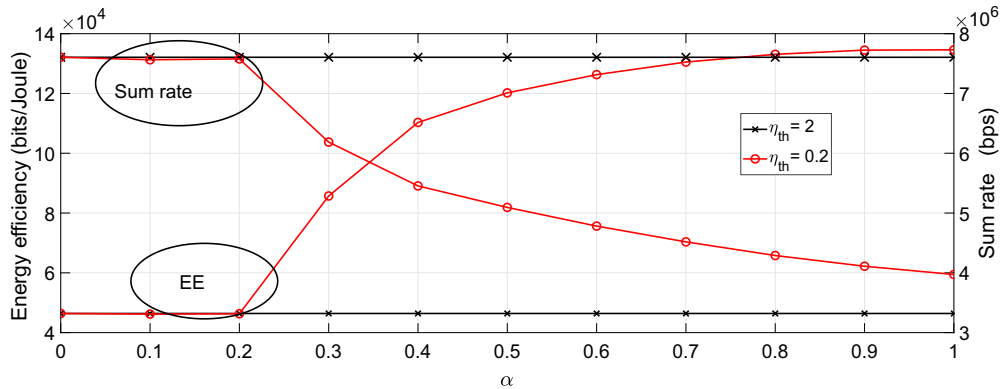


Fig. 5.4 Achieved EE and sum rate for the proposed design versus weight factors α , with different SINR thresholds η_{th} , TX-SNR= 20 dB.

Furthermore, Fig. 5.4 demonstrates the impact of the minimum SINR threshold η_{th} on the performance of the proposed design. In particular, with $\eta_{th} = 2$, the original optimization problem becomes infeasible as the minimum required transmit power P^* to achieve these minimum SINR requirements exceeds the available power P_{ava} . Hence, an alternative design,

namely the SE-Max is considered. As a result, the achieved sum rate is maximized under the available power constraint which provides constant sum rate and EE over the different weight factors α . However, choosing lower value of η_{th} ensures the feasibility of the design, which can be observed with $\eta_{th} = 0.2$, in Fig. 5.4.

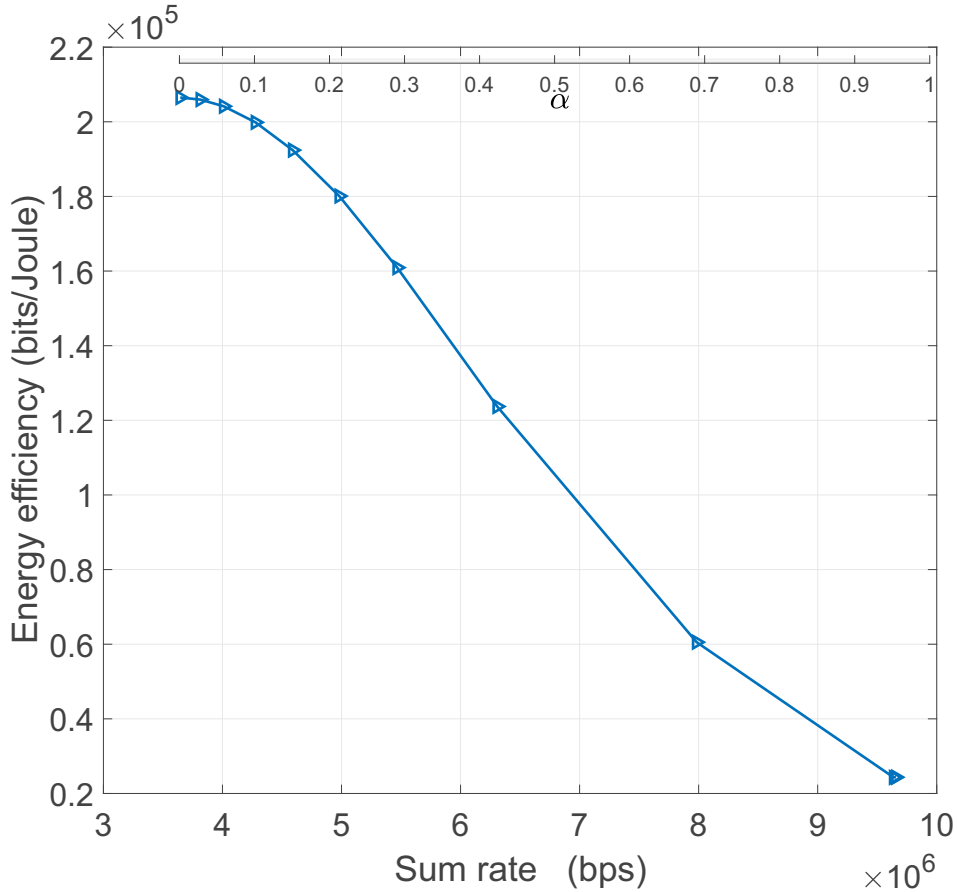


Fig. 5.5 Pareto front of SE-EE trade-off-based design for TX-SNR = 24 dB.

In addition, Fig. 5.5 presents the set of Pareto-optimal solutions (i.e., Pareto-front) with TX-SNR = 24 dB. In particular, this curve provides all best trade-off solutions (Pareto-optimal solutions) for the original SE-EE optimization problem. Furthermore, each point on this curve (sum rate and EE) corresponds to one of the best solutions that can be obtained with the corresponding weight factor. In other words, any improvement in either one of the performance metrics with a given weight factor can only be achieved by the degradation of the other performance metric.

Sum rate Fairness Trade-off Beamforming Design

Same simulation parameters that have been developed to demonstrate the performance of the SE-EE design will be exploited here. However, the number of transmit antennas at the base station is increased to four (i.e., $N = 4$), whereas the path loss exponent is set to 2 (i.e., $\kappa = 2$). Fig. 5.6 demonstrates the achieved sum rate and FI over the weight factor α . As

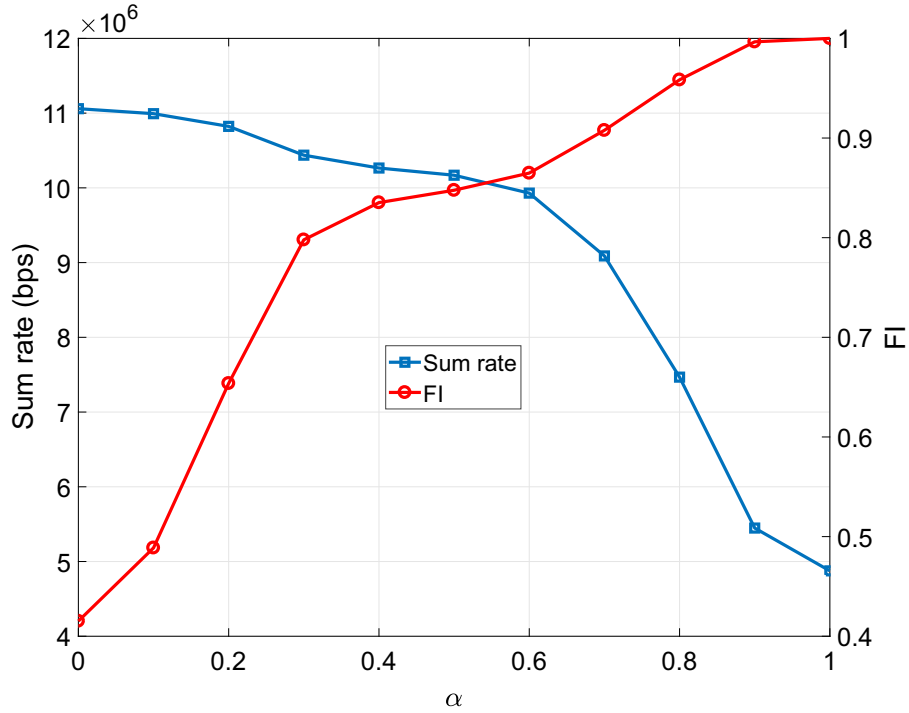


Fig. 5.6 Achieved sum rate and FI against the weight factor α , TX-SNR=30 dB.

expected, the problem \tilde{OP}_9 becomes SRM at $\alpha = 0$, and the maximum sum rate is achieved at the cost of lower FI. Furthermore, the optimal fairness is achieved when the weight factor is set to be one (i.e., $\alpha = 1$). In particular, the problem \tilde{OP}_9 turns out to be MMR with $\alpha = 1$. However, the base station can appropriately choose a value for the weight factor α so that a good balance between the sum rate and FI can be achieved. A good trade-off between these performance metrics can be achieved by choosing $\alpha = 0.5$, as shown in Fig. 5.6.

In addition, Table 5.1 demonstrates the importance of the proposed sum rate-fairness trade-off-based design over the other fixed beamforming design. In particular, the base station decides the weights of each of the conflicting performance metrics (i.e., sum rate and FI) based on the instantaneous channel state information of the users. To demonstrate this in a detailed manner, the rates of the weakest and strongest users, the achieved sum rate, and

Table 5.1 The impact of the weakest user distance (i.e., d_5) on the sum rate and FI with different weight factors, at TX-SNR=35 dB.

	Case 1, $d_5=10$ m				Case 2, $d_5=100$ m				Case 3 $d_5=1000$ m			
	R (Mbps)	R_5 (Mbps)	R_1 (Mbps)	FI	R (Mbps)	R_5 (Mbps)	R_1 (Mbps)	FI	R (Mbps)	R_5 (Mbps)	R_1 (Mbps)	FI
$\alpha = 0$	13.598	0.5537	8.9750	0.4224	13.4003	0.2033	9.2729	0.3845	13.2006	0.0042	9.2421	0.3750
$\alpha = 0.25$	13.1764	2.0968	3.6811	0.9571	12.9283	0.3935	4.2581	0.7974	12.9127	0.0057	5.1300	0.6559
$\alpha = 0.5$	12.9801	2.3456	3.0192	0.992	12.6967	0.4279	3.4141	0.8487	12.3254	0.0081	3.5196	0.7930
$\alpha = 0.75$	12.9111	2.3686	2.8195	0.9966	10.9714	0.9287	2.5853	0.9229	12.2129	0.0082	3.1948	0.8004
$\alpha = 1$	12.7126	2.6919	2.4219	0.999	7.6435	1.1216	1.3380	0.9484	0.1469	0.0340	0.0374	0.9951

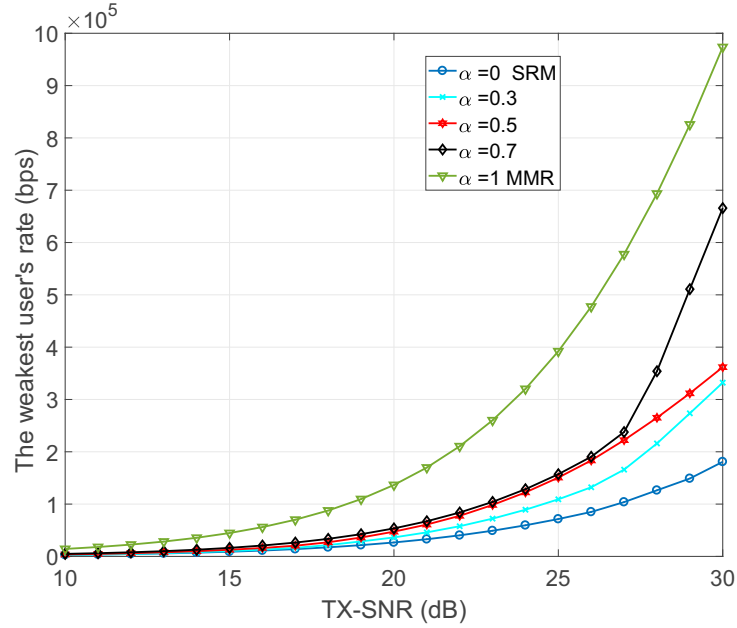


Fig. 5.7 The weakest user's rate against the available transmit power for different weight factors α .

the FI are presented through increasing the distance of the weakest user from 10 to 1000 meters, while the distances of the remaining four users in the system remain fixed. As seen in Table 5.1, the SRM beamforming design (i.e., $\alpha = 0$) does not provide a better QoS in terms of fairness and achievable rate of the weakest user as the distance of it increases. For example, when $d_5 = 1000$ meters, the weakest user achieves only a rate of 0.0042 Mbps while the strongest user enjoys a rate of 9.2421 Mbps, with FI of 0.375. Hence, the base station can intelligently assign appropriate weights to maintain a good fairness among the users, such that the weakest user rate is reasonably increased.

Fig. 5.7 illustrates the rate variation of the weakest user for different values of the weight factor α . For example, at TX-SNR= 30 dB, the rate of the weakest user achieves around 0.2 Mbps with $\alpha = 0$; however, this rate can be increased five times by setting the weight factor α to 1. Hence, the base station has the flexibility to determine the achievable rate of the weakest user by appropriately choosing the weight factor α .

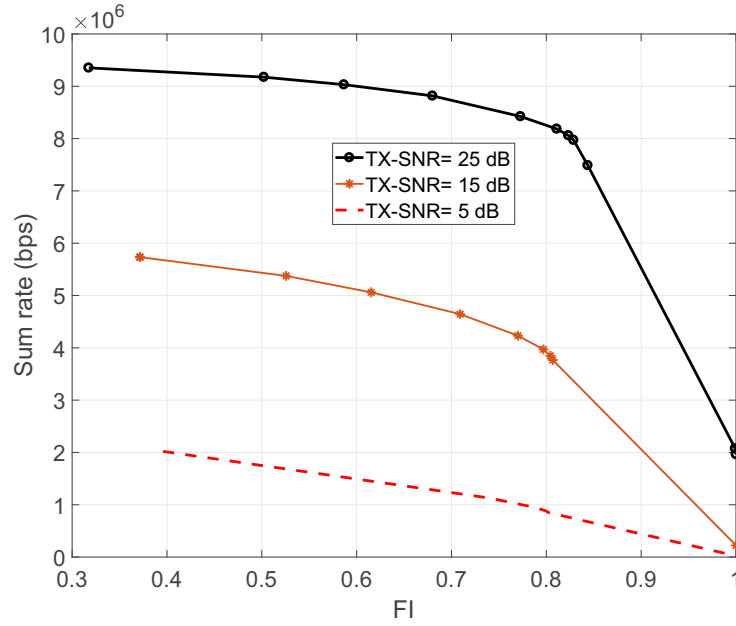


Fig. 5.8 Pareto-front for different TX-SNR thresholds.

Furthermore, the Pareto-optimal fronts of the proposed joint sum rate-fairness-based beamforming design for different TX-SNR thresholds are provided in Fig. 5.8. In particular, the Pareto-front is the set that consists of the best-trade off (i.e., Pareto-optimal) solutions for \tilde{OP}_9 . For instance, at TX-SNR=25 dB, each point on the curve represents the best (sum rate, FI) solution that could be achieved with a particular weight of α . It is worth mentioning that for a given value of α , one of the performance metrics can be improved. However, this improvement cannot be achieved without degrading the performance of the other metric.

5.4 Summary

In this chapter, two different multi-objective beamforming designs are proposed for MISO-NOMA system. Firstly, the spectral-energy efficiency trade-off based design is proposed to strike a good balance between the sum rate and EE. This design provides flexibility to the base station to select the importance for each performance metric based on the instantaneous transmission conditions and the requirement of the systems. Secondly, the sum rate fairness trade-off based design is proposed to strike a balance between the overall throughput of the system (i.e., sum rate) and the fairness between users. As such, the base station can assign more weight to sum rate if the fairness between users is not a key requirement of the system. These designs are formulated as MOO problems, which are difficult to solve directly. There-

fore, these MOO problem are first mapped to SOO form to evaluate the best-trade off solutions (Pareto-optimal solutions) by utilizing the weight-sum function. However, the developed SOO problems are non-convex in nature, therefore, SCA technique is exploited to evaluate the Pareto-optimal solution, iteratively. Then, the simulation results show that these multi-objective beamforming designs have multiple advantages over the conventional single-objective designs.

Chapter 6

Energy Harvesting of Hybrid TDMA-NOMA Technique

In this chapter, the EH capabilities of a hybrid TDMA-NOMA system is investigated. In particular, SWIPT technique is employed to simultaneously transfer information and power to users through wireless channels. As such, power allocation and power splitting ratios for all users to minimize the required transmit power under minimum rate and minimum EH requirements are jointly determined. In simulation results, the performance of the proposed hybrid TDMA-NOMA design is evaluated, where it is demonstrated that the proposed hybrid scheme outperforms the conventional TDMA system in terms of transmit power consumption.

6.1 Introduction

It is well known that NOMA can be integrated with the existing conventional OMA schemes, including TDMA and OFDMA [118]. In such hybrid systems, an orthogonal RB (i.e., time slot or frequency slot) is assigned to serve a group of users, whereas the users in each group are served based on NOMA. These hybrid systems can offer several advantages over the conventional systems with OMA schemes. Firstly, the integration of NOMA with the OMA schemes provides additional degrees of freedom which can be exploited with the available domains [118], [119]. Secondly, it is obvious that grouping the users (i.e., clustering) minimizes the effects of inevitable residual errors associated with SIC by significantly reducing the required number of SIC implementations [120], which facilitates employing NOMA in dense networks.

However, massive connectivity offered by these hybrid OMA-NOMA schemes has a direct negative impact on the power consumption of such systems. As a result, an explosive

growth in the power consumption is inevitable [61], which brings up different environmental issues including global warming and natural disasters, as well as financial pressures on both service providers and customers [61]. To address these issues, the power consumption in wireless transmission has been recently considered in the literature by either allocating the power resources to maximize the EE of systems [61], [9] or by incorporating the novel SWIPT technique [63]. In SWIPT, the receiver has the capability to simultaneously harvest energy and decode information [63]. In particular, this could be accomplished by splitting the received RF signal through either time splitting or power splitting techniques [64]. Despite of the low complexity of the former, this requires a better synchronization between the receiver and the transmitter to precisely perform the splitting [63], and thus, the latter is typically more desirable. In fact, SWIPT is expected to contribute in feeding the power-hungry users, especially in ultra-dense sensor networks, where hundreds of unreachable sensors seek power to extend their life-time [63]. Due to the co-channel interference introduced by exploiting the same RB to serve multiple users in the hybrid TDMA-NOMA systems, it is expected that these systems will have better EH capabilities compared to the conventional TDMA systems.

Motivated by that aforementioned discussion, the EH capabilities of the multi-user SISO hybrid TDMA-NOMA system is investigated in this chapter. As such, the hybrid TDMA-NOMA system model is firstly introduced with considering the EH capability of each user. Then, the required minimum transmit power at base station to meet QoS requirements is evaluated. In fact, these requirements include the minimum rate and minimum harvested power at each user. The design parameters, i.e., the power allocations and the power splitting ratios, corresponding to the minimum transmit power are jointly determined through solving a P-Min problem for the hybrid TDMA-NOMA scheme. However, due to the non-convexity of the P-Min problem, SCA is exploited to *jointly* optimize these design parameters. Finally, the performance of the proposed hybrid TDMA-NOMA design is compared with that of the conventional TDMA scheme.

6.2 System Model and Problem Formulation

6.2.1 System Model

A multi-user SISO hybrid TDMA-NOMA system with K users is considered, where the k^{th} single-antenna user (u_k) is located at a distance d_k (in meter) from the base station. Furthermore, the users are divided into C groups, and the available time for transmission (T) is divided equally among these groups, as shown in Fig. 6.1. The number of users in

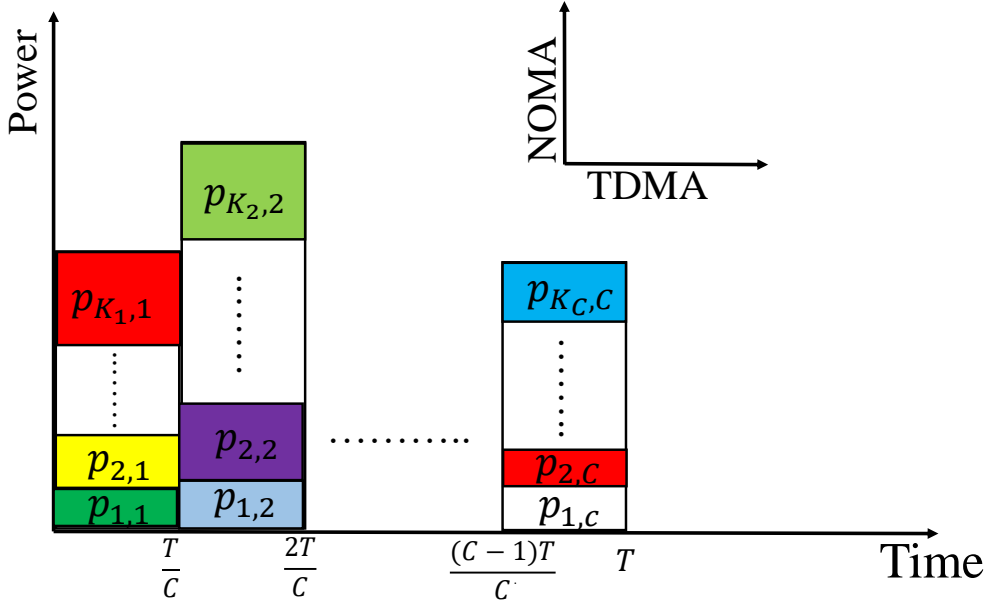


Fig. 6.1 Hybrid TDMA-NOMA system; the users are divided among C groups.

the i^{th} group (G_i) is denoted by $K_i, \forall i \in \mathcal{C} \triangleq \{1, 2, \dots, C\}$, such that $K = \sum_{i=1}^C K_i$. Note that the time slot allocated to serve group G_i is denoted by t_i , such that $T = \sum_{i=1}^C t_i$, and $t_i = \frac{T}{C}$. Furthermore, the j^{th} user in G_i is denoted by $u_{j,i}$. In particular, user grouping has a considerable impact on the performance of the hybrid TDMA-NOMA system. Hence, a user grouping strategy is discussed in the next section. Furthermore, multiple users in each group are served based on NOMA, such that the transmit signal at the base station at t_i is denoted by x_i , and it is expressed as

$$x_i = \sum_{j=1}^{K_i} p_{j,i} x_{j,i}. \quad (6.1)$$

Note that $p_{j,i}^2$ and $x_{j,i}$ denote the allocated power and the signal intended for the user j in G_i (i.e., $u_{j,i}$), respectively. Based on this, the received signal at $u_{j,i}$ can be expressed as

$$r_{j,i} = h_{j,i} x_i + n_{j,i}, \forall i \in \mathcal{C}, \forall j \in \mathcal{K}_i \triangleq \{1, 2, \dots, K_i\}, \quad (6.2)$$

where $h_{j,i}$ is the channel coefficient between the base station and $u_{j,i}$. In particular, the corresponding channel gain can be written as $|h_{j,i}|^2 = \frac{\eta}{(d_{j,i}/d_o)^\kappa}$ [121], where d_o and $d_{j,i}$ represent the reference distance and the distance between $u_{j,i}$ and the base station (in meters), respectively. Furthermore, η and κ represent the signal attenuation at d_o and the path loss exponent, respectively. In addition, $n_{j,i}$ is the AWGN with zero mean and variance $\sigma_{j,i}^2$ dBm. In fact, user ordering at each group plays a crucial role on the performance of NOMA systems

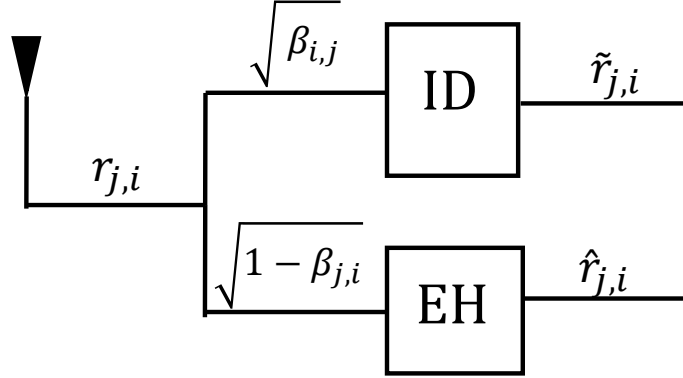


Fig. 6.2 Illustration of splitting the received signal at $u_{j,i}$.

[122]. Note that the optimal ordering can be determined through an exhaustive search among all ordering possibilities, which is not possible in practical scenarios, especially in dense networks [123], [124]. Hence, the users in each group are ordered based on their channel strengths [44], as follows:

$$|h_{1,i}|^2 \geq |h_{2,i}|^2 \geq \dots \geq |h_{K_i,i}|^2, \quad \forall i \in \mathcal{C}. \quad (6.3)$$

Now, it is assumed that each user has a potential capability to split the received signal into two parts such that $\sqrt{\beta_{j,i}}$ (i.e., $0 < \beta_{j,i} < 1$) of $r_{j,i}$ is used to decode information, whereas $\sqrt{1 - \beta_{j,i}}$ of $r_{j,i}$ is utilized to harvest energy, as shown in Fig. 6.2.

Information Decoding (ID) Stage

At this stage, the fraction of received signal $\sqrt{\beta_{j,i}} r_{j,i}$ is utilized to decode the information. Therefore, the signal split to the ID stage can be written as follows:

$$\tilde{r}_{j,i} = \sqrt{\beta_{j,i}} \left(h_{j,i} \sum_{s=1}^{K_i} p_{s,i} x_{s,i} + n_{j,i} \right) + \tilde{n}_{j,i}, \quad \forall i \in \mathcal{C}, \forall j \in \mathcal{K}_i, \quad (6.4)$$

where $\tilde{n}_{j,i}$ is AWGN with zero mean and variance $\tilde{\sigma}_{j,i}^2$ dBm, which is introduced due to processing $r_{j,i}$ on the ID stage [71], [63]. Based on the user ordering defined in (6.3), $u_{j,i}$ performs SIC to detect and remove the signals of the weaker users $u_{j+1,i} \dots u_{K_i,i}$ prior to decoding its own signal. Note that it is assumed that SIC is implemented with no errors.

Hence, the received signal at $u_{j,i}$ after employing SIC can be written as follows:

$$\tilde{r}_{j,i}^{\text{SIC}} = \sqrt{\beta_{j,i}} \left(h_{j,i} p_{j,i} x_{j,i} + h_{j,i} \sum_{s=1}^{j-1} p_{s,i} x_{s,i} + n_{j,i} \right) + \tilde{n}_{j,i}, \forall i \in \mathcal{C}, \forall j \in \mathcal{K}_i. \quad (6.5)$$

Accordingly, the SINR at which $u_{j,i}$ decodes the message of $u_{d,i} \forall d \in \{j+1, \dots, K_i\}$ can be written as

$$\text{SINR}_{j,i}^d = \frac{\beta_{j,i} |h_{j,i}|^2 p_{d,i}^2}{\beta_{j,i} |h_{j,i}|^2 \sum_{s=1}^{d-1} p_{s,i}^2 + \beta_{j,i} \sigma_{j,i}^2 + \tilde{\sigma}_{j,i}^2} \quad \forall i \in \mathcal{C}, \forall j \in \mathcal{K}_i, \forall d \in \{j+1, j+2, \dots, K_i\}. \quad (6.6)$$

Note that $u_{j,i}$ has the capability to decode the message of the weaker user $u_{d,i} \forall d \in \{j+1, \dots, K_i\}$ if and only if the messages intended for these weaker users are received at $u_{j,i}$ with higher SINR compared to that of the users with stronger channel conditions. In particular, this can be guaranteed by including the following condition:

$$p_{K_i,i}^2 \geq p_{K_i-1,i}^2 \geq \dots \geq p_{1,i}^2, \forall i \in \mathcal{C}. \quad (6.7)$$

The above constraint is referred as SIC constraint throughout this chapter. Based on this condition, the SINR of $u_{j,i}$ can be defined as [67]

$$\text{SINR}_{j,i} = \min\{\text{SINR}_{j,i}^1, \text{SINR}_{j,i}^2, \dots, \text{SINR}_{j,i}^j\}, \forall i \in \mathcal{C}, \forall j \in \mathcal{K}_i. \quad (6.8)$$

Therefore, the achieved rate at $u_{j,i}$ can be written as follows:

$$R_{j,i} = t_i \log_2(1 + \text{SINR}_{j,i}), \forall i \in \mathcal{C}, \forall j \in \mathcal{K}_i. \quad (6.9)$$

Note that the total required transmit power at the BS can be expressed as $P_t = \sum_{i=1}^C \sum_{j=1}^{K_i} p_{j,i}^2$.

EH Stage

Next, the received signal part at the EH stage is considered. In particular, the EH circuit consists of a matching network, a radio frequency to direct current (RF-DC) converter, and a storage unit [62]. The signal split to the EH stage can be written as

$$\hat{r}_{j,i} = \sqrt{(1 - \beta_{j,i})} \left(h_{j,i} \sum_{s=1}^{K_i} p_{s,i} x_{s,i} + n_{j,i} \right) + \hat{n}_{j,i}, \forall i \in \mathcal{C}, \forall j \in \mathcal{K}_i, \quad (6.10)$$

where $\hat{n}_{j,i}$ is AWGN introduced by the processing of the received signal at the EH stage with zero mean and variance $\hat{\sigma}_{j,i}^2$ dBm. Note that $\hat{r}_{j,i}$ is utilized to harvest the energy at $u_{j,i}$. Hence, the harvested power at $u_{j,i}$ can be defined as [64]

$$P_{j,i} = \eta (1 - \beta_{j,i}) \left(|h_{j,i}|^2 \sum_{s=1}^{K_i} p_{s,i}^2 \right), \forall i \in \mathcal{C}, \forall j \in \mathcal{K}_i, \quad (6.11)$$

where $\eta \in [0, 1]$ is the efficiency of the RF-DC in the EH stage [62]. Note that the total harvested power by all users in the system (P_H) can be written as $P_H = \sum_{i=1}^C \sum_{j=1}^{K_i} P_{j,i}$.

6.2.2 Problem Formulation

In this subsection, to investigate the EH capabilities of the hybrid TDMA-NOMA scheme, a P-Min design is formulated. In particular, the base station aims to minimize the transmit power (i.e., P_t) under minimum harvesting power and minimum data rate requirements at each user. Note that this design seeks to determine a power allocation (i.e., $p_{j,i}$) and a power splitting ratio (i.e., $\beta_{j,i}$) $\forall i \in \mathcal{C}, \forall j \in \mathcal{K}_i$ for each user in the system. These design parameters can be determined through solving the following P-Min problem:

$$OP_{10} \text{ minimize}_{\{p_{j,i}, \beta_{j,i}\}_{i=1}^C} \sum_{i=1}^C \sum_{j=1}^{K_i} p_{j,i}^2 \quad (6.12a)$$

$$\text{subject to} \quad R_{j,i} \geq R^{\min}, \forall i \in \mathcal{C}, \forall j \in \mathcal{K}_i, \quad (6.12b)$$

$$P_{j,i} \geq P^{\min}, \forall i \in \mathcal{C}, \forall j \in \mathcal{K}_i, \quad (6.12c)$$

$$p_{K_i,i}^2 \geq \dots \geq p_{1,i}^2, \forall i \in \mathcal{C}, \quad (6.12d)$$

$$0 \leq \beta_{j,i} \leq 1, \forall j \in \mathcal{K}_i, \forall i \in \mathcal{C}. \quad (6.12e)$$

Note that R^{\min} and P^{\min} denote the minimum rate and minimum harvested power requirements at each user, respectively. It is obvious that the optimization problem in (6.12) is non-convex due to the non-convex constraints in (6.12b) and (6.12c). Furthermore, the solution of this optimization problem needs to be determined by jointly optimizing the design parameters $\{p_{j,i}, \beta_{j,i}\} \forall i, \forall j$.

6.3 Proposed Methodology and Discussions

In this section, an iterative approach is proposed to jointly solve the original non-convex optimization problem OP_{10} in (6.12). Later in this section, some light is shed on the initial

parameters selection and convergence of the proposed iterative approach. However, a brief discussion is firstly presented on the proposed grouping strategy in the following subsection.

6.3.1 Grouping Strategy

Choosing an appropriate grouping strategy plays a crucial role on the performance of the hybrid TDMA-NOMA system, as the optimal solution of OP_{10} can be only determined by formulating the best groups. In particular, the required optimal transmit power can be only determined by solving OP_{10} with an exhaustive search among all possible set of groups. However, it is expensive in terms of computational complexity and unaffordable in practical systems, including IoTs in future wireless networks. Furthermore, the difference between the channel strengths of the users in the same group is another key factor that determines the overall performance of the system. As the users within each group are served based on NOMA, the practical implementation of the SIC technique requires the difference between the channel strengths of the users to be as large as possible [118], [38]. Furthermore, grouping users with a similar channel strength would introduce errors in the SIC implementation, which would degrade the overall performance of the system [34]. Based on this key fact, the users are grouped such that the difference between their channel strengths is as high as possible. For example, with two users in each group (i.e., $K_i = 2$), the user groups based on the proposed grouping strategy can be defined as

$$(\{u_{1,1}, u_{2,1}\}, \{u_{1,2}, u_{2,2}\}, \dots, \{u_{1,C}, u_{2,C}\}) \equiv \left(\{u_1, u_K\}, \{u_2, u_{K-1}\}, \dots, \{u_{\frac{K}{2}}, u_{\frac{K}{2}+1}\} \right). \quad (6.13)$$

It is worth to point out that this channel gain difference grouping technique has been widely employed in the context of different NOMA approach such as [125]. In particular, several sub-optimal clustering techniques can also be proposed, however, the performance of such techniques can be investigated in future work.

6.3.2 Proposed Algorithm

With the assumption that the users have been already grouped into groups as in (6.13), the non-convex optimization problem OP_{10} is now solved through the SCA technique. In SCA, the non-convex terms are approximated by a set of lower bounded convex terms, and then, the original non-convex problem is solved with these approximated convex problem. The non-convexity of the constraint in (6.12b) is firstly handled by introducing new slack

variables $\vartheta_{j,i}$ and $\theta_{j,i}$, such that,

$$R_{j,i} \geq \vartheta_{j,i}, \forall i \in \mathcal{C}, \forall j \in \mathcal{K}_i. \quad (6.14a)$$

$$(1 + \text{SINR}_{j,i}^d) \geq \theta_{j,i}, \forall i \in \mathcal{C}, \forall j \in \mathcal{K}_i, \forall d \in \{j+1, \dots, \mathcal{K}_i\}, \quad (6.14b)$$

$$\theta_{j,i} \geq 2^{\vartheta_{j,i}} \forall i \in \mathcal{C}, \forall j \in \mathcal{K}_i. \quad (6.14c)$$

To handle the non-convexity of (6.14b), a slack variable $\chi_{j,i}$ is inserted such that

$$\frac{\beta_{j,i} |h_{j,i}|^2 p_{d,i}^2}{\beta_{j,i} |h_{j,i}|^2 \sum_{s=1}^{d-1} p_{s,i}^2 + \beta_{j,i} \sigma_{j,i}^2 + \tilde{\sigma}_{j,i}^2} \geq \frac{(\theta_{j,i} - 1) \chi_{j,i}^2}{\chi_{j,i}^2}, \quad \forall i \in \mathcal{C}, \forall j \in \mathcal{K}_i, \forall d \in \{j+1, j+2, \dots, \mathcal{K}_i\}. \quad (6.15)$$

Then, the constraint in (6.15) is decomposed into the following two constraints:

$$\beta_{j,i} |h_{j,i}|^2 p_{d,i}^2 \geq (\theta_{j,i} - 1) \chi_{j,i}^2, \forall i \in \mathcal{C}, \forall j \in \mathcal{K}_i, \forall d \in \{j+1, j+2, \dots, \mathcal{K}_i\}, \quad (6.16)$$

$$\beta_{j,i} |h_{j,i}|^2 \sum_{s=1}^{d-1} p_{s,i}^2 + \beta_{j,i} \sigma_{j,i}^2 + \tilde{\sigma}_{j,i}^2 \leq \chi_{j,i}^2, \forall i \in \mathcal{C}, \forall j \in \mathcal{K}_i, \forall d \in \{j+1, j+2, \dots, \mathcal{K}_i\}. \quad (6.17)$$

To handle the non-convexity of these constraints, another slack variable $\alpha_{j,i}^d$ is incorporated such that

$$\beta_{j,i} p_{d,i}^2 \geq \alpha_{j,i}^d \forall i \in \mathcal{C}, \forall j \in \mathcal{K}_i, \forall d \in \{j+1, j+2, \dots, \mathcal{K}_i\}. \quad (6.18)$$

It is obvious that the constraint in (6.18) is still non-convex. Therefore, the first-order Taylor series is exploited to approximate the left-hand side of (6.18) with a linear term. Doing so, the approximated convex form of (6.18) can be written as

$$\beta_{j,i}^{(t)} p_{d,i}^{2(t)} + 2p_{d,i}^{(t)} \beta_{j,i}^{(t)} (p_{d,i} - p_{d,i}^{(t)}) + p_{d,i}^{2(t)} (\beta_{j,i} - \beta_{j,i}^{(t)}) \geq \alpha_{j,i}^d, \quad \forall i \in \mathcal{C}, \forall j \in \mathcal{K}_i, \forall d \in \{j+1, j+2, \dots, \mathcal{K}_i\}, \quad (6.19)$$

where $\beta_{j,i}^{(t)}$ and $p_{d,i}^{(t)}$ represent the approximations of $\beta_{j,i}$ and $p_{d,i}$ at the t^{th} iteration, respectively. By incorporating these slack variables, the non-convex constraint in (6.16) can be approximately replaced by the following convex constraint:

$$|h_{j,i}|^2 \alpha_{j,i}^d \geq \chi_{j,i}^{2(t)} (\theta_{j,i}^{(t)} - 1) + 2 (\theta_{j,i}^{(t)} - 1) \chi_{j,i}^{(t)} (\chi_{j,i} - \chi_{j,i}^{(t)}) + \chi_{j,i}^{2(t)} (\theta_{j,i} - \theta_{j,i}^{(t)}), \quad \forall i \in \mathcal{C}, \forall j \in \mathcal{K}_i, \forall d \in \{j+1, j+2, \dots, \mathcal{K}_i\}. \quad (6.20)$$

Note that the non-convex right-hand side of inequality (6.16) is approximated with a linear term. Similarly, the approximated convex form of constraint (6.17) is written as

$$\chi_{j,i}^{2(t)} + 2\chi_{j,i}^{(t)} \left(\chi_{j,i} - \chi_{j,i}^{(t)} \right) \geq \gamma \left(|h_{j,i}|^2 \sum_{s=1}^{d-1} \alpha_{j,i}^s + \beta_{j,i} \sigma_{j,i}^2 + \tilde{\sigma}_{j,i}^2 \right). \quad (6.21)$$

Based on these multiple slack variables, the achieved rate at each user (i.e., $R_{j,i}$) can be equivalently approximated by $\vartheta_{j,i}$ with the constraints in (6.14c), (6.19), (6.20), and (6.21). Next, the non-convexity of the constraint in (6.12c) is tackled by incorporating slack variables $\rho_{i,j}$ and $\varrho_{i,j}$, such that

$$(1 - \beta_{j,i}) p_{s,i}^2 \geq \rho_{j,i}^s, \forall i \in \mathcal{C}, \forall j \in \mathcal{K}_i, \forall s \in \mathcal{K}_i, \quad (6.22a)$$

$$\eta |h_{j,i}|^2 \sum_{s=1}^{K_i} \rho_{j,i}^s \geq \varrho_{i,j}, \forall i \in \mathcal{C}, \forall j \in \mathcal{K}_i. \quad (6.22b)$$

Without loss of generality, the non-convex constraint in (6.22a) can be tackled by following the same approximations developed to handle the previous constraint in (6.18). Hence,

$$\left(1 - \beta_{j,i}^{(t)} \right) p_{s,i}^{2(t)} + 2p_{s,i}^{(t)} \left(1 - \beta_{j,i}^{(t)} \right) \left(p_{s,i} - p_{s,i}^{(t)} \right) - p_{s,i}^{2(t)} \left(\beta_{j,i} - \beta_{j,i}^{(t)} \right) \geq \rho_{j,i}^s, \\ \forall i \in \mathcal{C}, \forall j \in \mathcal{K}_i, \forall s \in \mathcal{K}_i. \quad (6.23)$$

Finally, the non-convexity of the SIC constraint in (6.12d) is tackled by replacing each element in this constraint by the following linear approximation:

$$p_{K_i,i}^2 \geq p_{K_i,i}^{2(t)} + 2p_{K_i,i}^{(t)} \left(p_{K_i,i} - p_{K_i,i}^{(t)} \right), \forall i. \quad (6.24)$$

Based on these multiple slack variable incorporations, the non-convex optimization problem in (6.12) can be equivalently written as

$$\tilde{O}P_{10}: \underset{\Gamma}{\text{minimize}} \quad \sum_{i=1}^C \sum_{j=1}^{K_i} p_{j,i}^2 \quad (6.25a)$$

$$\text{subject to} \quad r_{j,i} \geq R^{\min}, \varrho_{j,i} \geq P^{\min}, \forall i \in \mathcal{C}, \forall j \in \mathcal{K}_i, \quad (6.25b)$$

$$(6.12d), (6.12e), (6.14c), (6.19), (6.20), (6.21), (6.23), \quad (6.25c)$$

where Γ includes all the optimization variables involved in the P-Min design:

$$\Gamma = \{p_{j,i}, r_{j,i}, \beta_{j,i}, \varrho_{j,i}, \rho_{j,i}, \alpha_{j,i}\}_{i=1}^K.$$

The solution of the optimization problem in (6.25) requires an appropriate selection of the initial variables (i.e., $\Gamma^{(0)}$). Therefore, random initial power allocations $\{p_{j,i}^{(0)}\}_{i=1}^K$ are assumed. Then, the corresponding initial power splitting ratios (i.e., $\{\beta_{j,i}^{(0)}\}_{i=1}^K$) that satisfy the constraints of the original optimization problem OP_{10} , are evaluated. Furthermore, the remaining slack variables $\rho_{j,i}^{(0)}$ and $\alpha_{j,i}^{(0)}$ can be determined by substituting $\{p_{j,i}^{(0)}\}_{i=1}^K$ and $\{\beta_{j,i}^{(0)}\}_{i=1}^K$ in (6.19) and (6.20), respectively. The algorithm proposed to solve the original P-Min problem is summarized in Algorithm 6. The algorithm terminates when the absolute difference between two sequential optimal values is less than a defined threshold μ .

Algorithm 6 P-Min Design using SCA.

Step 1: Group users based on (6.13)

Step 2: Initialize all design parameters $\Gamma^{(0)}$

Step 3: Repeat

1. Solve the optimization problem in (6.25)
2. Update $\Gamma^{(n+1)}$

Step 3: Until required accuracy is achieved.

To demonstrate the performance of the proposed EH design of the hybrid TDMA-NOMA system, the performance of it is compared with that of the conventional TDMA system. In the TDMA system, each time slot ($t_i^{\text{TDMA}} = \frac{T}{K}$) is employed to serve only one user. Based on this time slot assignment, the achieved rate at u_i can be written as

$$R_i^{\text{TDMA}} = t_i^{\text{TDMA}} \log_2 \left(1 + \frac{\beta_i |h_i|^2 p_i^2}{\beta_i \sigma_i^2 + \tilde{\sigma}_i^2} \right), \forall i \in \mathcal{K}. \quad (6.26)$$

On the other hand, the harvested power at u_i in this conventional TDMA can be represented as

$$P_i^{\text{TDMA}} = \eta (1 - \beta_i) |h_i|^2 p_i^2, \forall i \in \mathcal{K}. \quad (6.27)$$

Now, a similar P-Min problem in a TDMA system with minimum rate and minimum EH constraints is formulated. As such,

$$OP_{11} : \underset{\{p_i, \beta_i\}_{i=1}^K}{\text{minimize}} \quad \sum_{i=1}^K p_i^2 \quad (6.28a)$$

$$\text{subject to} \quad R_i^{\text{TDMA}} \geq R^{\min}, \forall i \in \mathcal{K}, \quad (6.28b)$$

$$P_i^{\text{TDMA}} \geq P^{\min}, \forall i \in \mathcal{K}. \quad (6.28c)$$

Note that the developed optimization problem in (6.28) for the TDMA system is solved using the same SCA technique.

6.4 Simulation Results

In this section, the EH capability of the proposed hybrid TDMA-NOMA scheme is demonstrated by evaluating and comparing its performance with that of the conventional TDMA scheme. In these numerical simulations, ten users (i.e., $K = 10$) that are uniformly distributed in a circle of radius 10 meter from the base station are considered. In addition, these users are divided into five groups (i.e., $C = 5$), where T is chosen to be 1 second. Table 6.1 summarizes the different parameters adopted in simulations [121]. In addition, the CVX toolbox [90] is used to generate results in this section.

Table 6.1 Parameter values used in simulations.

Parameter	Value
Number of users (K)	10
Number of groups (C)	5
Number of users in each group (K_i)	2
Path loss exponent (κ)	2
Reference distance (d_0)	1
Signal attenuation at d_0 (η)	-30 dB
$\sigma_i^2, \hat{\sigma}_{j,i}^2, \tilde{\sigma}_{j,i}^2$ (dBm)	-100
Efficiency of converter (η)	0.75

Table 6.2 Splitting ratio $\beta_{j,i}$ for all users, with a minimum rate requirement $R^{\min} = 10^{-1}$ bit/Hz .

Cluster 1		Cluster 2		Cluster 3		Cluster 4		Cluster 5	
$\beta_{1,1}$	$\beta_{2,1}$	$\beta_{1,2}$	$\beta_{2,2}$	$\beta_{1,3}$	$\beta_{2,3}$	$\beta_{1,4}$	$\beta_{2,4}$	$\beta_{1,5}$	$\beta_{2,5}$
0.8738	0.0062	0.5807	0.0063	0.4250	0.0063	0.3343	0.0064	0.2757	0.0064

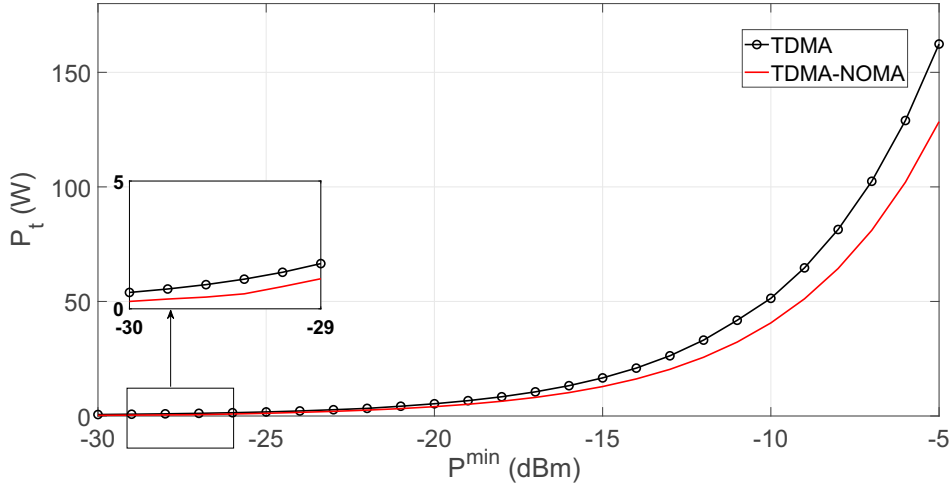


Fig. 6.3 The required transmit power versus different minimum harvest power requirements P^{\min} , with a minimum rate requirement $R^{\min} = 10^{-1}$ bit/Hz.

Fig. 6.3 illustrates and compares the minimum required transmit power (i.e., P_t) against a range of minimum harvest power requirements P^{\min} for the hybrid TDMA-NOMA and the conventional TDMA systems. As expected, P_t of both systems increases with the increase of P^{\min} . Furthermore, as shown in Fig. 6.3, the hybrid TDMA-NOMA scheme exhibits a better performance, as it consumes less P_t compared to the conventional TDMA system. In particular, users grouping in the hybrid TDMA-NOMA system introduces higher interference levels, which facilitates the satisfaction of the minimum harvested power requirements with lower P_t compared to the conventional TDMA system.

Now, the splitting ratios $\beta_{i,j}$ associated with solving the optimization problem OP_{10} are introduced in Table 6.2. As seen, these ratios depend on the channel conditions of the users. Next, the effect of minimum rate requirement R^{\min} in the required transmit value is shown in Table 6.3. Clearly, the required transmit power decreases with the lower minimum rate requirements.

Next, the number of iterations required for the convergence of SCA algorithm to solve OP_{10} for two different minimum harvested power requirements are evaluated in Fig. 6.4. As seen, the algorithm converges to the solution within a few iterations.

Table 6.3 The required transmit power for different minimum rate requirement R^{\min} , with a minimum harvest power requirement $P^{\min} = -30$ dBm.

R^{\min} (bit/Hz)	10^{-1}	10^{-2}	10^{-3}
P_t (W)	2.4154	2.2071	1.6581

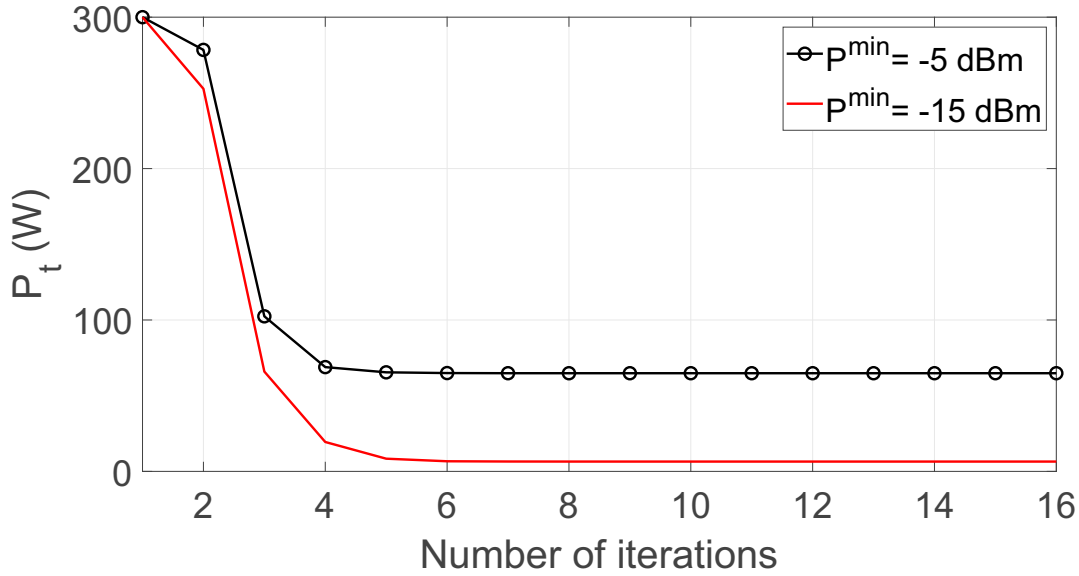


Fig. 6.4 The convergence of the SCA algorithm to solve OP_{10} for different values of the minimum harvest power requirement P^{\min} , $R^{\min} = 10^{-2}$ bit/Hz.

6.5 Summary

In this chapter, the EH capabilities of a multi-user SISO hybrid TDMA-NOMA system is investigated. In such a hybrid system, users are divided into a number of groups, with a time slot assigned to serve each group and NOMA employed to serve users within a group. For the proposed scheme, the required minimum power to meet the minimum rate and minimum harvest energy requirements at each user is evaluated. Simulation results confirmed that the proposed hybrid TDMA-NOMA system outperforms the conventional TDMA system in terms of the minimum required transmit power.

Chapter 7

Conclusions and Future Work

7.1 Conclusions

NOMA has been recently envisioned as a promising MA scheme that can meet the demanding requirements in 5G and beyond wireless networks. The key advantage behind NOMA is that users can be served simultaneously using same RB by employing power-domain superposition coding. Furthermore, stronger users in NOMA can decode the messages of users with weaker channel conditions by exploiting SIC. To offer additional degrees of freedom, and hence to cultivate its underlying potential benefits, different key technologies have been combined with NOMA. These techniques include multiple antennas-NOMA and hybrid OMA-NOMA systems. In particular, it is expected that these hybrid systems play a crucial role towards significantly improving the performance of 5G and beyond wireless communication systems. However, allocating available resources between users in such systems has a direct impact on their performance. Therefore, different resource allocation techniques have been investigated for different types of NOMA systems throughout this thesis.

In Chapter 4 and Chapter 5, the integration between multiple antennas and NOMA is mainly focused. In particular, beamformer-based MISO-NOMA system is considered where each user is served by a dedicated beamforming vector. In such a system, the performance is determined based on the beamforming design criteria and several beamforming designs have been proposed in Chapter 4 and Chapter 5 to cope with demanding requirements of future wireless communication networks. Specifically, due to the importance of both the power consumption and the achieved rate, three EE-aware beamforming designs have been proposed in Chapter 4. In the first EE-based design, the overall EE of the system is considered with the GEE-Max beamforming design, in which EE of the system is maximized subject to a set of

constraints. The developed GEE-Max optimization problem is non-convex in nature, hence, two iterative algorithms have been developed to obtain solution of this non-convex problem. In particular, SCA algorithm has been firstly proposed to approximate each non-convex term in the problem by a lower bounded convex term, and then the problem is iteratively solved. Furthermore, the Dinkelbach's algorithm has been also exploited to provide an alternative algorithm to solve the GEE-Max optimization problem. In this algorithm, the fractional objective function is parametrized by a non-fractional one, and then, the non-fractional problem is solved using SCA technique. However, due to the unfairness associated with the proposed GEE-Max design, the performance of weaker users are enhanced through developing two EE-fairness designs, namely MMEE and PF designs. As such, the optimal fairness is achieved through the MMEE design, however, this fairness enhancement is achieved at the cost of the overall EE degradation of the system. Therefore, the PF based beamforming design is proposed to offer a good balance between the fairness and the GEE of the system. Simulation results have been also provided to evaluate the performance of the proposed designs through comparing them with other beamforming designs in the literature.

Next, owing the fact that 5G and beyond wireless networks aim to simultaneously improve different conflicting performance metrics, novel multi-performance metrics based beamforming designs have been developed in Chapter 5. In the first design, the SE-EE based beamforming design has been proposed, in which the aim was to consider the conflicting performance metrics, namely SE and EE. In this SE-EE trade-off design, the relative importance of each performance metric is considered through assigning a weight factor. With this weight factor assignment, base station has the flexibility to choose the importance of each objective based on the conditions and environments of the systems. In the second design, the achieved sum rate and the achieved rate at each user is considered through proposing a novel sum rate fairness trade-off beamforming design. In this design, the base station can determine the relative importance of each performance metric based on service requirements and channel conditions of users in the system. In fact, these multi-performance beamforming metric based designs are formulated into MOO problems, which are challenging to solve and cannot be solved directly using classical techniques. Therefore, the weighted-sum approach combined with priori-articulations methods are jointly exploited to transform the original MOO problems into tractable SOO forms. Then, classical optimization techniques are exploited to evaluate Pareto-Optimal solutions of these problems. Simulation results showed that the proposed multi-performance designs have flexible performance compared to the conventional single-performance designs. Particularity, with these multi-performance designs, base station has potential capabilities to strike a good balance between the conflicting metrics through a

possibility of simply tuning the weight factor of each metric.

In Chapter 6, the EH capabilities of a hybrid TDMA-NOMA is considered through employing the SWIPT technique. In such hybrid system, users are divided into a number of groups, with a time slot is assigned to serve each group while NOMA is employed to serve users within a group. Furthermore, each user splits the received signal into two parts, namely EH and ID parts, as such the EH part is utilized to harvest energy while the ID part is assigned to decode information. In particular, the required minimum transmit power to meet the minimum rate and minimum harvest energy requirements at each user is evaluated. This has been achieved through developing P-Min design, in which, the allocated power and power splitting ratio for each user are obtained. Simulation results confirmed that the proposed hybrid TDMA-NOMA system outperforms the conventional TDMA system in terms of the minimum required transmit power.

7.2 Future work

The presented work in this thesis investigated the combination of NOMA with multiple antennas and OMA techniques, these combinations play crucial role in deployment of future wireless networks. Furthermore, several resource allocation techniques have been developed for these NOMA systems, in which different considerations have been taken into account to make these systems reliable in terms of practical implementation. However, there is a number of future work directions that need to be investigated to cultivate additional underlying benefits of NOMA systems, which are summarized as follows.

Error Propagation in SIC

In most existing work on NOMA including the work presented throughout this thesis, it is assumed that stronger users are able to perfectly decode the signals of weaker users prior to decode their own signals using the SIC technique. However, through this SIC process, if any signal is decoded erroneously, then, this error will effect sequentially both, the decoding of the remaining signals in the sequence and decoding of the strong user's signal itself. In particular, practical implementation of NOMA should take this SIC errors into consideration. Therefore, it is important to extend the work of this thesis with considering residual error propagation produced by imperfect SIC receivers.

Cluster-based MISO-NOMA/ Cooperative Transmission

In this thesis, different designs have been developed for a beamformer-based MISO-NOMA system, at which each user is served by a beamforming vector. In particular, the proposed designs can be extended to cluster-based MISO-NOMA systems, where users are grouped into clusters, such that each cluster is served with a beamforming vector whereas the users inside each cluster are served based on NOMA. In addition, cooperative transmission for this cluster-based MISO-NOMA system can be also investigated. With cooperative transmission scenario, stronger user acts as relay to decode and forward the signals of weaker users in the cluster, which can be easily performed as the strong user decodes the signals of weaker users prior to decoding its own signal using the SIC. In particular, the performance of weaker users are expected to be enhanced in this cooperative scenario as they receive two copies of their intended signals, one of them is received in a direct transmission phase, while the second is received in a cooperative transmission phase. Investigating this cluster-based-cooperative MISO-NOMA system through developing different beamforming designs will be an interesting topic.

Resource Allocations using Machine Learning

The proposed resource allocations techniques for NOMA systems throughout the literature including this thesis are mainly solved through iterative algorithms, which introduce challenges on meeting the stringent latency requirements for envisioned real-time applications in future wireless networks. To overcome this processing delay issues, the resource allocation techniques developed in this thesis can be alternatively handled using machine learning (ML) techniques which have potential capabilities to reduce the computational complexity of the solutions. Therefore, through applying appropriate ML techniques, such as deep neural networks, base station can allocate resources by exploiting the previously developed solutions to establish a relationship between the input parameters and corresponding outputs. In other words, these solutions can be used to train different network models that suitably developed these kind of resource allocation problems.

Appendix A

Proofs for Chapter 4

A.1 Proof of Theorem 1

To prove Theorem 1, we firstly rewrite (4.42) such as

$$\chi^* = \frac{f_1(\{\mathbf{w}_i^*\}_{i=1}^K)}{f_2(\{\mathbf{w}_i^*\}_{i=1}^K)} \geq \frac{f_1(\{\mathbf{w}_i\}_{i=1}^K)}{f_2(\{\mathbf{w}_i\}_{i=1}^K)}, \quad (\text{A.1})$$

where $\{\mathbf{w}_i^*\}_{i=1}^K$ denote the beamforming vectors that maximize the original problem OP_1 . Without loss of generality, the condition in (A.1) can be decomposed as

$$f_1(\{\mathbf{w}_i\}_{i=1}^K) - \chi^* f_2(\{\mathbf{w}_i\}_{i=1}^K) \leq 0, \quad (\text{A.2a})$$

$$f_1(\{\mathbf{w}_i^*\}_{i=1}^K) - \chi^* f_2(\{\mathbf{w}_i^*\}_{i=1}^K) = 0, \quad (\text{A.2b})$$

where the left side of (A.2a) denotes the objective function of the parametrized optimization problem OP_5 (i.e., $F(\{\mathbf{w}_i\}_{i=1}^K, \chi^*)$). The inequality in (A.2a) reveals that any feasible beamforming set $\{\mathbf{w}_i\}_{i=1}^K$ (rather than the optimal set) will provide $F(\{\mathbf{w}_i\}_{i=1}^K, \chi^*)$ to be less than zero, whereas the optimal beamforming vectors $\{\mathbf{w}_i^*\}_{i=1}^K$ could be achieved if and only if the condition in (A.2b) is satisfied. Hence, we can determine the optimal beamforming vectors of the original fractional problem OP_1 by solving the non-fractional one in OP_5 with the assumption that the maximum objective value of OP_5 is zero. This completes the proof of Theorem 1. ■

A.2 Proof of Lemma 1

In order to prove the convergence of the Dinkelbach's iterative approach to the optimal solution, the following conditions can be equivalently proven [95]:

$$\chi^{(n+1)} \geq \chi^{(n)}, \quad (\text{A.3a})$$

$$\lim_{n \rightarrow \infty} \chi^{(n)} = \chi^*. \quad (\text{A.3b})$$

We start with $\chi^{(n+1)} \geq \chi^{(n)}$, and it is known that $F(\chi)$ is a non-decreasing function. Therefore

$$\{F(\chi^{(n)}) \geq F(\chi^*) \geq 0 | \chi^{(n)} \leq \chi^*\},$$

which implies that

$$f_1(\{\mathbf{w}_i^{(n)}\}_{i=1}^K) - \chi^n f_2(\{\mathbf{w}_i^{(n)}\}_{i=1}^K) \geq 0. \quad (\text{A.4})$$

On the other hand, the following holds based on (4.44):

$$f_1(\{\mathbf{w}_i^n\}_{i=1}^K) = \chi^{(n+1)} f_2(\{\mathbf{w}_i^{(n)}\}_{i=1}^K). \quad (\text{A.5})$$

By substituting (A.5) in (A.4), then we have;

$$(\chi^{(n+1)} - \chi^{(n)}) f_2(\{\mathbf{w}_i^{(n)}\}_{i=1}^K) > 0.$$

Since $f_2(\{\mathbf{w}_i^{(n)}\}_{i=1}^K)$ is assumed to be always positive, then

$$(\chi^{(n+1)} - \chi^{(n)}) > 0,$$

which confirms the inequality in (A.3a). Now, we consider the second condition in (A.3b) and prove this through contradiction. First, we assume that the condition in (A.3b) does not hold and there exists another non-negative parameter (χ^+) such that

$$\lim_{n \rightarrow \infty} \chi^{(n)} = \chi^+ < \chi^*.$$

Based on this argument, the following holds:

$$F(\chi^+) = 0.$$

However, $F(\chi)$ is a non-decreasing function, which means that

$$\{F(\chi^+) = 0 > F(\chi^*) = 0 | \chi^+ < \chi^*\}, \quad (\text{A.6})$$

which is obviously not true and contradicts the assumption made in the beginning of this proof. Therefore,

$$\lim_{n \rightarrow \infty} \chi^{(n)} = \chi^*.$$

This confirms that the Dinkelbach's iterative algorithm converges to the optimal solution, which completes the proof of Lemma 1. ■

Appendix B

Proofs for Chapter 5

B.1 Proof of Theorem 1

First, we denote the beamforming vectors that provide an optimal solution to \tilde{OP} as $\{\mathbf{w}_i^*\}_{i=1}^K$. Therefore,

$$f_{EE-SE}(\{\mathbf{w}_i^*\}_{i=1}^K) \geq f_{EE-SE}(\{\mathbf{w}_i\}_{i=1}^K), \quad (\text{B.1})$$

which can be rewritten as

$$\sum_{l=1}^2 \alpha_l f_l^{Norm}(\{\mathbf{w}_i^*\}_{i=1}^K) - \sum_{l=1}^2 \alpha_l f_l^{Norm}(\{\mathbf{w}_i\}_{i=1}^K) \geq 0. \quad (\text{B.2})$$

The inequality in (B.2) can be equivalently reformulated as

$$\sum_{l=1}^2 \frac{\alpha_l}{f_l^*} (f_l(\{\mathbf{w}_i^*\}_{i=1}^K) - f_l(\{\mathbf{w}_i\}_{i=1}^K)) \geq 0. \quad (\text{B.3})$$

In particular, we prove Theorem 1 by using a contradiction argument, as follows. First, we assume that $\{\mathbf{w}_i^*\}_{i=1}^K$ is not a Pareto-optimal solution to the original optimization problem OP . This assumption implies that there exists another feasible solution $\{\mathbf{w}_i'\}_{i=1}^K$ such that

$$\mathbf{f}\{\mathbf{w}_i'\}_{i=1}^K \succ \mathbf{f}\{\mathbf{w}_i^*\}_{i=1}^K. \quad (\text{B.4})$$

The condition in (B.4) can be equivalently written as

$$(f_l(\{\mathbf{w}_i'\}_{i=1}^K) - f_l(\{\mathbf{w}_i^*\}_{i=1}^K)) > 0, \forall l \in 1, 2. \quad (\text{B.5})$$

Without loss of generality, each element in (B.5) can be scaled by a positive constant (i.e., $\frac{\alpha_l}{f_l^*}, \forall l \in \{1, 2\}$). Furthermore, both of these inequalities can be added

$$\sum_{l=1}^2 \frac{\alpha_l}{f_l^*} (f_l(\{\mathbf{w}'_i\}_{i=1}^K) - f_l(\{\mathbf{w}^*_i\}_{i=1}^K)) > 0, \forall l \in 1, 2. \quad (\text{B.6})$$

However, the inequality in (B.6) contradicts the fact that $\{\mathbf{w}^*_i\}_{i=1}^K$ is the optimal solution of \tilde{OP} . Therefore, the optimal solution of \tilde{OP} satisfies the Pareto-optimality condition, and hence, it gives the Pareto-solutions of the original SE-EE trade-off OP problem. This completes the proof of Theorem 1. \blacksquare

B.2 Proof of Lemma 1

Lemma 1 presents that f_1^{Norm} and f_2^{Norm} remain constant with the different weight factors while the available power is less than green power. This can be equivalently written as

$$\{f_1^{Norm}(\beta_1)\}_{P_{ava}=P_1} = \{f_1^{Norm}(\beta_2)\}_{P_{ava}=P_1}, \quad (\text{B.7a})$$

$$\{f_2^{Norm}(\beta_1)\}_{P_{ava}=P_1} = \{f_2^{Norm}(\beta_2)\}_{P_{ava}=P_1}, \quad (\text{B.7b})$$

where P_1 is less than the green power, and $\beta_1, \beta_2 \in [0, 1]$. In order to prove this, we validate (B.7a) and (B.7b) with the extreme conditions of $\beta_1 = 0$ and $\beta_2 = 1$. We start with $\beta_1 = 0$, in which case \tilde{OP} turns out to be an SE-Max problem, and thus, the maximum SE is achieved. Therefore,

$$\{f_1^{Norm}(\beta_1 = 0)\}_{P_{ava}=P_1} = 1. \quad (\text{B.8})$$

Furthermore, it has been already verified in [101] that both SE-Max and GEE-Max problem provide the same optimal beamforming vectors with an available power less than the green power. This means that $\{f_2(\beta_1 = 0)\}_{P_{ava}=P_1} = f_2^*$, therefore,

$$\{f_2^{Norm}(\beta_1 = 0)\}_{P_{ava}=P_1} = 1. \quad (\text{B.9})$$

Similarly, we follow the same approach for the case with $\beta_2 = 1$, where \tilde{OP} becomes the GEE-Max problem. The maximization of EE with an available power less than the green power will simultaneously achieve the maximum sum rate and the maximum EE. Hence,

$$\{f_1^{Norm}(\beta_2 = 1)\}_{P_{ava}=P_1} = 1, \quad (\text{B.10a})$$

$$\{f_2^{Norm}(\beta_2 = 1)\}_{P_{ava}=P_1} = 1. \quad (\text{B.10b})$$

It is can be easily noticed that (B.8), (B.9), (B.10a), and (B.10b) validate the conditions provided in (B.7a), (B.7b). This completes the proof of Lemma 2. ■

References

- [1] Y. Liu, Z. Qin, M. ElKashlan, Z. Ding, A. Nallanathan, and L. Hanzo, "Non-orthogonal multiple access for 5G and beyond," *Proc. IEEE*, vol. 105, no. 12, pp. 2347–2381, Dec. 2017.
- [2] R. Vannithamby and S. Talwar, *Towards 5G Applications: Requirements and Candidate Technologies*. John Wiley & Sons, 2017.
- [3] M. Benisha, R. T. Prabu, and V. T. Bai, "Requirements and challenges of 5G cellular systems," in *Proc. IEEE 2nd International Conference on Advances in Electrical, Electronics, Information, Communication and Bio-Informatics (AEEICB)*, 2016, pp. 251–254.
- [4] G. Liu and D. Jiang, "5G: Vision and requirements for mobile communication system towards year 2020," *Chin. J. Eng.*, vol. 2016, Mar. 2016, Art. no. 5974586.
- [5] L. Atzori, A. Iera, and G. Morabito, "The Internet of Things: A survey," *Comput. Netw.*, vol. 54, no. 15, pp. 2787–2805, Oct. 2010.
- [6] D. Evans, "The internet of things; how the next evolution of the internet is changing everything," CISCO, 2011.
- [7] X. Krasniqi and E. Hajrizi, "Use of IoT technology to drive the automotive industry from connected to full autonomous vehicles," *IFAC PapersonLine*, vol. 49, no. 29, pp. 269–274, 2016.
- [8] S. R. Islam, N. Avazov, O. A. Dobre, and K.-S. Kwak, "Power-domain non-orthogonal multiple access (NOMA) in 5G systems: potentials and challenges," *IEEE Commun. Surveys Tuts.*, vol. 19, no. 2, pp. 721–742, Oct. 2017.
- [9] A. Zappone and E. Jorswieck, "Energy efficiency in wireless networks via fractional programming theory," *Found. Trends Commun. Inf. Theory*, vol. 11, no. 3-4, pp. 185–396, Jan. 2015.

- [10] J. Wu, S. Rangan, and H. Zhang, *Green Communications: Theoretical Fundamentals, Algorithms, and Applications*. CRC press, 2016.
- [11] H. Shi, R. V. Prasad, E. Onur, and I. Niemegeers, “Fairness in wireless networks: Issues, Measures and Challenges,” *IEEE Commun. Surveys Tuts.*, vol. 16, no. 1, pp. 5–24, 1st Quart. 2014.
- [12] S. Tomida and K. Higuchi, “Non-orthogonal access with SIC in cellular downlink for user fairness enhancement,” in *Proc. IEEE Inter. Symp. on Intell. Signal Process. and Comm. Sys. (ISPACS), 2011*, pp. 1–6.
- [13] W. Roh, J.-Y. Seol, J. Park, B. Lee, J. Lee, Y. Kim, J. Cho, K. Cheun, and F. Aryanfar, “Millimeter-wave beamforming as an enabling technology for 5G cellular communications: Theoretical feasibility and prototype results,” *IEEE Commun. Mag.*, vol. 52, no. 2, pp. 106–113, Feb. 2014.
- [14] E. G. Larsson, O. Edfors, F. Tufvesson, and T. L. Marzetta, “Massive MIMO for next generation wireless systems,” *IEEE Commun. Mag.*, vol. 52, no. 2, pp. 186–195, Feb. 2014.
- [15] M. Aldababsa, M. Toka, S. Gökçeli, G. K. Kurt, and O. Kucur, “A tutorial on nonorthogonal multiple access for 5G and beyond,” *Wireless Commun. Mobile Computing*, vol. 2018, Feb. 2018, Art. no. 9713450.
- [16] A. Goldsmith, *Wireless Communications*. Cambridge University Press, 2005.
- [17] J. Winters, “Optimum combining for indoor radio systems with multiple users,” *IEEE Trans. Commun.*, vol. 35, no. 11, pp. 1222–1230, Nov. 1987.
- [18] G. J. Foschini and M. J. Gans, “On limits of wireless communications in a fading environment when using multiple antennas,” *Wireless Personal Commun.*, vol. 6, no. 3, pp. 311–335, Mar. 1998.
- [19] J. Mietzner, R. Schober, L. H.-J. Lampe, W. H. Gerstacker, P. A. Hoeher *et al.*, “Multiple-antenna techniques for wireless communications—a comprehensive literature survey,” *IEEE Commun. Surveys Tut.*, vol. 11, no. 2, pp. 87–105, 2nd Quart. 2009.
- [20] A. M. Hunter, J. G. Andrews, and S. Weber, “Transmission capacity of ad hoc networks with spatial diversity,” *IEEE Trans. Wireless Commun.*, vol. 7, no. 12, pp. 5058–5071, Dec. 2008.

- [21] L. Zheng and D. N. C. Tse, "Diversity and multiplexing: A fundamental tradeoff in multiple-antenna channels," *IEEE Transactions on information theory*, vol. 49, no. 5, pp. 1073–1096, 2003.
- [22] H. Bolcskei, D. Gesbert, and A. J. Paulraj, "On the capacity of OFDM-based spatial multiplexing systems," *IEEE Trans. Commun.*, vol. 50, no. 2, pp. 225–234, Feb. 2002.
- [23] H. Weingarten, Y. Steinberg, and S. Shamai, "The capacity region of the Gaussian MIMO broadcast channel," in *Proc. IEEE Int. Symp. Inf. Theory (ISIT)*, 2004.
- [24] P. Saxena and A. Kothari, "Performance analysis of adaptive beamforming algorithms for smart antennas," *Proc. IERI Procedia*, vol. 10, pp. 131–137, 2014.
- [25] B. Widrow, P. Mantey, L. Griffiths, and B. Goode, "Adaptive antenna systems," *Proc. IEEE*, vol. 55, no. 12, pp. 2143–2159, Dec. 1967.
- [26] B. D. Van Veen and K. M. Buckley, "Beamforming: A versatile approach to spatial filtering," *IEEE ASSP Mag.*, vol. 5, no. 2, pp. 4–24, Apr. 1988.
- [27] S. Tomida and K. Higuchi, "Non-orthogonal access with SIC in cellular downlink for user fairness enhancement," in *Proc. IEEE Inter. Symp. on Intell. Signal Process. and Comm. Sys. (ISPACS), 2011*, pp. 1–6.
- [28] Y. Saito, Y. Kishiyama, A. Benjebbour, T. Nakamura, A. Li, and K. Higuchi, "Non-orthogonal multiple access (NOMA) for cellular future radio access," in *Proc. IEEE VTC Spring 2013*, pp. 1–5.
- [29] S. Vanka, S. Srinivasa, Z. Gong, P. Vizi, K. Stamatiou, and M. Haenggi, "Superposition coding strategies: Design and experimental evaluation," *IEEE Trans. Wireless Commun.*, vol. 11, no. 7, pp. 2628–2639, Jul. 2012.
- [30] Z. Ding, Y. Liu, J. Choi, Q. Sun, M. Elkashlan, and H. V. Poor, "Application of non-orthogonal multiple access in LTE and 5G networks," *IEEE Commun. Mag.*, vol. 55, no. 2, pp. 185–191, Feb. 2017.
- [31] Z. Ding, F. Adachi, and H. V. Poor, "The application of MIMO to non-orthogonal multiple access," *IEEE Trans. Wireless Commun.*, vol. 15, no. 1, pp. 537–552, Jan. 2016.
- [32] Z. Ding, Y. Liu, J. Choi, Q. Sun, M. Elkashlan, I. Chih-Lin, and H. V. Poor, "Application of non-orthogonal multiple access in LTE and 5G networks," *IEEE Commun. Mag.*, vol. 55, no. 2, pp. 185–191, Feb. 2017.

- [33] Z. Ding, L. Dai, and H. V. Poor, "MIMO-NOMA design for small packet transmission in the Internet of Things," *IEEE access*, vol. 4, pp. 1393–1405, Apr. 2016.
- [34] J. Kim, J. Koh, J. Kang, K. Lee, and J. Kang, "Design of user clustering and precoding for downlink non-orthogonal multiple access (NOMA)," in *Proc. IEEE Military Communications Conference (MILCOM), 2015*, pp. 1170–1175.
- [35] M. Zeng, A. Yadav, O. A. Dobre, and H. V. Poor, "Energy-efficient joint user-RB association and power allocation for uplink hybrid NOMA-OMA," *IEEE Internet of Things J.*, vol. 6, no. 3, pp. 5119–5131, Jun. 2019.
- [36] Y. Sun, Y. Guo, S. Li, D. Wu, and B. Wang, "Optimal resource allocation for NOMA-TDMA scheme with α -fairness in industrial internet of things," *Sensors*, vol. 18, no. 5, p. 1572, 2018, <https://doi.org/10.3390/s18051572>.
- [37] D. Zhai and J. Du, "Spectrum efficient resource management for multi-carrier-based NOMA networks: A graph-based method," *IEEE Wireless Commun. Lett.*, vol. 7, no. 3, pp. 388–391, Jun. 2018.
- [38] Z. Ding, X. Lei, G. K. Karagiannidis, R. Schober, J. Yuan, and V. Bhargava, "A survey on non-orthogonal multiple access for 5G networks: Research challenges and future trends," *IEEE J. Sel. Areas Commun.*, vol. 35, no. 10, pp. 2181 – 2195, Oct. 2017.
- [39] A. Benjebbour, Y. Saito, Y. Kishiyama, A. Li, A. Harada, and T. Nakamura, "Concept and practical considerations of non-orthogonal multiple access (NOMA) for future radio access," in *Proc. IEEE Intell. Signal Process. and Commun. Syst. (ISPACS), 2013*, pp. 770–774.
- [40] T. Cover, "Broadcast channels," *IEEE Trans. Inf. Theory*, vol. 18, no. 1, pp. 2–14, Jan. 1972.
- [41] P. Patel and J. Holtzman, "Analysis of a simple successive interference cancellation scheme in a DS/CDMA system," *IEEE Sel. Areas in Commun.*, vol. 12, no. 5, pp. 796–807, Jun. 1994.
- [42] E. Gelal, J. Ning, K. Pelechrinis, T.-S. Kim, I. Broustis, S. V. Krishnamurthy, and B. D. Rao, "Topology control for effective interference cancellation in multiuser MIMO networks," *IEEE/ACM Transactions on Networking (TON)*, vol. 21, no. 2, pp. 455–468, Apr. 2013.

- [43] Z. Chen, Z. Ding, X. Dai, and R. Zhang, "A mathematical proof of the superiority of NOMA compared to conventional OMA," [Online]. Available: <https://arxiv.org/abs/1612.01069>.
- [44] Z. Ding, F. Adachi, and H. V. Poor, "The application of MIMO to non-orthogonal multiple access," *IEEE Trans. Wireless Commun.*, vol. 15, no. 1, pp. 537–552, Jan. 2016.
- [45] Q. Sun, S. Han, I. Chin-Lin, and Z. Pan, "On the ergodic capacity of MIMO NOMA systems," *IEEE Wireless Commun. Lett.*, vol. 4, no. 4, pp. 405–408, Aug. 2015.
- [46] L. Lv, J. Chen, and Q. Ni, "Cooperative non-orthogonal multiple access in cognitive radio," *IEEE Commun. Lett.*, vol. 20, no. 10, pp. 2059–2062, Oct. 2016.
- [47] B. Wang, L. Dai, Z. Wang, N. Ge, and S. Zhou, "Spectrum and energy-efficient beamspace MIMO-NOMA for millimeter-wave communications using lens antenna array," *IEEE J. Sel. Areas Commun.*, vol. 35, no. 10, pp. 2370–2382, Oct. 2017.
- [48] Z. Wei, L. Zhao, J. Guo, D. W. K. Ng, and J. Yuan, "A multi-beam NOMA framework for hybrid mmwave systems," in *Proc. IEEE International Conference on Communications (ICC) 2018*, pp. 1–7.
- [49] Z. Chen, Z. Ding, P. Xu, and X. Dai, "Optimal precoding for a QoS optimization problem in two-user MISO-NOMA downlink," *IEEE Commun. Lett.*, vol. 20, no. 6, pp. 1263–1266, Jun. 2016.
- [50] G. L. Stuber, J. R. Barry, S. W. McLaughlin, Y. Li, M. A. Ingram, and T. G. Pratt, "Broadband MIMO-OFDM wireless communications," *Proc. IEEE*, vol. 92, no. 2, pp. 271–294, 2004.
- [51] T. L. Marzetta, "Noncooperative cellular wireless with unlimited numbers of base station antennas," *IEEE Trans. Wireless Commun.*, vol. 9, no. 11, pp. 3590–3600, Nov. 2010.
- [52] T. L. Marzetta and A. Ashikhmin, "MIMO system having a plurality of service antennas for data transmission thereof," Nov. 26 2013, uS Patent 8,594,215.
- [53] H. Huh, G. Caire, H. C. Papadopoulos, and S. A. Ramprasad, "Achieving "Massive MIMO" spectral efficiency with a not-so-large number of antennas," *IEEE Trans. Wireless Commun.*, vol. 11, no. 9, pp. 3226–3239, Sep. 2012.

- [54] M. Bengtsson and B. Ottersten, "Optimal downlink beamforming using semidefinite optimization," in *Proc. Annual Allerton Conf. on Commun., Control and Computing*, 1999, pp. 987–996.
- [55] S. K. Joshi, P. C. Weeraddana, M. Codreanu, and M. Latva-Aho, "Weighted sum-rate maximization for MISO downlink cellular networks via branch and bound," *IEEE Trans. Signal Process.*, vol. 60, no. 4, pp. 2090–2095, Dec. 2012.
- [56] O. Tervo, L.-N. Tran, and M. Juntti, "Optimal energy-efficient transmit beamforming for multi-user MISO downlink," *IEEE Trans. Signal Process.*, vol. 63, no. 20, pp. 5574–5588, Oct. 2015.
- [57] J. Kim, J. Koh, J. Kang, K. Lee, and J. Kang, "Design of user clustering and precoding for downlink non-orthogonal multiple access (NOMA)," in *Proc. IEEE Military Communications Conference (MILCOM), 2015*, pp. 1170–1175.
- [58] B. Kim, S. Lim, H. Kim, S. Suh, J. Kwun, S. Choi, C. Lee, S. Lee, and D. Hong, "Non-orthogonal multiple access in a downlink multiuser beamforming system," in *Proc. IEEE Military Communications Conference (MILCOM), 2013*, pp. 1278–1283.
- [59] S. Ali, E. Hossain, and D. I. Kim, "Non-orthogonal multiple access (NOMA) for downlink multiuser MIMO systems: User clustering, beamforming, and power allocation," *IEEE Access*, vol. 5, pp. 565–577, Dec. 2017.
- [60] F. Fang, H. Zhang, J. Cheng, and V. C. Leung, "Energy-efficient resource allocation for downlink non-orthogonal multiple access network," *IEEE Trans. Commun.*, vol. 64, no. 9, pp. 3722–3732, Sep. 2016.
- [61] P. Gandotra, R. K. Jha, and S. Jain, "Green communication in next generation cellular networks: a survey," *IEEE Access*, vol. 5, pp. 11 727–11 758, Jun. 2017.
- [62] X. Lu, P. Wang, D. Niyato, D. I. Kim, and Z. Han, "Wireless networks with RF energy harvesting: A contemporary survey," *IEEE Commun. Surveys Tuts.*, vol. 17, no. 2, pp. 757–789, Sec. Quarter 2015.
- [63] L. R. Varshney, "Transporting information and energy simultaneously," in *Proc. IEEE ISIT 2008.*, 2008, pp. 1612–1616.
- [64] I. Krikidis, S. Timotheou, S. Nikolaou, G. Zheng, D. W. K. Ng, and R. Schober, "Simultaneous wireless information and power transfer in modern communication systems," *IEEE Commun. Mag.*, vol. 52, no. 11, pp. 104–110, Nov. 2014.

- [65] T. N. Do and B. An, "Optimal sum-throughput analysis for downlink cooperative SWIPT NOMA systems," in *Proc. IEEE 2nd SigTelCom, 2018*, pp. 85–90.
- [66] F. Alavi, K. Cumanan, Z. Ding, and A. G. Burr, "Beamforming techniques for non-orthogonal multiple access in 5G cellular networks," *IEEE Trans. Veh. Technol.*, vol. 67, no. 10, pp. 9474–9487, Oct. 2018.
- [67] M. F. Hanif, Z. Ding, T. Ratnarajah, and G. K. Karagiannidis, "A minorization-maximization method for optimizing sum rate in the downlink of non-orthogonal multiple access systems," *IEEE Trans. Signal Process.*, vol. 64, no. 1, pp. 76–88, Jan. 2016.
- [68] J. Wang, Q. Peng, Y. Huang, H.-M. Wang, and X. You, "Convexity of weighted sum rate maximization in NOMA systems," *IEEE Signal Process. Lett.*, vol. 24, no. 9, pp. 1323–1327, Sept. 2017.
- [69] M. S. Ali, H. Tabassum, and E. Hossain, "Dynamic user clustering and power allocation for uplink and downlink non-orthogonal multiple access (NOMA) systems," *IEEE Access*, vol. 4, pp. 6325–6343, Aug. 2016.
- [70] T. D. P. Perera, D. N. K. Jayakody, S. K. Sharma, S. Chatzinotas, and J. Li, "Simultaneous wireless information and power transfer (SWIPT): Recent advances and future challenges," *IEEE Commun. Surveys Tuts.*, vol. 20, no. 1, pp. 264–302, 1st Quart. 2017.
- [71] N. Zhao, S. Zhang, F. R. Yu, Y. Chen, A. Nallanathan, and V. C. Leung, "Exploiting interference for energy harvesting: A survey, research issues, and challenges," *IEEE Access*, vol. 5, pp. 10 403–10 421, May 2017.
- [72] J. Xu, L. Liu, and R. Zhang, "Multiuser MISO beamforming for simultaneous wireless information and power transfer," *IEEE Trans. Signal Process.*, vol. 62, no. 18, pp. 4798–4810, Sep. 2014.
- [73] H. Zhang, K. Song, Y. Huang, and L. Yang, "Energy harvesting balancing technique for robust beamforming in multiuser MISO SWIPT system," in *Proc. IEEE International Conference on Wireless Communications & Signal Processing (WCSP)*, 2013, pp. 1–5.
- [74] Q. Shi, L. Liu, W. Xu, and R. Zhang, "Joint transmit beamforming and receive power splitting for MISO SWIPT systems," *IEEE Trans. Wireless Commun.*, vol. 13, no. 6, pp. 3269–3280, Jun. 2014.

- [75] Y. Dong, X. Ge, M. J. Hossain, J. Cheng, and V. C. Leung, "Proportional fairness-based beamforming and signal splitting for MISO-SWIPT systems." *IEEE Commun. Lett.*, vol. 21, no. 5, pp. 1135–1138, May 2017.
- [76] R. Sun, Y. Wang, X. Wang, and Y. Zhang, "Transceiver design for cooperative non-orthogonal multiple access systems with wireless energy transfer," *IET Commun.*, vol. 10, no. 15, pp. 1947–1955, 2016.
- [77] P. D. Diamantoulakis, K. N. Pappi, Z. Ding, and G. K. Karagiannidis, "Wireless-powered communications with non-orthogonal multiple access," *IEEE Trans. Wireless Commun.*, vol. 15, no. 12, pp. 8422–8436, Dec. 2016.
- [78] Y. Liu, Z. Ding, M. ElKashlan, and H. V. Poor, "Cooperative non-orthogonal multiple access with simultaneous wireless information and power transfer." *IEEE J. Sel. Areas Commun.*, vol. 34, no. 4, pp. 938–953, Apr. 2016.
- [79] Z. Ding, M. Peng, and H. V. Poor, "Cooperative non-orthogonal multiple access in 5G systems," *IEEE Commun. Lett.*, vol. 19, no. 8, pp. 1462–1465, Aug. 2015.
- [80] J. Zander, S.-L. Kim, M. Almgren, and O. Queseth, *Radio resource management for wireless networks*. Artech House, Inc., 2001.
- [81] S. Stanczak, M. Wiczanowski, and H. Boche, *Fundamentals of resource allocation in wireless networks: theory and algorithms*. Springer Science & Business Media, 2009, vol. 3.
- [82] Y. Tang, C. Sheng, Y. Hu, H. Yu, and X. Zhang, "Low-complexity beamforming designs of sum secrecy rate maximization for the Gaussian MISO multi-receiver wiretap channel," in *Proc. IEEE International Conference on Acoustics, Speech and Signal Processing (ICASSP)*, 2016, pp. 2174–2178.
- [83] L.-N. Tran, M. F. Hanif, A. Tolli, and M. Juntti, "Fast converging algorithm for weighted sum rate maximization in multicell MISO downlink," *IEEE Signal Process. Lett.*, vol. 19, no. 12, pp. 872–875, Dec. 2012.
- [84] B. Radunović and J.-Y. L. Boudec, "A unified framework for Max-Min and Min-Max fairness with applications," *IEEE/ACM Transactions on Networking (TON)*, vol. 15, no. 5, pp. 1073–1083, Oct. 2007.
- [85] L. Deng, Y. Rui, P. Cheng, J. Zhang, Q. Zhang, and M. Li, "A unified energy efficiency and spectral efficiency tradeoff metric in wireless networks," *IEEE Commun. Lett.*, vol. 17, no. 1, pp. 55–58, Jan. 2013.

- [86] O. Amin, E. Bedeer, M. H. Ahmed, and O. A. Dobre, "Energy efficiency–spectral efficiency tradeoff: A multiobjective optimization approach," *IEEE Trans. Veh. Technol.*, vol. 65, no. 4, pp. 1975–1981, Apr. 2016.
- [87] S. Boyd and L. Vandenberghe, *Convex Optimization*. Cambridge Univ. Press, 2004.
- [88] Y. Nesterov and A. Nemirovskii, *Interior-point Polynomial Algorithms in Convex Programming*. Philadelphia, PA: SIAM, 1994.
- [89] Z.-Q. Luo and W. Yu, "An introduction to convex optimization for communications and signal processing," *IEEE Journal on selected areas in communications*, vol. 24, no. 8, pp. 1426–1438, 2006.
- [90] M. Grant, S. Boyd, and Y. Ye, "CVX: Matlab software for disciplined convex programming," [Online]. Available: <http://www.stanford.edu/boyd/cvx>.
- [91] J. Löfberg, "Yalmip: A toolbox for modeling and optimization in matlab," in *Proc. IEEE CACSD Conference*, vol. 3, 2004.
- [92] A. Beck, A. Ben-Tal, and L. Tetrushvili, "A sequential parametric convex approximation method with applications to nonconvex truss topology design problems," *J. Global Optimiz.*, vol. 47, no. 1, pp. 29–51, May 2010.
- [93] A. L. Yuille and A. Rangarajan, "The concave-convex procedure," *Neural computation*, vol. 15, no. 4, pp. 915–936, 2003.
- [94] D. R. Hunter and K. Lange, "A tutorial on MM algorithms," *Amer. Statistician*, vol. 58, no. 1, pp. 30–37, 2004.
- [95] W. Dinkelbach, "On non linear fractional programming," *Manage. Sci.*, vol. 13, no. 7, pp. 492–498, Mar. 1967.
- [96] A. Konak, D. W. Coit, and A. E. Smith, "Multi-objective optimization using genetic algorithms: A tutorial," *Reliability Engineering & System Safety*, vol. 91, no. 9, pp. 992–1007, Sept. 2006.
- [97] A. Zhou, B.-Y. Qu, H. Li, S.-Z. Zhao, P. N. Suganthan, and Q. Zhang, "Multiobjective evolutionary algorithms: A survey of the state of the art," *Swarm and Evolutionary Computation*, vol. 1, no. 1, pp. 32–49, 2011.

- [98] R. T. Marler and J. S. Arora, "Survey of multi-objective optimization methods for engineering," *Structural and multidisciplinary optimization*, vol. 26, no. 6, pp. 369–395, Apr. 2004.
- [99] ———, "The weighted sum method for multi-objective optimization: new insights," *Structural and multidisciplinary optimization*, vol. 41, no. 6, pp. 853–862, Jun. 2010.
- [100] K. Cumanan, R. Krishna, L. Musavian, and S. Lambotharan, "Joint beamforming and user maximization techniques for cognitive radio networks based on branch and bound method," *IEEE Trans. Wireless Commun.*, vol. 9, no. 10, pp. 3082–3092, Oct. 2010.
- [101] H. M. Al-Obiedollah, K. Cumanan, J. Thiyagalingam, A. G. Burr, Z. Ding, and O. A. Dobre, "Energy efficient beamforming design for MISO non-orthogonal multiple access systems," *IEEE Trans. Commun.*, vol. 67, no. 6, pp. 4117–4131, Jun. 2019.
- [102] M. S. Lobo, L. Vandenberghe, S. Boyd, and H. Le Bret, "Applications of second-order cone programming," *Linear Algebra and its Appl.*, vol. 284, pp. 193–228, Nov. 1998.
- [103] M. Grant, S. Boyd, and Y. Ye, "CVX: Matlab software for disciplined convex programming," 2008.
- [104] D. Feng, C. Jiang, G. Lim, L. J. Cimini, G. Feng, and G. Y. Li, "A survey of energy-efficient wireless communications," *IEEE Communications Surveys & Tutorials*, vol. 15, no. 1, pp. 167–178, 2012.
- [105] K.-G. Nguyen, L.-N. Tran, O. Tervo, Q.-D. Vu, and M. Juntti, "Achieving energy efficiency fairness in multicell MISO downlink," *IEEE Communications Letters*, vol. 19, no. 8, pp. 1426–1429, 2015.
- [106] S. He, Y. Huang, S. Jin, F. Yu, and L. Yang, "Max-min energy efficient beamforming for multicell multiuser joint transmission systems," *IEEE Communications Letters*, vol. 17, no. 10, pp. 1956–1959, 2013.
- [107] Y. Li, M. Sheng, X. Wang, Y. Zhang, and J. Wen, "Max–min energy-efficient power allocation in interference-limited wireless networks," *IEEE Transactions on Vehicular Technology*, vol. 64, no. 9, pp. 4321–4326, 2014.
- [108] D. Bertsimas, V. F. Farias, and N. Trichakis, "The price of fairness," *Operations research*, vol. 59, no. 1, pp. 17–31, Feb. 2011.
- [109] F. Kelly, "Charging and rate control for elastic traffic," *Transactions on Emerging Telecommunications Technologies*, vol. 8, no. 1, pp. 33–37, 1997.

- [110] C. Peel, Q. Spencer, A. L. Swindlehurst, and B. Hochwald, "Downlink transmit beamforming in multi-user MIMO systems," in *Proc. IEEE Sensor Array Multichannel Signal Process. Workshop*, 2004, pp. 43–51.
- [111] A. Wiesel, Y. C. Eldar, and S. Shamai, "Zero-forcing precoding and generalized inverses," *IEEE Trans. Signal Process.*, vol. 56, no. 9, pp. 4409–4418, Sep. 2008.
- [112] J. Lorincz and I. Bule, "Renewable energy sources for power supply of base station sites," *International Journal of Business Data Communications and Networking (IJBDCN)*, vol. 9, no. 3, pp. 53–74, 2013.
- [113] L.-C. Wang and S. Rangapillai, "A survey on green 5G cellular networks," in *Proc. IEEE International Conference on Signal Processing and Communications (SPCOM)*, 2012, pp. 1–5.
- [114] C. Xiong, G. Y. Li, S. Zhang, Y. Chen, and S. Xu, "Energy-and spectral-efficiency tradeoff in downlink OFDMA networks," *IEEE Trans. Wireless Commun.*, vol. 10, no. 11, pp. 3874–3886, Dec. 2011.
- [115] R. Jain, D.-M. Chiu, and W. R. Hawe, *A quantitative measure of fairness and discrimination for resource allocation in shared computer system*. Eastern Research Laboratory, Digital Equipment Corporation Hudson, MA, 1984, vol. 38.
- [116] K. Proos, G. Steven, O. Querin, and Y. Xie, "Multicriterion evolutionary structural optimization using the weighting and the global criterion methods," *AIAA journal*, vol. 39, no. 10, pp. 2006–2012, 2001.
- [117] K. Cumanan, L. Musavian, S. Lambotharan, and A. B. Gershman, "SINR balancing technique for downlink beamforming in cognitive radio networks," *IEEE Signal Process. Lett.*, vol. 17, no. 2, pp. 133–136, Feb. 2010.
- [118] Y. Liu, Z. Qin, M. El Kashlan, Z. Ding, A. Nallanathan, and L. Hanzo, "Non-orthogonal multiple access for 5G and beyond," *Proc. IEEE*, vol. 105, no. 12, pp. 2347–2381, Dec. 2017.
- [119] Q. Yang, H.-M. Wang, D. W. K. Ng, and M. H. Lee, "NOMA in downlink SDMA with limited feedback: Performance analysis and optimization," *IEEE J. Sel. Areas Commun.*, vol. 35, no. 10, pp. 2281–2294, Oct. 2017.
- [120] M. Zeng, A. Yadav, O. A. Dobre, and H. V. Poor, "Energy-efficient power allocation for MIMO-NOMA with multiple users in a cluster," *IEEE Access*, vol. 6, pp. 5170–5181, Feb. 2018.

-
- [121] T. N. Do and B. An, "Optimal sum-throughput analysis for downlink cooperative SWIPT NOMA systems," in *Proc. IEEE 2nd SigTelCom, 2018*, pp. 85–90.
- [122] S. Islam, M. Zeng, O. A. Dobre, and K.-S. Kwak, "Resource allocation for downlink NOMA systems: Key techniques and open issues," *IEEE Wireless Commun.*, vol. 25, no. 2, pp. 40–47, Apr. 2018.
- [123] H. Alobiedollah, K. Cumanan, J. Thiyagalingam, A. G. Burr, Z. Ding, and O. A. Dobre, "Energy efficiency fairness beamforming design for MISO NOMA systems," in *Proc. IEEE WCNC, 2019*.
- [124] ———, "Sum rate fairness trade-off-based resource allocation technique for MISO NOMA systems," in *Proc. IEEE WCNC, 2019*.
- [125] Z. Ding, P. Fan, and H. V. Poor, "Impact of user pairing on 5G nonorthogonal multiple-access downlink transmissions," *IEEE Transactions on Vehicular Technology*, vol. 65, no. 8, pp. 6010–6023, 2015.